



AVIATION FUEL PRODUCTION FROM RENEWABLE FEEDSTOCK BY A  
SINGLE-STEP HYDROTREATING PROCESS



By  
MISS Boontarika AKASSUPHA

A Thesis Submitted in Partial Fulfillment of the Requirements  
for Master of Engineering (CHEMICAL ENGINEERING)  
Department of CHEMICAL ENGINEERING  
Graduate School, Silpakorn University  
Academic Year 2017  
Copyright of Graduate School, Silpakorn University

การผลิตเชื้อเพลิงอากาศยานจากวัตถุดิบหมุนเวียนด้วยกระบวนการไฮโดรทรีตใน  
ขั้นตอนเดียว



วิทยานิพนธ์นี้เป็นส่วนหนึ่งของการศึกษาตามหลักสูตรวิศวกรรมศาสตรมหาบัณฑิต

สาขาวิชาวิศวกรรมเคมี แผน ก แบบ ก 2 ระดับปริญญามหาบัณฑิต

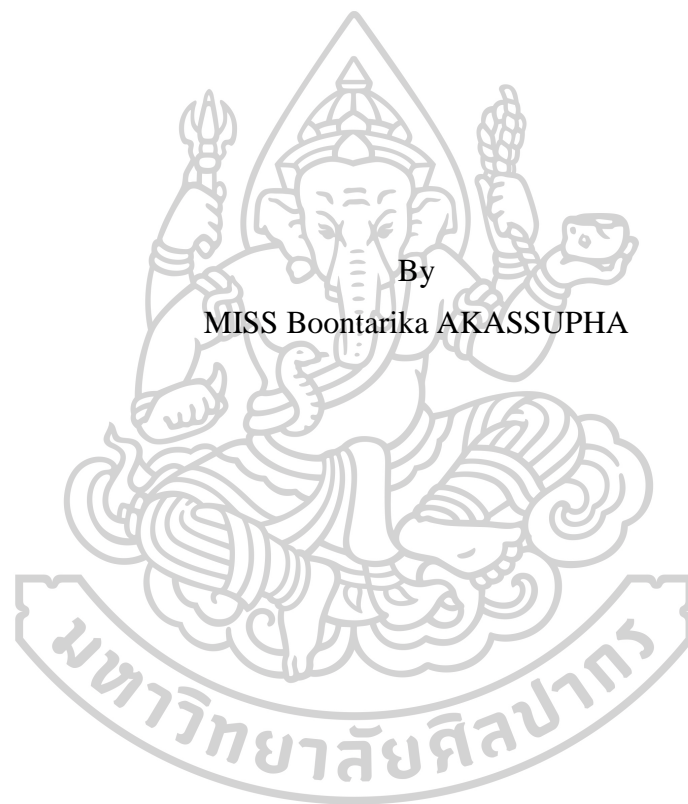
ภาควิชาวิศวกรรมเคมี

บัณฑิตวิทยาลัย มหาวิทยาลัยศิลปากร

ปีการศึกษา 2560

ลิขสิทธิ์ของบัณฑิตวิทยาลัย มหาวิทยาลัยศิลปากร

AVIATION FUEL PRODUCTION FROM RENEWABLE  
FEEDSTOCK BY A SINGLE-STEP HYDROTREATING PROCESS



By  
MISS Boontarika AKASSUPHA

A Thesis Submitted in Partial Fulfillment of the Requirements  
for Master of Engineering (CHEMICAL ENGINEERING)  
Department of CHEMICAL ENGINEERING  
Graduate School, Silpakorn University  
Academic Year 2017  
Copyright of Graduate School, Silpakorn University

Title Aviation fuel production from renewable feedstock by a  
single-step hydrotreating process  
By Boontarika AKASSUPHA  
Field of Study (CHEMICAL ENGINEERING)  
Advisor Worapon Kiatkitipong

---

Graduate School Silpakorn University in Partial Fulfillment of the  
Requirements for the Master of Engineering

..... Dean of graduate school  
(Associate Professor Jurairat Nunthanid, Ph.D.)

Approved by

..... Chair person  
(Assistant Professor Tarawipa Puangpetch , Ph.D.)

..... Advisor  
(Assistant Professor Worapon Kiatkitipong , D.Eng.)

..... Examiner  
( Sunthon Piticharoenphun , Ph.D.)

..... Examiner  
( NUTCHAPON CHOTIGKRAI , D.Eng.)

..... External Examiner  
(Professor Navadol Laosiripojana , Ph.D.)

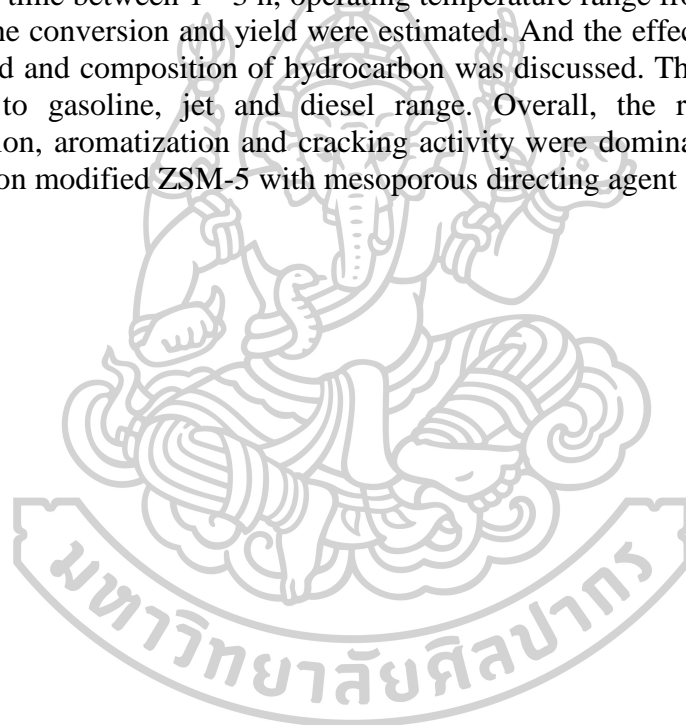


56404206 : Major (CHEMICAL ENGINEERING)

Keyword : Hydrotreated jet fuel (HJF); Hydroprocessing; NiMo; ZSM-5

MISS BOONTARIKA AKASSUPHA : AVIATION FUEL PRODUCTION FROM RENEWABLE FEEDSTOCK BY A SINGLE-STEP HYDROTREATING PROCESS THESIS ADVISOR : ASSISTANT PROFESSOR WORAPON KIATKITIPONG, D.Eng.

The catalytic hydroprocessing of palm fatty acid distillate (PFAD) over NiMo supported on ZSM-5, modified ZSM-5 with mesoporous directing agent, and modified ZSM-5 using rice husk ash or TEOS as a Si source was carried out to produce biojet fuel. The physicochemical properties of the catalyst were investigated by X-ray diffraction (XRD), scanning electron microscopy (SEM), Transmission Electron Microscope (TEM), ammonia temperature program desorption (NH<sub>3</sub>-TPD) and N<sub>2</sub> adsorption-desorption isotherm. The effect of reaction parameter such as reaction time between 1 - 3 h, operating temperature range from 360 - 390 °C were studied. The conversion and yield were estimated. And the effect of modified-ZSM-5 on the yield and composition of hydrocarbon was discussed. The liquid product were identified to gasoline, jet and diesel range. Overall, the result showed that the isomerization, aromatization and cracking activity were dominant when using NiMo supported on modified ZSM-5 with mesoporous directing agent as a catalyst.



## ACKNOWLEDGEMENTS

First and foremost, I would like to express my very great appreciation to my thesis advisor, Assist. Prof. Worapon Kiatkitipong for the continuous support of my study and research, for his patience, motivation, and immense knowledge. His guidance helped me in all the time of my research and my life. Even when i fall down, he never left and embolden me to move on. I would also like to show gratitude to my committee, including Assist. Prof. Tarawipa Puangpetch, Mr. Sunthon Piticharoenphun, Mr Nutchapon Chotigkrai and Prof. Navadol Laosiripojana for their encouragement and wisely comments.

Most importantly, none of this could have happened without my family. who always show unconditional love and encouragement throughout my life. Last but not least,I would also like to extend my thanks to my friends and my special friend who give me an important life lesson. This accomplishment would not have been possible without them. Thank you.

Boontarika AKASSUPHA

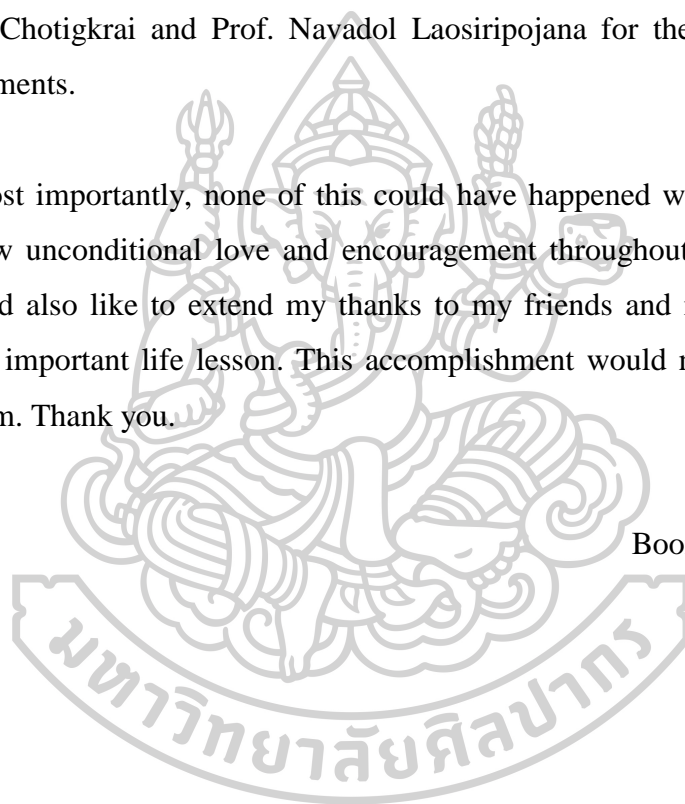


## TABLE OF CONTENTS

	<b>Page</b>
ABSTRACT.....	D
ACKNOWLEDGEMENTS.....	E
TABLE OF CONTENTS.....	F
TABLE OF TABLES .....	H
TABLE OF FIGURES .....	I
LIST OF ABBREVIATIONS.....	L
CHAPTER 1 INTRODUCTION.....	1
1.1. Introduction.....	1
1.2. Objective of Research.....	3
1.3. Scope of Research.....	3
CHAPTER 2 THEORY .....	6
2.1. Hydroprocessing process .....	6
2.2. Palm fatty acid distillate (PFAD) .....	8
2.3. Zeolite .....	9
CHAPTER 3 LITERATURE REVIEWS .....	13
3.1. Zeolite .....	13
3.2. Renewable aviation fuel production .....	14
CHAPTER 4 RESEARCH PROCEDURE.....	22
4.1 Chemicals .....	22
4.2. Catalyst preparation .....	23
4.3. Catalyst Characterization .....	27
4.4. Catalyst activity .....	27
CHAPTER 5 RESULTS AND DISCUSSION.....	28
5.1. Characterization of ZSM-5 supports .....	28
5.2. Hydroprocessing of PFAD .....	40

Chapter 6 Conclusions and recommendations .....	62
6.1 . Conclusion .....	62
6.2. Recommendations.....	62
REFERENCES .....	63
INDEX .....	72
Appendix A.....	73
A.1.Calculation H <sub>2</sub> to feed ratio .....	73
A.2. Calculation of metal loading for catalyst preparation .....	74
A.3. The calculation of the composition solution used to synthesize ZSM-5 from rice husk ash as a Si precursor.....	75
A.4. The calculation of selectivity and yield of liquid hydrocarbon and conversion of PFAD .....	78
A.4. The SEM-EDX images of catalysts.....	80
VITA.....	81

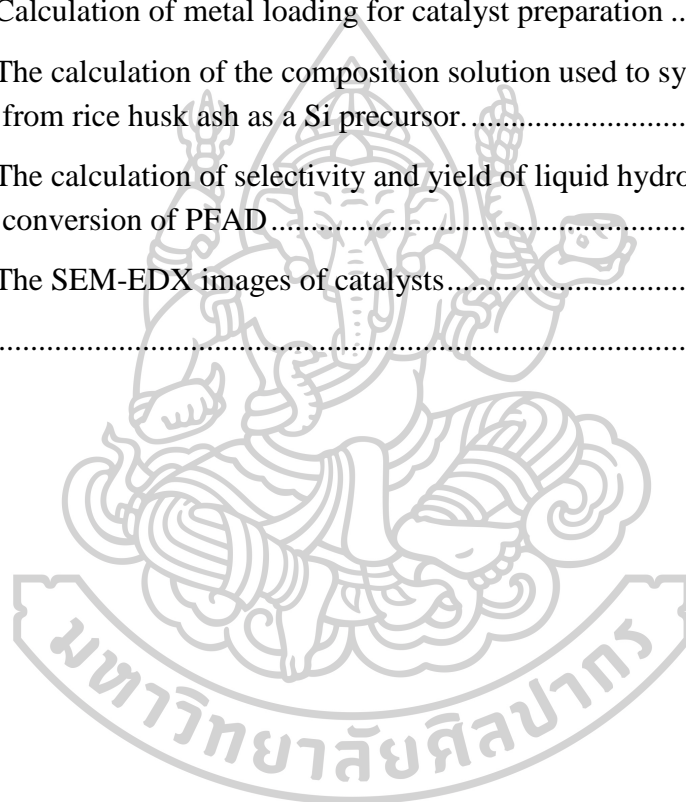




**TABLE OF TABLES**

	Page
Table 1. Distribution of fatty acids in PFAD.....	8
Table 2. The chemicals used to prepare the catalysts .....	22
Table 3. Acidity of ZSM-5 supports determined by temperature programmed desorption of ammonia .....	35
Table 4. Textural properties of the samples	38
Table 5. Fatty acid distribution of <i>Pongamia Pinnata</i> oil .....	59
Table 7. Fatty acid distribution of palm fatty acid distilled (PFAD).....	73
Table 8. The chemical composition of rice husk ash (RHA).....	79

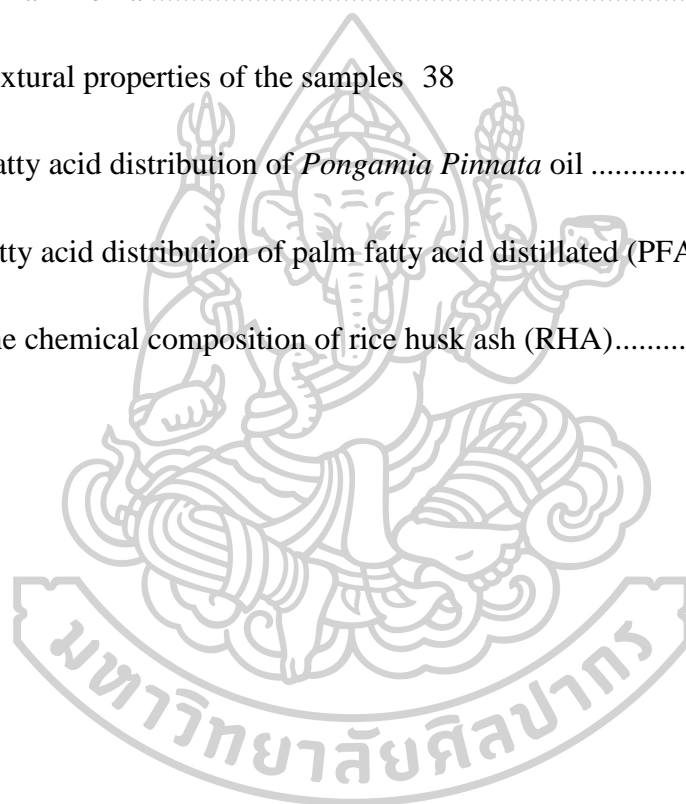


## TABLE OF FIGURES

	Page
Figure 1. Hydroprocessing pathways.....	6
Figure 2. (a) Diagram of the (100) face of ZSM-5. (b) Channel structure of ZSM-5. .	9
Figure 3 hierarchical systems were defined 4 types. A non-hierarchical with only microporous structure represented by the sticks (a). A small agglomerated-crystal produced a mesoporous framework by intercrystalline space (b). The intracconnected systems were showed in (c) and (d). The microporous structures were intervened with large molecule resulting to present the accessible mesoporous of the zeolite (c). The non-accessible mesoporous in the microporous system (d).[20] .....	11
Figure 4. The possible deoxygenation pathways .....	16
Figure 5 schematic of variation to the parameter in hydrothermal synthesis of ZSM-5 supports. Path 4.2.1 was ZSM-5 synthesis without mesoporous modification (ZNwo). Path 4.2.2 was ZSM-5 synthesis with added mesoporous directing agent with Si source (ZNco). Path 4.2.3 was ZSM-5 synthesis with added mesoporous directing agent after added Si source (ZNpost).....	26
Figure 6. XRD pattern of ZSM-5 synthesized by using (a) Sodium silicate (ZNwo), (b) Sodium silicate and add ODAC with Si sources (ZNco), (c) Sodium silicate and add ODAC after add Si source (ZNpost), (d) TEOS and add ODAC with Si sources (ZTco). And (e) rice husk ash and add ODAC with Si sources (ZRco). .....	30
Figure 7. SEM images for the major morphology of ZSM-5 using (a) Sodium silicate (ZNwo), (b) Sodium silicate and add ODAC with Si sources (ZNco), (c) Sodium silicate and add ODAC after add Si source (ZNpost).....	31
Figure 8. SEM images of ZSM-5 synthesized from TEOS and add ODAC with Si sources (ZTco). And (e) rice husk ash and add ODAC with Si sources (ZRco) .....	32

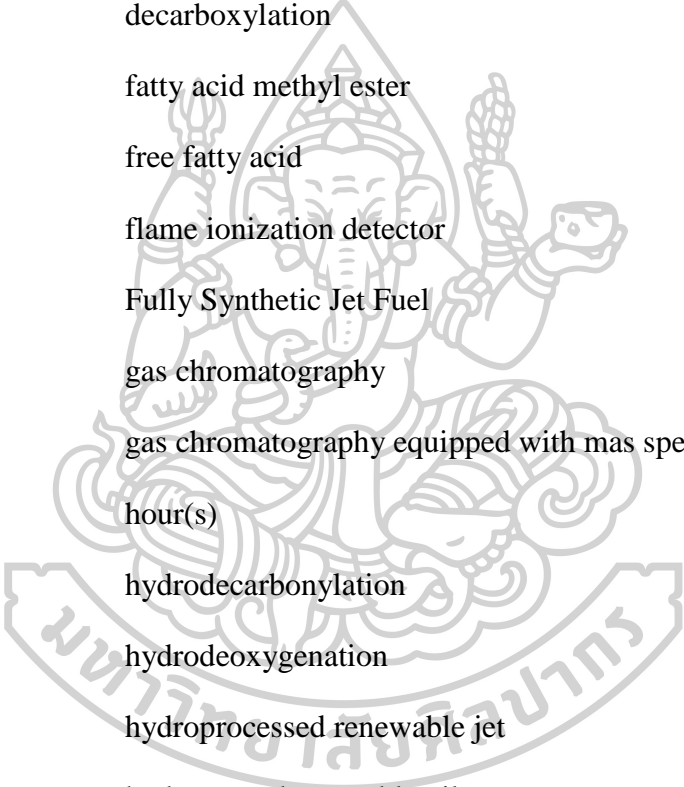
- Figure 9. TEM images of catalysts at 200 nm. (a) ZNwo, (b) NiMo/ZNwo, (c) NiMo/ZNco and (d) NiMo/ZNpost.....33
- Figure 10. NH<sub>3</sub>-TPD profiles of NaZNwo, ZNwo, ZNco, ZNpost ZTco, and ZRco. ....34
- Figure 11. NH<sub>3</sub>-TPD profiles of NiMo/ZNwo, NiMo/ZNco and NiMo/ZNpost .....34
- Figure 12. Nitrogen adsorption – desorption isotherm of ZSM-5 supports with different Si source and modified with ODAC as a mesoporous directing agent.....37
- Figure 13. Nitrogen adsorption – desorption isotherm of NiMo impregnated on ZSM-5 and modified ZSM-5 with ODAC .....37
- Figure 14. The effect of operating pressure on conversion and yield of NiMo/ZNco at operating temperature = 360°C and reaction time = 1 h.....40
- Figure 15. The effect of operating temperature on conversion (a) and yield of gasoline (b) of all catalysts (operating pressure = 40 bar and reaction time = 2 h).....41
- Figure 16. The effect of operating temperature on yield of jet fuel (a) and yield of diesel (b) of all catalysts (operating pressure = 40 bar and reaction time = 2 h).....42
- Figure 17. The effect of reaction time on conversion (a) and yield of gasoline (b) of all catalysts (operating pressure = 40 bar and operating temperature = 375°C).....43
- Figure 18. The effect of reaction time on yield of jet fuel (a) and diesel fuel (b) of all catalysts (operating pressure = 40 bar and operating temperature = 375°C).....44
- Figure 19. The effect of operating temperature on n-alkanes distribution (a), and hydrocarbon composition using NiMo/ZNco at operating temperature = 360°C and 375°C (b) (operating pressure = 40 bar and reaction time = 2 h) .....45
- Figure 20. The effect of operating temperature on hydrocarbon distributions in gasoline, jet and diesel range using NiMo/ZNco at operating temperature = 360°C (a)

and at operating temperature = 375°C (b) (operating pressure = 40 bar and reaction time = 2 h).....	46
Figure 21. The effect of operating time on n-alkanes distribution (a), and hydrocarbon distributions in gasoline, jet and diesel range at reaction time = 1 h (b) using NiMo/ZNwo (operating pressure = 40 bar and operating temperature = 375°C ) .....	47
Figure 22. The hydrocarbon distributions in gasoline, jet and diesel range at reaction time = 2 h (a), and 3 h (b) using NiMo/ZNwo (operating pressure = 40 bar and operating temperature = 375°C ) .....	48
Figure 23. The effect of reaction time on hydrocarbon composition using NiMo/ZNwo (operating pressure = 40 bar and operating temperature = 375°C).....	49
Figure 24. Mole fraction of gaseous products using NiMo/ZNwo at operating temperature = 360°C (a), 375°C (b), and 390°C (c) (operating pressure = 40 bar).....	52
Figure 25. Mole fraction of gaseous products using NiMo/ZNco at operating temperature = 360°C (a), 375°C (b), and 390°C (c) (operating pressure = 40 bar).....	53
Figure 26. The effect of reaction time on conversion, yield of gasoline, jet and diesel when using <i>Pongamia Pinnata</i> oil as feedstock and using NiMo/ZNwo (a) and NiMo/ZNco (b) (operating pressure = 40 bar and operating temperature = 360°C) ...	55
Figure 27. The effect of reaction time on gaseous products when using <i>Pongamia Pinnata</i> oil as feedstock and using NiMo/ZNwo (a) and NiMo/ZNco (b) (operating pressure = 40 bar and operating temperature = 360°C) .....	56
Figure 28. The effect of reaction time on n-alkanes distribution when using <i>Pongamia Pinnata</i> oil as feedstock and using NiMo/ZNwo (a) and NiMo/ZNco (b) (operating pressure = 40 bar and operating temperature = 360°C).....	57
Figure 29. structure of triglyceride. ....	58
Figure 30. TG-DTA profiles of used NiMo/ZNwo (a) and used NiMo/ZNco (b). ....	60

Figure 31 SEM-EDX images of NiMo/ZNwo (a), NiMo/ZNco (b), and NiMO/ZNpost (c).....80

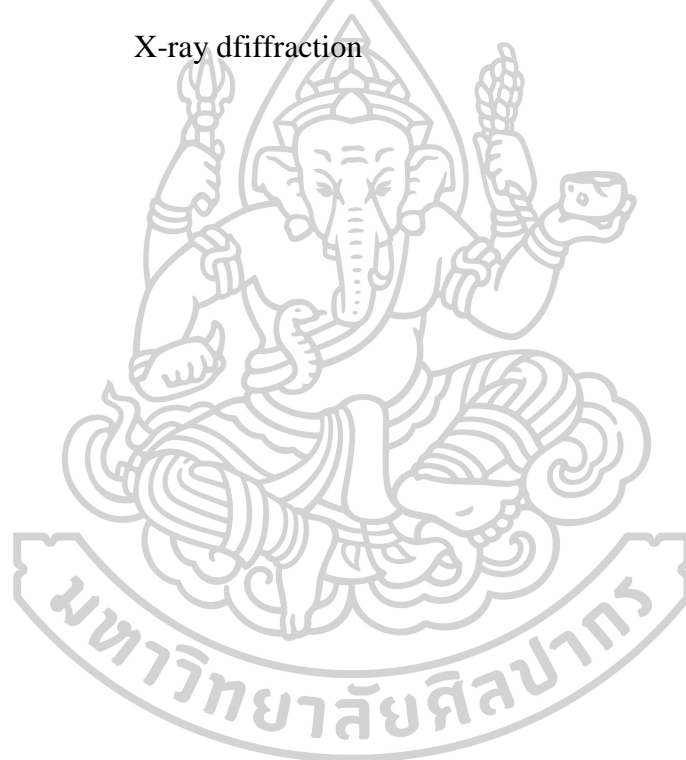


## LIST OF ABBREVIATIONS



BHD	bio-hydrotreated diesel
Bio-SPK	bio-derived synthetic paraffinic kerosene
°C	degree Celsius
DCO	decarbonylation
DCO <sub>2</sub>	decarboxylation
FAME	fatty acid methyl ester
FFA	free fatty acid
FID	flame ionization detector
FSJF	Fully Synthetic Jet Fuel
GC	gas chromatography
GM-MS	gas chromatography equipped with mass spectroscopy
h	hour(s)
HDCO	hydrodecarbonylation
HDO	hydrodeoxygenation
HRJ	hydroprocessed renewable jet
HVO	hydrotreated vegetable oil
ODAC	octadecyldimethyl(3-trimethoxysilylpropyl)ammoniumchloride
PFAD	palm fatty acid distillate
RBD	Refined-bleached-deodorized
RHA	rice husk ash
SEM	scanning electron microscopy
SPK	synthetic paraffinic kerosene
TCD	thermal conductivity

TEOS	Tetraethyl orthosilicate
TEM	Transmission electron microscopy
TPABr	Tetrapropyl ammonium bromide
TG	triglyceride
TGA	thermogravimetric analysis
DTG	derivative thermogravimetric analysis
wt. %	percent weight by weight
XRD	X-ray diffraction



# CHAPTER 1

## INTRODUCTION

### 1.1. Introduction

Emissions of aviation burning fuel cause global climate change by release greenhouse gases, especially carbon dioxide (CO<sub>2</sub>), which is proportional to the growth in aircraft transport. The emissions are also including oxide of nitrogen (NO<sub>x</sub>) and oxide of sulphur (SO<sub>x</sub>). NO<sub>x</sub> lead to the ozone formation in lower atmosphere which is a toxic and also enhance the global warming. Sulphur in the emission can oxidize to SO<sub>2</sub> and SO<sub>4</sub><sup>2-</sup>, which is form sulphuric acid may produce acid rain and air pollutants[1, 2]. Because the concerns of the environment and the CO<sub>2</sub> emissions from the aviation are increasing [3]. In European countries, in 2012, EU Emissions Trading System (EU ETS) included emissions from international aviation. Like industrial installations covered by the EU ETS, airlines receive tradable allowances covering a certain amount of CO<sub>2</sub> emissions that can be emitted by their flights per year. In addition, “European Advanced Biofuels Flight Path” taken by the International Civil Aviation Organization (ICAO), which is a UN specialized agency and works with the Convention’s 192 Member States and industry groups, leading European airlines and biofuel producers are trying to achieve a target of 2 million tons of sustainable biofuels used in European civil aviation by 2020. Due to the increasing emission from aviation transport, limited fossil fuel, and legislative constraints, interested in alternative and sustainable fuels are continuously higher.

Currently, there are some promising alternative jet fuels that can replace for conventional petroleum based fuel, for instance, Synthetic paraffinic kerosene (SPK), which was licensed by Syntroleum’s S-8, Shell’s GTL, and Sasol’s GTL-1 and GTL-2, Fully Synthetic Jet Fuel (FSJF), was licensed by Sasol, and Bio-Jet Fuel. However, to meet the specification ASTM D7566 (The American Society for Testing and Material), SPK that manufactured by Fischer-Tropsch (F-T) process using biomass as feedstock should blend with Jet-A only up to 50%. Fully Synthetic Jet Fuel (FSJF) was claimed by Sasol that they are the first company produced FSJF from coal and



natural gas by coal-to-liquid (CTL) process and Sasol's FSJF was included in ASTM D1655[4]. But, FSJF shown higher carbon emissions than petroleum based jet fuel in lifecycle assessment studies, and feedstock of FSJF did not from biomass [3, 5]. Therefore, there are still many attempts to synthesis renewable and sustainable aviation fuel. Biojet or biofuels are derived from biomass by hydroprocessing. Primary process for biofuel production, known as first-generation biofuel, is transesterification of triglycerides with alcohols. This reaction will produce fatty acid methyl esters (FAME) [6, 7]. FAMEs, also known as first-generation biodiesel, are produced from lipids by transesterification. In common, petroleum based jet fuel blend with biodiesel can use as alternative jet fuel but FAME is not hydrocarbon. So, it is not a "drop-in" fuel. The problem with FAME in the engine is that it has the ability to be absorbed by metal surface. And fuel in an aircraft engine transport in a joint systems, so FAME can stick in pipes or pumps of the system. There is a limit for blending jet fuel with FAME. The limitation for combination of jet A-1 with FAME of waste vegetable and Jatropha oil is up to 10% and 20% [8]. Because FAME contains oxygen and has undesirable cold flow properties and lower heat content comparing to petroleum based fuel [6, 9]. The next generation of biofuel is "Hydroprocessed renewable jet" (HRJ), which was converted from triglycerides by hydroprocessing process. This fuel was also call bio-SPK. HRJ is got more interest than FAME due to its properties satisfied the petroleum based jet fuel. This HRJ has good cold flow properties, high heating content, and it can act like a drop-in fuel. This is because HRJ is a hydrocarbon based, mainly n-alkanes. Triglycerides in animal fats or vegetable oils are converted to paraffinic hydrocarbons in the present of hydrogen. The mechanism of the reaction is complex and consists of a group of many reactions such as hydrotreating (hydrodesulfurization and hydrodenitrogenation), hydrogenation, hydrodeoxygenation, hydrocracking and hydroisomerization [10, 11]. HJF is currently produced by 2 reaction stages and include multiple reactors or multi-step reactions. In order to generate a product having paraffinic hydrocarbon in aviation boiling point range, in first step, the feed oil is converted to the straight chain diesel-range paraffins, by removing oxygen molecules and converted any olefins to paraffins by the reaction with hydrogen. Second step are isomerization and cracking to produce carbon numbers in the aviation range which have lower carbon number

than diesel. However, this process is complicated and many details are required between the first and second steps such as a portion of paraffins need to recycle to reaction zone to increase solubility of hydrogen and minimize hydrocracking and recycle of excess H<sub>2</sub> that are not consume need to pass through scrubber system to remove CO<sub>2</sub> [12]. However, single step economical processes to convert lipids into aviation ranges are still limited [13].

In this study, hydroprocessing in a single-step process of palm fatty acid distillate (PFAD) is investigated. Catalysts employed in this study includes 5wt% Ni and 18wt% Mo supported on ZSM-5 (ZNwo), modified ZSM-5 with mesoporous-directing agent (ZNco and ZNpost), ZSM-5 using rice husk ash as a silica source (ZRco) and ZSM-5 from TEOS as a silica source (ZTco).

## 1.2. Objective of Research

1.2.1. To synthesize ZSM-5 from low cost material, modified ZSM-5 with mesoporous-directing agent and ZSM-5 from rice husk ash.

1.2.2. To evaluate the hydroprocessing activities and selectivity of bimetallic (NiMo) sulfides catalysts supported on ZSM-5, modified ZSM-5 with mesoporous-directing agent and ZSM-5 from rice husk ash for aviation production.

## 1.3. Scope of Research

1.3.1. ZSM-5 synthesis (all sample used Tetrapropylammonium bromide (TPABr) as a ZSM-5 template)

1.3.1.1. Synthesized hierarchical ZSM-5 as follows Verma [13].

- SiO<sub>2</sub>/Al<sub>2</sub>O<sub>3</sub> equal to 40, hydrothermal method at 220°C with autogenously pressure for 24 h.
- Using tetraethyl orthosilicate (TEOS), aluminium nitrate as Si and Al sources with constant SiO<sub>2</sub>/Al<sub>2</sub>O<sub>3</sub> ratio.

- Tetrapropylammonium bromide, TPABr (denoted here as TPABr) and octadecyldimethyl (3-trimethoxysilylpropyl) ammonium chloride, ODAC (denoted here as ODAC) were used as microporous and mesoporous templates, respectively.
- The synthesized hierarchical ZSM-5 using TEOS as a Si source is denoted as ZTco.

1.3.1.2. Synthesized under similar procedure follows 1.3.1.1 but changing Si sources by using sodium silicate and Al source is aluminium nitrate. The synthesized ZSM-5 is denoted as ZNwo.

- Hydrothermal method at 220°C with autogenously pressure for 24 hr. with constant SiO<sub>2</sub>/Al<sub>2</sub>O<sub>3</sub> ratio at 40.
- For ZNwo, not using ODAC, but only using TPABr for zeolite template.

1.3.1.3. Synthesized ZSM-5 under similar procedure follows 1.3.1.2 and using ODAC as a mesoporous directing agent. ODAC adding procedures were varied by adding as the same time with sodium silicate (denote as ZNco) or after adding sodium silicate (denote as ZNpost).

1.3.1.4. To synthesize ZSM-5 from rice husk ash using hydrothermal method under procedure follows by 1.3.1.2 and using rice husk ash and Sodium aluminate as Si and Al sources respectively. The synthesized ZSM-5 is denoted as ZRco.

1.3.1.5. To synthesize ZSM-5 from TEOS using hydrothermal method under procedure follows by 1.3.1.2 and using TEOS and Sodium aluminate as Si and Al sources respectively. The synthesized ZSM-5 is denoted as ZTco.

1.3.1.6. Ni and Mo loaded on ZNwo, ZNco, ZNpost, ZRco and ZTco by impregnation method using solutions of the 5 wt% Ni(NO<sub>3</sub>)<sub>2</sub> and 18wt% (NH<sub>4</sub>)<sub>6</sub>Mo<sub>7</sub>O<sub>24</sub>. The ZSM-5 supports were mixed with the impregnation solution and stirred for 6 h. Then the catalysts were dried at 110°C and calcined at 550°C for 5 hr.

### 1.3.2. Material and catalyst characterization

All ZSM-5 supports were characterized by X-ray Diffraction, Siemens D5000, in order to obtain XRD patterns representing ZSM-5 framework. Catalyst morphology was investigated with a scanning electron microscopy (SEM) which was JEOL model JSM-5410LV and Transmission Electron Microscopy (TEM) ) which was Hitachi model S-4800. The nitrogen adsorption-desorption isotherm, specific BET surface area, pore volume and pore size was examined in BELsorp instrument.

### 1.3.3. Hydroprocessing evaluation

Hydroprocessing reaction was conducted in stainless steel batch reactor. For each batch, 1 g. of catalyst and 2 ml. of palm fatty acid distillate feed were loaded in the reactor. The reaction conditions for all catalysts were varied: temperature 360 - 390°C, H<sub>2</sub> Pressure 40 bar, reaction time 1 – 3 hr.

1.3.4. Hydroprocessing product characterization The liquid product from the reaction was collected and analyzed by FID detector, the Shimadzu 14B gas chromatography equipped with an Agilent DB-2887 column. The gas product was collected and analyzed by TCD detector, the Shimadzu 14B gas chromatography equipped with a Porapak Q column.



## CHAPTER 2

### THEORY

This chapter provided some knowledges about hydroprocessing process, some pathways and property of feedstock for more understanding of the research.

#### 2.1. Hydroprocessing process

The reaction pathways of hydroprocessing process consisted of liquid and gas phase reactions. During hydroprocessing process, many reaction routes of liquid phase have occurred. The possible pathways to convert triglyceride to hydrocarbon might consisted of four deoxygenation reactions for example, decarboxylation ( $\text{DCO}_2$ ), decarbonylation ( $\text{DCO}$ ), hydrodecarbonylation ( $\text{HDCO}$ ), and hydrodeoxygenation ( $\text{HDO}$ ) as showed in Figure 1 [10, 14, 15]

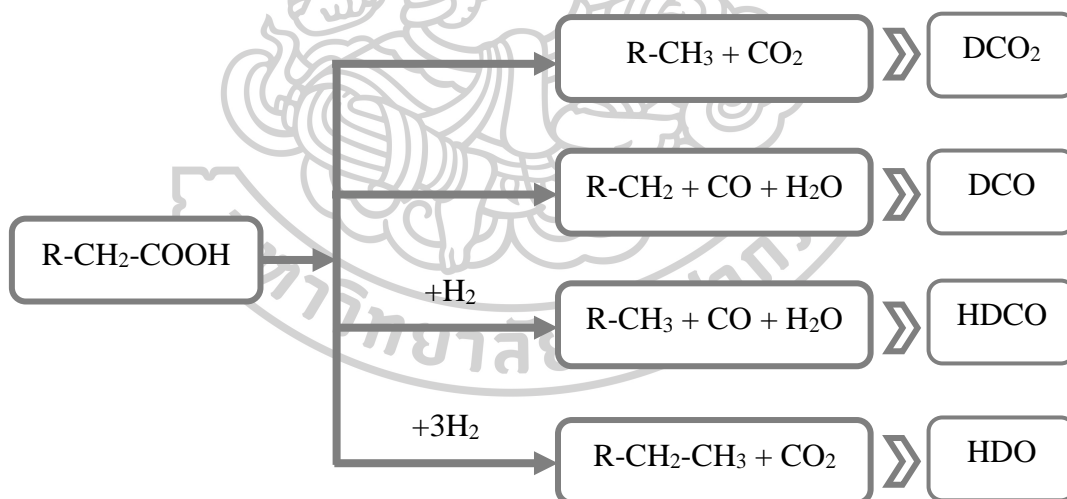


Figure 1. Hydroprocessing pathways

### 2.1.1. Decarboxylation and decarbonylation

If hydrocarbons are produced through DCO<sub>2</sub>, carboxyl group in fatty acid group will release carbon dioxide and produce alkanes. In the other hands, DCO pathway will generate carbon monoxide and water while produce alkene. The major advantage of these two reactions is no need of hydrogen in the reaction. Which is outstanding in economics.

### 2.1.2. Hydrodecarbonylation

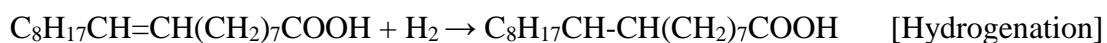
The carboxyl group in fatty acid that reacted through HDCO with hydrogen will release alkane, carbon monoxide, and water. In the case of DCO<sub>2</sub>, DCO, and HDCO, the hydrocarbon product will have one carbon atom shorter (C<sub>n-1</sub>) than fatty acid (C<sub>n</sub>) in feed.

### 2.1.3. Hydrodeoxygenation

Hydrodeoxygenation reaction can produce maximum carbon atom of hydrocarbon product or same carbon atom of fatty acid chain (C<sub>n</sub>). In this reaction, oxygen atom will remove out from the fatty acid then oxygen atom will gather with hydrogen to form water as a product too. However, HDO consumes more hydrogen than HDCO.

### 2.1.4. Other possible reactions

It is possible that triglycerides can get saturated via hydrogenation reaction first and then transform to hydrocarbon through DCO<sub>2</sub>, DCO, and HDCO. In addition, the present of CO<sub>2</sub>, CO and H<sub>2</sub> in the system, gas phase reaction can be occurred i.e. water –gas shift and methanation reaction. The hydrocarbon product can also go further to cracking and isomerization reaction.



## 2.2. Palm fatty acid distillate (PFAD)

PFAD is a residue from the refining of edible palm oil. PFAD consists of free fatty acids, which are undesired for edible oil. In palm oil refinery, there are 4 - 5% of PFAD as a residue. The advantages of PFAD are low cost and non-edible feedstock. PFAD is one of more promising feedstock for biodiesel production due to high conversion and yield in biodiesel. And biodiesel product from PFAD can decrease greenhouse gas emissions up to 80 - 90% compared to conventional diesel[16, 17].

In this research, PFAD was obtain from Pathum Vegetable Oil, Co. Ltd. In Thailand. The distribution of fatty acids in PFAD was showed in table 2.1.

Table 1. Distribution of fatty acids in PFAD.

Fatty acid	Wt.%
C 12:0 (Lauric acid)	-
C 14:0 (Myristic acid)	1.1
C 16:0 (Palmitic acid)	49.0
C 16:1 (Palmitoleic acid)	0.2
C 18:0 (Steric acid)	4.1
C 18:1 (Oleic acid)	35.8
C 18:2 (Linoleic acid)	8.3
C 18:3 (Lonoleic acid)	0.3
C 20:0 (Arachidic acid)	0.3
C 20:1 (Eicosenoic acid)	0.2
C 24:1 (Tetracosenoic acid)	0.6

### 2.3. Zeolite

Zeolitic material is aluminosilicates compound contains of aluminum oxygen tetrahedron ( $\text{AlO}_4$ ) and silicon oxygen tetrahedron ( $\text{SiO}_4$ ) bonded together to form a triangular structure. The general formula is  $\text{M}_{x/m}\text{Al}_x\text{Si}_{2-x}\text{O}_4 \cdot n\text{H}_2\text{O}$  where  $m$  is a valance electron of cation of  $M$  and  $n$  is water content. These zeolite structure are builded by the combination of secondary building units (SBUs). Channel or cage are appeared when SBUs coalesce together. The porous zeolite has small cavities or channels structures which connect neatly in three dimensions. These structures are uniform in size and shape. The uniform pores accept the same certain dimension molecule while reject larger molecule. This advantage property known as molecular sieve. Zeolites can be classified to about 40 species differences based on the type of structure, which has variety properties of the zeolite crystal structure, density, size and strength of the bond.[18] In this work, MFI framework, ZSM-5, was interesting. ZSM-5 exhibit the  $\text{Pnma}$  orthorhombic space group which has two type of channels. The ZSM-5 channel systems consist of a straight channel running parallel to (010) and a sinusoidal channel parallel to the (100) axis.[19]

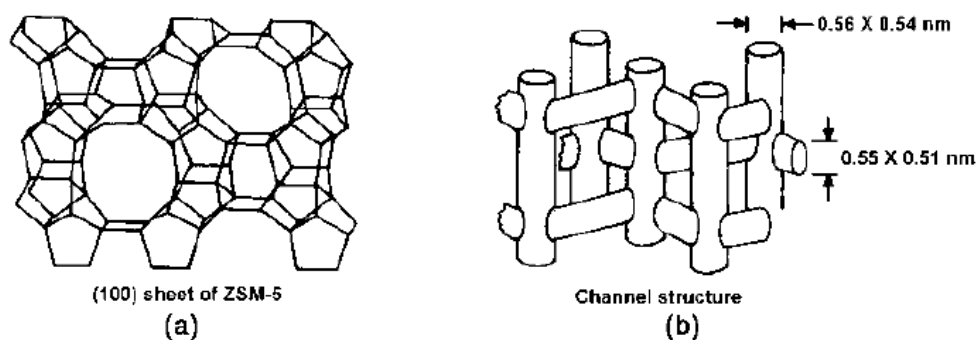


Figure 2. (a) Diagram of the (100) face of ZSM-5. (b) Channel structure of ZSM-5.

A net negative charge in ZSM-5 framework was introduced by +3 valance electrons of Al which reacted with Si atom in ZSM-5 system leading to require cations to remain neutral. The presence of cations allow ZSM-5 to be used in ion-



exchange reaction and the created the acid site by the protons. ZSM-5 consists of hydroxyl group with silicon and aluminum atom resulting to a strong Brønsted site. The Brønsted acid site is formed by exchange sodium ion with hydrogen ion via ion-exchange reaction. ZSM-5 is widely used for cracking, isomerization and other petroleum refining industry. Not only the specific in size and shape, the acid property is one in the advantages of ZSM-5. The acid sites i.e. Brønsted and Lewis, are important sites in zeolites as the site that catalytic reactions take place. The active sites also appear on the external surface and at the pore mouth of zeolite crystals [19]. In addition, there are some modifications on ZSM-5 molecular which result to change shape selectivity or channel property. From the modification, the certain molecule can pass through the zeolite pore.

However, many catalytic reactions have limitations using microporous zeolite as a catalyst. This limitations are involving the accessibility of bulky molecule of feedstock and the pore-blocked by large molecule resulting to coke form. More recently, the modification or improvement of zeolite properties are required in many reaction especially in hydrocarbon processes. To decreased the disadvantages of microporous and increased the accessibility and activity or shortening the micropore path length, mesoporous is introduced in the zeolite. “Hierarchical” system, which possesses two pore structures, is the combination of microporous and mesoporous structure. There are many methods such as dual templating, colloid-imprint carbon, desilication, dealumination, recrystallization, and mesoporous directing agent were studied to modified zeolite.

The hierarchical system was showed in Figure 3. The advantage of hierarchical system was to improve the accessibility of micropores. The interconnected system refer to a mesoporous framework which was produced by a small agglomerated-crystal (Figure 3 (b)). The intraconnected system showed that there was mesoporous in the microporous system (Figure 3 (c and d)) which could shorten the length of microporous. The mesopores in Figure 3 c. allowed the molecule to access from the surface of ZSM-5. But in Figure 3 d., the mesopores was inside the micropores system therefore there are the accessible ways only by the micropores. Hence, the method to add the mesopores in a zeolite could be unsuitable for some

applications. It is necessary to concern the accessibility simultaneous with the generating a large pore.

Several synthesis methods studied the material to improve the accessibility. Generally, most of synthesis method used a template to generate the mesopores. However the mesoporous could be also produce without template.

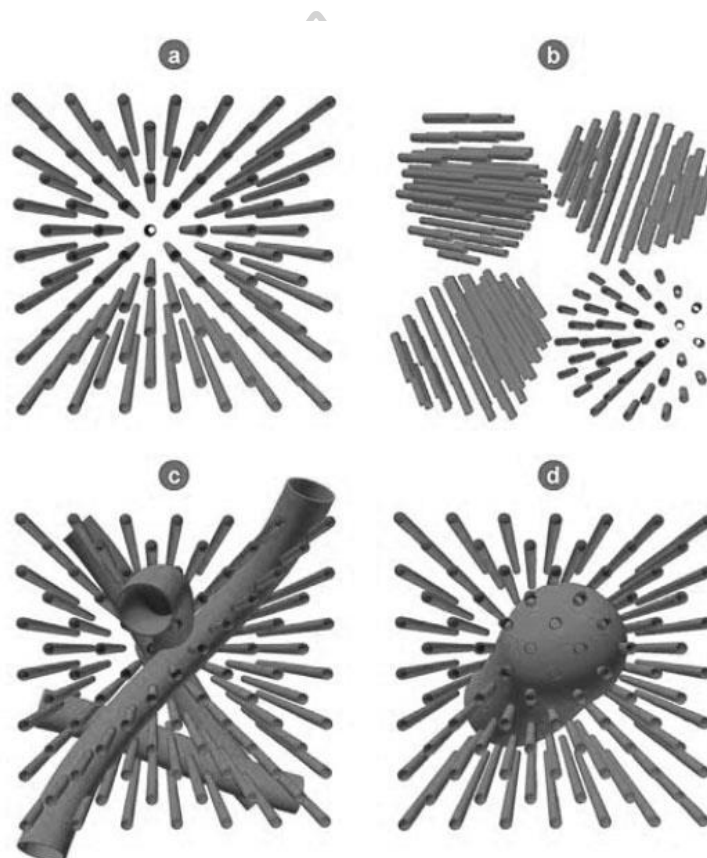


Figure 3 hierarchical systems were defined 4 types. A non-hierarchical with only microporous structure represented by the sticks (a). A small agglomerated-crystal produced a mesoporous framework by intercrystalline space (b). The intraconnected systems were showed in (c) and (d). The microporous structures were intervened with large molecule resulting to present the accessible mesoporous of the zeolite (c). The non-accessible mesoporous in the microporous system (d).[20]

### 2.3.1. Templating method

Templating methods can be classified to 3 types: solid templating, supramolecule templating, and indirect templating. The first type, solid templating, the zeolite was contacted with porous carbon template and then the solid was removed to produce mesoporous. Carbon templating can be tuned the porous system between nanosized to mesoporous zeolite crystal. The second type, supramolecular templating method, this method used surfactant molecule or organosilanes to directly generate large micropores or mesopores. A large surfactant molecule template allowed the crystallization of zeolite to take place on the surface of surfactant to lead to have a large pore. On the other hand, the organosilanes allowed the crystallization of zeolite to take place inside. The last one is the indirect templating method which gives composite materials into zeolite structure. In this method, the important part is to partial or secondary crystallization of the mesoporous material into zeolite structure in the crystallization process.

### 2.3.2. Non-templating method

The two important methods in non-templating method are demetallation and controlled crystallization. One of the examples of the demetallations is dealumination which aluminums are extracted from a zeolite framework by steaming or acid leaching to generate mesoporous zeolite. Steam treatment is a well-known method to selectively remove silicon out of the zeolite framework to engender the mesoporous zeolite. In the controlled crystallization method, the conditions of crystallization are adjusted to favor in the nucleation process. This method is about to develop the synthesis methodology to favor the nucleation more than crystal growth. The main disadvantage of this method is the trial-error on the synthesis condition which is hard to control the pore size or particle size [19, 20].

## CHAPTER 3

### LITERATURE REVIEWS

This chapter reviews various articles of interest that relate with the aviation fuel production from renewable feedstock, including acid support, production conditions, feedstocks, hydroprocessing catalysts and reaction mechanism. This review is divided into two parts, zeolite support and renewable aviation fuel production.

#### 3.1. Zeolite

Zeolites are one of the most significant materials in chemistry; especially in petroleum processes such as catalytic cracking, hydrocracking, isomerization, aromatics alkylation, methanol to gasoline. Zeolites have been defined as microporous crystalline aluminosilicates which have high adsorption capacity due to the high surface area of the microporous structure [21, 22]. Zeolite pores can selectively sort molecules depending on their sizes and shapes. This “molecular sieving” effect has enabled the development of molecular size- or shape-selective applications in adsorption and a strong Brønsted acidity of bridging Si–(OH)–Al sites generated by the presence of aluminum inside the silicate framework [23]. But in the case of the catalytic reaction of larger molecules, zeolites showed low activities, since the larger molecules cannot access the active sites located inside the zeolite micropores [24, 25].

The strategy recently for improving the accessibility in zeolites is likely the case of hierarchical zeolites. These materials are characterized by the presence of a bimodal pore size distribution, formed by both micropores and mesopores. The secondary mesoporous structure can be generated by using mesopore templates which should have sufficiently high affinity with zeolite frameworks. After removal of the template through calcination, the zeolite can possess open mesoporous structure in addition to the zeolitic micropores in a hierarchical manner. This type of zeolites is often called “hierarchically nanoporous zeolites” or “hierarchical zeolites” for short [26, 27]. Recently, Choi and coworkers reported a new method for the preparation of mesoporous material having the strong acidity. They proposed to use an amphiphilic

organosilane template molecule, [3-(trimethoxysilyl)propyl] hexadecyl-dimethylammonium (TPHAC), and reported a successful preparation of mesoporous HZSM-5 [28]. The same method were proposed by Serrano, They used a silanization agent; phenylaminopropyl-trimethoxysilane (PHAPTMS) as the silylating agent to prevent the total aggregation of protozeolitic nanounits during the crystallization step, leading to zeolitic materials containing a hierarchical porosity [25]. The other way to synthesis of hierarchical mesoporous ZSM-5 was investigated by Verma, octadecyldimethyl(3-trimethoxysilylpropyl) ammonium chloride (ODAC) was added to a conventional alkaline mixture for zeolite ZSM-5 synthesis as a mesopore template to control the crystallinity [13]. Hierarchical zeolites have been also reported by Serrano and coworkers to show a better resistance to deactivation by coking. Moreover, the availability of the additional mesoporosity provides an ideal space for supporting other active phase with a high dispersion and strong interaction with the support, opening new ways for the development of improved bifunctional zeolitic catalysts [25].

### **3.2. Renewable aviation fuel production**

Craig and Soveran applied for a U.S. Patent No.4992605 in 1989, referred to a production of hydrocarbons by the hydroprocessing of vegetable oil. In this patent, Hydroprocessing feedstock selected from a group consisting of canola oil, sunflower oil, soybean oil, rapeseed oil, palm oil and tall oil under conditions of temperature about 360-390 °C, pressure about 4.8-15.2 MPa and liquid hourly space velocity (LHSV) of 0.5-5.0 hr<sup>-1</sup>. In the presence of two commercial hydroprocessing catalysts including Co-Mo or Ni-Mo were employed to convert many feedstock into linear hydrocarbon compound mixtures. The obtained products have a boiling point in 210-343 °C range of diesel with carbon atom ranging from C15 to C18. The liquid product was almost completely converted to a high quality (high cetane) diesel boiling range material. Although some residual material (at T>343°C) was formed. Super cetane has a linear additive effect on cetane number [29]. The similar process was proposed in U.S. patent No. 5705722, was investigated by J. Monnier and his colleagues in 1995. Tall oil, wood oils from the pulping of hardwood species and animal fats which contain unsaturated fatty acids, were carried to hydroprocessing with hydrogen gas

and suitable catalysts such as Co-Mo, Ni-Mo and transition metal based catalysts. This process is a process for producing additives for diesel fuels having high cetane numbers and improving ignition. The reactions were carried out in temperature ranges of 370-450 °C, the hydrogen pressure 4-15 MPa and the liquid hourly space velocity (LHSV) are 0.5 to 5.0 hr<sup>-1</sup>. They found that the unsaturated fatty acids, the diterpenic acids and unsaponifiable in tall oil can be converted into cetane improver [30]. Generally, the cetane number of commercial diesel fuel can be improved by addition of the additive. However, the major drawbacks of these additives are their relatively high cost and a non-linear impact on mixture cetane number. The studies of SRC (The Saskatchewan Research Council), Natural Resources Canada and Agriculture and Agri-Food Canada, super cetane were performed by Stumborg and his coworkers. They converted canola oil and tall oil, using conventional technology, into a hydrocarbon in diesel range with high cetane number almost 100 is called "SCR super cetane". SRC can blend with conventional diesel at any proportion with specific gravity property of SRC same as diesel fuel. Viscosity is higher than conventional diesel fuel but similar to FAME from canola oil. The major concerns were the poor cold flow characteristics which higher than 20 °C and the corrosion properties which did not meet the 1A requirement for diesel fuel. Gaseous emission was decreased with an addition of SRC super cetane. Therefore, SCR super cetane is a more effective cetane additive than commercial alkyl-nitrate cetane enhancers [31]. Due to the challenging issues of conventional petroleum fuel is a scarcity of fossil fuel, cause of the increasing use of fuel for transportation. There is a need to find alternative renewable fuel that can be used in place of fossil fuel. Hydroprocessing has now become a well and established process e.g. Neste oil corporation and UOP to produce straight chain alkanes in diesel range from fatty acid triglycerides of animal fat, tall oil, and other vegetable oils [7, 32]. Neste oil process relates to chemical industry and is directed to the production of middle distillate. The process consists of two step, hydrogenated process follows by catalytically converted to paraffins with branched chains [33]. The UOP process has a pretreatment step to remove contaminants such as alkali metals in the feedstock followed by hydrogenation, decarboxylation and/or hydrodeoxygenation and optionally hydroisomerization in one step [34]. Renewable hydrocarbon-based diesel obtained by hydroprocessing is also called as second

generation biodiesel or green diesel. Generally, supported noble metal catalysts, sulfide metal catalysts and reduced metal catalysts are used for this process. The reaction pathway involves hydrogenation of the C=C bonds of the vegetable oils followed by alkane production by three different pathways: decarbonylation, decarboxylation and hydrodeoxygenation (or dehydration/hydrogenation). The routes in Figure 3 depends on the reaction temperature, pressure, liquid hourly space velocity and the catalyst used [7, 35].

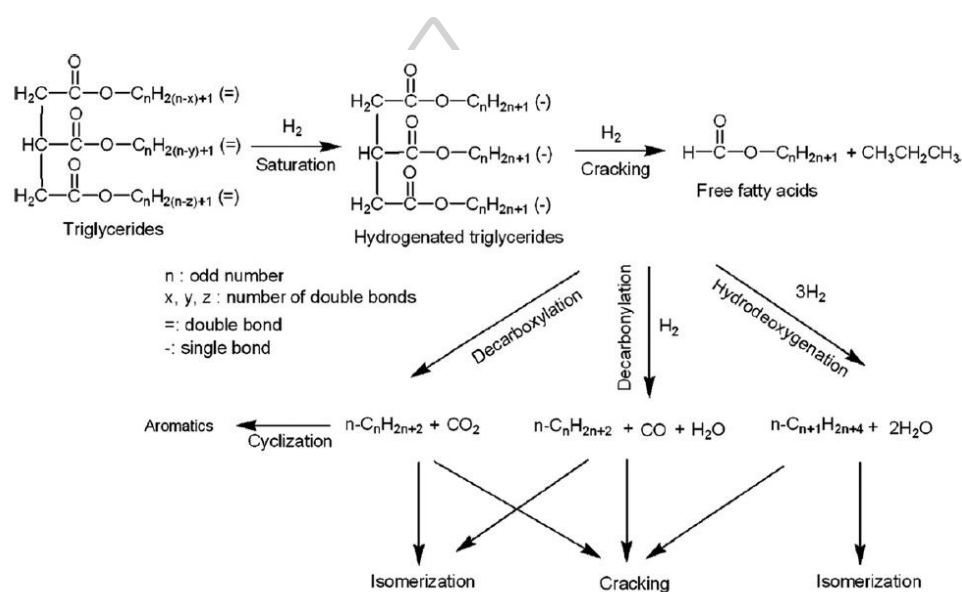


Figure 4. The possible deoxygenation pathways

The major advantages of hydroprocessing over trans-esterification are compatibility with current refinery infrastructure, engine compatibility and feedstock flexibility [35].

Hydrogenating and deoxygenating of the renewable feedstock with the presence of a hydrotreating catalyst at proper condition reaction can produce straight chain hydrocarbon, which have carbon atom similar to, or shorter than, the fatty acid composition of the feedstock. The general product was in the diesel boiling range. Clearly, this approach was suitable for diesel fuel production, but not an aviation fuel production. Alternatively, the selective hydrocracking and hydroisomerization

reaction can reduce the carbon chain length to aviation fuel range paraffins and improve properties such as low freezing point, high density, low viscosity etc. It is worth to note that there are many terms that can represent in similar meaning to “hydrotreated jet fuel (HJF)” such as hydrotreated vegetable oil (HVO), hydrotreated renewable jet (HRJ), bio-derived synthetic paraffinic kerosene (Bio-SPK) or hydroprocessed esters and fatty acids (HEFA) which named by the ASTM.

The aviation industry has recently begun investigating alternative fuel sources to replace the conventional fuel, paraffin (also known as kerosene) from crude oil. First generation biofuels, such as bio ethanol from sugarcane and bio diesel palm oil are not sufficient to substitute for fossil fuels in large quantities to fulfill the required need so far industries, especially the aviation industry [7]. Fatty acid methyl esters (also known as biodiesel) are renewable fuels manufactured by the transesterification of vegetable oils or animal fats. It was also considered as an alternative to jet fuel components with the reason that it can be used as a substitute for or as an additive to mineral diesel [36]. Llamas and his colleagues reported the blending of FAME from oils rich in shorter chain fatty acids, such as coconut, palm kernel, babassu and camelina oils, and then the fraction which approaches the distillation range of fossil kerosene, from 175–185°C to 240–275°C at atmospheric pressure, was separated. Then blends containing 5, 10 and 20 vol% of biokerosene with fossil kerosene and Jet A1. The blends of FAME and Jet A1 up to 10 vol% can meet the following ASTM D1655 specifications: color, acidity, density, lower heating value, copper strip corrosion, oxidation stability. However, the major drawbacks of FAME blends is a linear impact on density, kinematic viscosity, heating value, cloud point, pour point, and flash point. So, the possibility of biofuels replacing conventional jet fuel is limited, considering the large amount of FAME would make the blends of jet biofuel out of the standard [37, 38]. This is similar with the blended aviation biofuel from *Jatropha* oils and waste vegetable oils, investigated by Baroutian and his associates. The methyl esters of waste vegetable and *jatropha* oil were separately blended with Jet A-1 aviation fuel at various volumetric ratios. The jet biofuel with not more than 10 and 20% esters of waste vegetable and *jatropha* oils have similar characteristics with the commercial available Jet A1 aviation fuel [8]. The major disadvantages of FAME are poor heating value, low storage stability due to a high degree of



unsaturation, corrosivity because of the presence of moisture, ease of hydrolysis, undesired low temperature properties and relatively low energy content. Hydrocarbon fuels are mainly characterized by their cold flow properties. Compared to FAMEs and conventional petroleum-based fuels, Hydrocarbon fuels from hydro-deoxygenation are recognized by high cetane numbers [7].

From limitation of blending jet biofuel, the aviation fuel from catalytic hydro-processing is getting interest. A multi-step, multi-catalyst traditional process (deoxygenation followed by selective cracking and isomerization) has been claimed to convert lipids into jet-range hydrocarbons [39]. A process can produce a diesel boiling point range and an aviation boiling point range product from plant and animal oils. The process involves in hydrogenation, deoxygenation (decarboxylation, decarbonylation, and/or hydrodeoxygenation) in at least a first zone and then hydroisomerization and selective hydrocracking in a second zone. Products from the first reaction zone are n-paraffins and oxygenate compounds. But the presence of oxygen containing molecules including water, CO<sub>2</sub> and CO may result in the deactivation of the isomerization catalyst. The performance of the isomerization and selective hydrocracking catalyst is improved by removing oxygen containing molecules from the feed to the isomerization and selective hydrocracking zone using a selective hot high pressure hydrogen stripper. In addition, a portion of this hydrocarbon fraction (after separation from the gaseous portion) may be used as the hydrocarbon recycle, since hydrogen has a great solubility in the hydrocarbon product rather than in the feedstock. Moreover, a portion of the lighter hydrocarbons generated in the deoxygenation zone may be also carried with the hydrogen in the hot high pressure hydrogen stripper and removed in the overhead stream. Therefore, in some applications, it is advantageous to take steps to prevent normal hydrocarbons from being removed in the hot high pressure hydrogen stripper overhead and bypassing the isomerization zone. Rectification agents may be optionally introduced into the hot high pressure hydrogen stripper to reduce the amount of hydrocarbons in the hot high pressure hydrogen stripper overhead stream. Some suitable examples of additional rectification agents include a diesel range stream, a naphtha range stream, a naphtha and LPG range stream, or any mixture thereof. In some embodiment, a portion of branched enriched product is optionally used as a rectification agent.

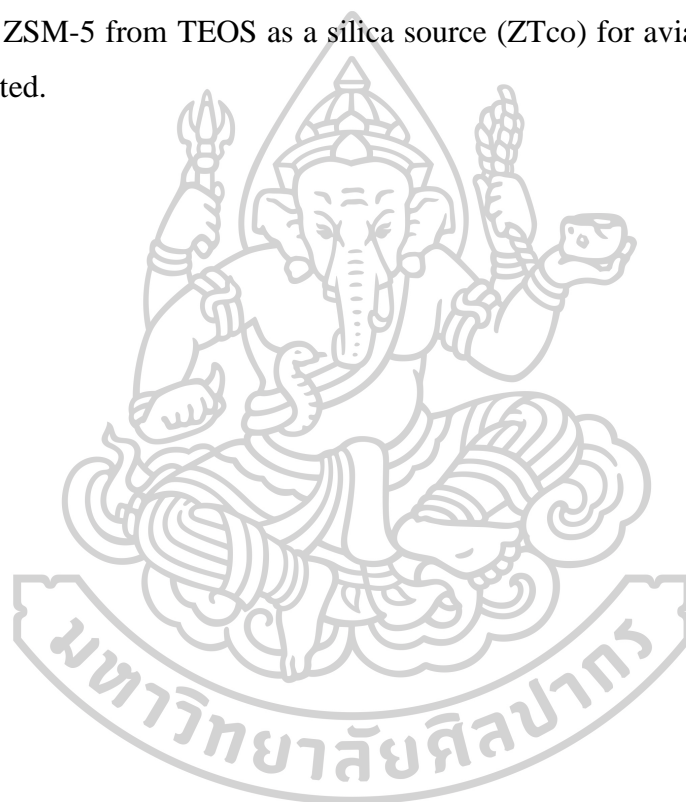
Typically, sulfided NiMo, NiW, CoMo supported on  $\gamma$ -Al<sub>2</sub>O<sub>3</sub> are used to provide hydrogenation and deoxygenation function while isomerization catalyst contains Pt, Pd or Ni on SAPO-11, Al<sub>2</sub>O<sub>3</sub>, ZSM-22, SiO<sub>2</sub> support. Many catalysts well known for isomerization can also become selective cracking catalyst functions at more severe conditions [39].

In 2009, McCall and his colleagues studied process which comprises a single reaction zone to hydrogenate, deoxygenate, isomerize and selectively hydrocrack a renewable feedstock, in order to generate a paraffinic hydrocarbon products in the aviation fuel range and a high iso/normal ratio was provided in Patent US 2009/0283442 A1. The examples of multifunctional catalysts, successful in catalyzing the deoxygenation, hydrogenation, isomerization and selective hydrocracking in the same reaction zone include noble metals, sulfide metals, sulfide base metals, zeolite, non-crystalline silica-aluminas, and alumina. The reaction was carried on tubular furnace which using Refined-bleached-deodorized (RBD) soybean oil as feedstock and two different multifunctional catalysts in series. The operating temperature of Catalyst 1 (hydrogenate, deoxygenate) is 332 °C while that of Catalyst 2 (isomerizes, hydrocrack) is 398 °C. The LHSV normally is within range of about 0.5 to 1 hr<sup>-1</sup>. The yield of aviation fuel (132°C-279°C) in range having approximately about 9 to 18 carbon atoms of 54.7% could be obtained and meeting the specification of MTL-DTL-83133. Successfully conducting the required reactions in a single reaction zone resulted in a lower capital and operating cost structure was claimed in the patent [12].

Recently, there are several studies about a single step process for hydroprocessing of lipids to obtain an aviation fuel. Verma and his coworkers studied the single step process for aviation fuel production. They used 5% NiO, 18% MoO<sub>3</sub> supported on a hierarchical mesoporous ZSM-5 with higher acidity, higher surface area but semi zeolitic crystallinity catalyst as a catalyst for producing jet-fuel range hydrocarbons, almost completed conversion of Jatropha oil (1.7% FFA, 19.5% C16:0, 7.9% C18:0, 45.4% C18:1, 27.3% C18:2) and algae oil (1.6% FFA, 51% C16:0, 2% C18:0, 39% C18:1, 7% C18:2) was obtained with aviation fuel (C9-C15) yield of 54.3% and 78.5% and iso/*n*-paraffins ratio of 2.6 and 2.5, respectively. The jet-fuel range products from the single-step route met all the basic requirements of the desired

freezing point ( $-55\text{ }^{\circ}\text{C}$ ), density ( $0.78\text{ gcc}^{-1}$  at  $15\text{ }^{\circ}\text{C}$ ), flash point ( $>38\text{ }^{\circ}\text{C}$ ), heat of combustion ( $>44\text{ MJ kg}^{-1}$ ), and viscosity ( $<8.0\text{ mm}^2\text{ S}^{-1}$ ). Sulfur content ( $<20\text{ ppm}$ ), olefins content ( $1\text{--}2\%$ ) and aromatics content ( $<1\%$ ) of the products were very low. The used catalysts could be easily regenerated at  $450\text{ }^{\circ}\text{C}$  in a stream of air and could be reused after resulfidation without any significant decrease in performance [13]. However, a much higher yield of aviation fuel from algae oil over *Jatropha* oil has not been discussed or elucidated yet. The similar reaction was performed by Chen and colleagues. They used hierarchical ZSM-5 catalysts which prepared by desilication with different NaOH concentrations to obtain a mesoporous structure and differences of acid strength. The ZSM-5 supports were impregnated with 4 wt% Ni and 12 wt% Mo. The hydroprocessing reaction was performed in a fixed-bed reactor at 653 K under 3 MPa with the liquid hourly space velocity of  $3.8\text{ h}^{-1}$  and a  $\text{H}_2/\text{oil}$  ratio (v/v) of 500 and used *jatropha* oil as feedstock. All catalysts gave almost complete conversion. The highest yield of liquid product was 83.7% when using ZSM-5 support which had hierarchical and amorphous structure. The most interesting notice was about ZSM-5 with collapsed structure. It could supply more accessible active sites for gaseous olefins to be converted to larger molecules and also allow large molecule to access the active site. The result indicated that the mesoporous structure with larger intracrystal mesopores provided shape-selective catalytic cracking for C9–C15 paraffins [40]. Another studied about hydrotreatment of *jatropha* oil was investigate by Gong and coworkers. They studied a series of sulfided NiMo/SiO<sub>2</sub>–Al<sub>2</sub>O<sub>3</sub> and NiMo/ZSM-5–Al<sub>2</sub>O<sub>3</sub> catalysts in a fixed-bed reactor in this follow condition: 330–370 °C, 3 MPa of total pressure, liquid hourly space velocity equal to  $2\text{ h}^{-1}$  and  $\text{H}_2/\text{feed}$  ratio of 600 (v/v). When increasing amounts of ZSM-5 in ZSM-5–Al<sub>2</sub>O<sub>3</sub> support, the ratio of decarboxylation and/or decarbonylation versus hydrodeoxygenation did not change. Because total acid sites of catalyst prefer the decarboxylation and/or decarbonylation pathways. They found that the highest yields (about 25%) of isomerized products occur when using NiMo/SiO<sub>2</sub>–Al<sub>2</sub>O<sub>3</sub> catalysts while using NiMo/ZSM-5–Al<sub>2</sub>O<sub>3</sub> catalysts had the highest yields (about 30%) of cracked products. These results were affected by the acid site of catalyst. The isomerization reaction favored weak and middle acidic sites and the cracking reaction favored strong acidic sites [41].

As shown above, very limited study of aviation fuel production in one step has been reported. Moreover, the understanding on the effect of support on isomerization and cracking reactions in hydrotreatment of vegetable oils is scarce. Thus, in this work, the effect of active sites and supports will be investigated for the hydroprocessing of lipids to produce aviation fuel in a single-step process. Different conditions of hydroprocessing of palm fatty acid distillate with bimetallic (NiMo) sulfides catalysts supported on ZSM-5 (ZNwo), modified ZSM-5 with mesoporous-directing agent (ZNco and ZNpost), ZSM-5 using rice husk ash as a silica source (ZRco) and ZSM-5 from TEOS as a silica source (ZTco) for aviation production will be investigated.



## CHAPTER 4

### RESEARCH PROCEDURE

#### 4.1 Chemicals

Table 2. The chemicals used to prepare the catalysts

Chemicals	Formula	Grade	Manufacture
Sodium silicate	SiO <sub>2</sub>	Assay 27% SiO <sub>2</sub>	Riedel-de Haen
Tetraethyl orthosilicate	C <sub>8</sub> H <sub>20</sub> O <sub>4</sub> Si	Assay 99.0%	ALDRICH
Aluminium nitrate	Al(NO <sub>3</sub> ) <sub>3</sub> ·9H <sub>2</sub> O	Assay 99.99%	UNILAB
Tetrapropyl ammonium bromide	C <sub>12</sub> H <sub>28</sub> BrN	98%	ALDRICH
Sodium Hydroxide	NaOH	≥98%	UNIVAR
Hydrochloric acid	HCl	37%	Merck
Octadecyldimethyl (3- trimethoxysilylpropyl) ammonium chloride	[(CH <sub>3</sub> O) <sub>3</sub> Si(CH <sub>2</sub> ) <sub>3</sub> N(CH <sub>3</sub> ) <sub>2</sub> (CH <sub>2</sub> ) <sub>17</sub> CH <sub>3</sub> ]Cl	42 wt% in methanol	ALDRICH

Sulfuric acid	$\text{H}_2\text{SO}_4$	95-97%	Merck
Nickel nitrate	$\text{Ni}(\text{NO}_3)_2 \cdot 6\text{H}_2\text{O}$	Assay 97.0%	UNILAB
Ammonium molybdate	$(\text{NH}_4)_6\text{Mo}_7\text{O}_{24} \cdot 4\text{H}_2\text{O}$	Assay 81.0- 83.0%	UNIVAR
Ammonium nitrate	$\text{NH}_4\text{NO}_3$	$\geq 98\%$	Italmar

## 4.2. Catalyst preparation

### 4.2.1. ZSM-5 (ZNwo) preparation

The ZNwo synthesis was performed in a stainless steel reactor line with PTFE under autogenous pressure at constant  $\text{SiO}_2/\text{Al}_2\text{O}_3$  ratio at 40, under  $220^\circ\text{C}$  for 24 hr.

The preparation of the ZSM-5 gel, first, 0.8 g. of Tetrapropyl ammonium bromide (TPABr) as a structure-directing substance was dissolved in 50 ml. DI water, 22.22 g. of Sodium silicate and 1.875 g. of Aluminium nitrate was dissolved in 20 ml DI water respectively. Second, the Si and Al precursors were added to TPABr solution drop by drop under vigorous stirring. Then, the pH of the mixture was adjusted to approximately 11 by the addition of 1 M HCl solution. The final mixture was further stirred for 30 minutes at room temperature to obtain the homogeneous mixture. The mixture then was transferred to a reactor. The reactor was heated hydrothermally to  $220^\circ\text{C}$  for 24 hr. The participated product was separated by centrifugation, washed with DI water until pH equal to neutral, dried at  $110^\circ\text{C}$  for 1 day and subsequently calcined in air at  $550^\circ\text{C}$  for 5 hr.

4.2.2. Modified ZSM-5 by adding mesoporous-directing agent with ZSM-5 source preparation (ZNco)

To synthesis ZNco 13.12 g. of Otadecyldimethyl (3-trimethoxysilylpropyl) ammonium chloride (ODAC) was added to the conventional ZSM-5 mixture. The important part is to adding 3.47 g. of ODAC solution drop by drop into TPABr solution while adding Si and Al precursors. The other steps were same as conventional ZSM-5 synthesis.

4.2.3. Modified ZSM-5 by adding mesoporous-directing agent after adding ZSM-5 source preparation (ZNpost)

To synthesis ZNpost 3.47 g. of Otadecyldimethyl (3-trimethoxysilylpropyl) ammonium chloride (ODAC) was added to the conventional ZSM-5 mixture. The important part is to adding 3.47 g. of ODAC solution into the final mixture after add Si and Al precursors and adjust the pH of solution. The other steps were same as conventional ZSM-5 synthesis.

4.2.4. ZSM-5 from rice husk ash and modified ZSM-5 by adding mesoporous-directing agent preparation (ZRco)

Rice husk ash (RHA) silica was prepared by leaching rice husk by 1 M HCl solution at 120°C for 3 hr. Then washing and dried at 110°C for 24 hr. To get white powder silica, the RHA was pyrolyzed at 700°C for 1 hr. in air. Next, 4.49 g. of the final powder was dissolved in a specific amount of NaOH solution to obtain the desire composition of sodium silicate solution.

When obtain the 50 ml of 27wt% of SiO<sub>2</sub> in NaOH solution. Sodium silicate solution was combined with 0.35 g. of sodium aluminate, 0.2531 g. of TPABr and 50 ml. of 0.001 M NaOH solution. The pH of the mixture was adjusted to approximately 11 by the addition of 1 M HCl solution. The final mixture was further stirred for 30 minutes at room temperature to obtain the homogeneous mixture. The mixture then was transferred to a reactor. The reactor was heated hydrothermally to 220°C for 24 hr. The participated product was separated by centrifugation, washed with DI water

until pH equal to neutral, dried at 110°C for 1 day and subsequently calcined in air at 550°C for 5 hr.

#### 4.2.5. ZSM-5 from TEOS and modified ZSM-5 by adding mesoporous-directing agent preparation (ZTco)

Synthesized hierarchical ZSM-5 as follows Verma [13] using 31.7 g. of tetraethyl orthosilicate (TEOS) and aluminium nitrate as Si and Al sources. The important part is to adding 3.47 g. of ODAC solution drop by drop into TPABr solution while adding Si and Al precursors. The other steps were same as conventional ZSM-5 synthesis.

#### 4.2.6. NiMo supported on ZNwo, ZNco, ZNpost, ZRco and ZTco preparation

All supports were performed ion-exchange by stirred with 1 M  $\text{NH}_4\text{NO}_3$  solution 3 times, each time stirred for 2 hr., washed with DI water and calcined at 550°C for 5 hr., to get HZNwo, HZNco, HZNpost, HZRco and HZTco before impregnate with Ni and Mo. 5wt% of Ni and 18wt% were subjected to deposit on the supports by conventional impregnation. An aqueous solutions of  $(\text{NH}_4)_6\text{Mo}_7\text{O}_{24}$  and  $\text{Ni}(\text{NO}_3)_2$  were mixed with the supports, stirred for 8 hr., dried at 100°C and calcined in an air at 400°C for 1 hr.

All NiMo catalysts were presulfided using 4L/min total flowrate of 15vol% of  $\text{H}_2$  and 85vol% of  $\text{H}_2\text{S}$  stream at 430°C for 4 hr with 10°C/min of ramp rate. Then, cooled down with the  $\text{N}_2$  flow.



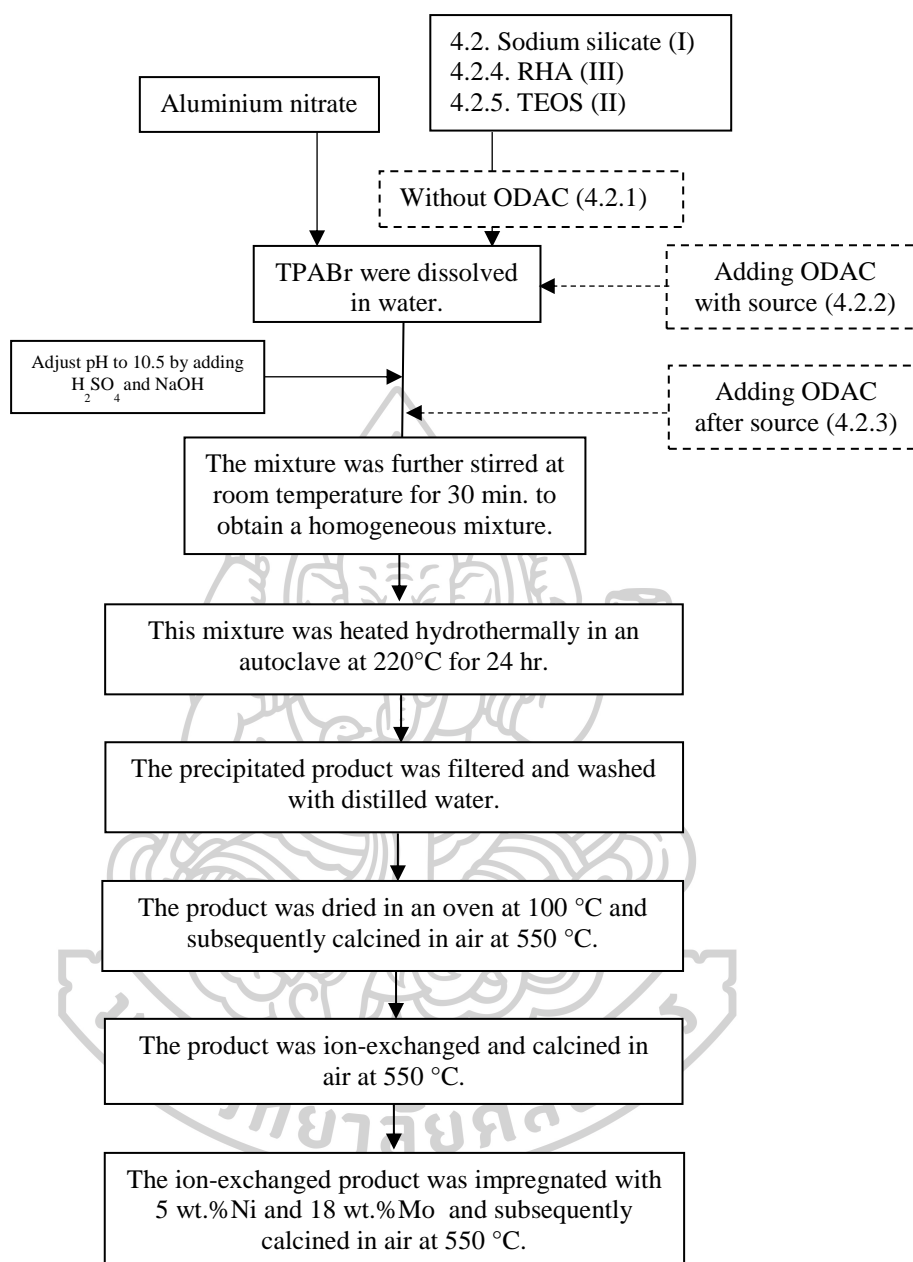


Figure 5 schematic of variation to the parameter in hydrothermal synthesis of ZSM-5 supports. Path 4.2.1 was ZSM-5 synthesis without mesoporous modification (ZNwo). Path 4.2.2 was ZSM-5 synthesis with added mesoporous directing agent with Si source (ZNco). Path 4.2.3 was ZSM-5 synthesis with added mesoporous directing agent after added Si source (ZNpost).

### 4.3. Catalyst Characterization

All ZSM-5 supports were characterized by X-ray Diffraction with  $5^\circ - 80^\circ$  range of  $2\theta$ , Siemens D5000, in order to obtain XRD patterns representing ZSM-5 framework.

Catalyst morphology were investigated with a scanning electron microscopy (SEM) which was JEOL model JSM-5410LV.

The nitrogen adsorption-desorption was examined in BELsorp instrument (BEL japan) to determine surface area pore volume and pore diameter.

Acidic property of supports were determined by ammonia – temperature program ( $\text{NH}_3$  -TPD) desorption method (Micromeritics Chemisorb 2750 Pulse Chemisorption System). The condition was  $550^\circ\text{C}$  at ramp rate of  $10^\circ\text{C}/\text{min}$  to desorb ammonia.

The used catalyst was investigated by thermogravimetric analysis (TGA). The sample was heated up to  $1000^\circ\text{C}$  with the ramp rate of  $10^\circ\text{C}/\text{min}$  to determine coke deposited on catalyst.

### 4.4. Catalyst activity

The catalyst activities were tested in hydroprocessing reaction, which was conducted in stainless steel batch reactor. For each batch, 1 g. of catalyst and 2 ml. of the feed of palm fatty acid distillate (PFAD) were loaded in the reactor. The liquid product from the reactor was collected and analyzed by FID detector, the Shimadzu 14B gas chromatography equipped with an Agilent DB-2887 column,  $30\text{ m}\times 0.25\text{ mm}$  and GC-MS (Shimadzu QP2010) equipped with a capillary column (Rtx-5MS,  $30\text{ m}\times 0.25\text{ mm}$ ) and MS detector. The gas product from the reactor was collected and analyzed by TCD detector, the Shimadzu 14B gas chromatography equipped with a Poropak Q column,  $30\text{ m}\times 0.25\text{ mm}$ .

## CHAPTER 5

### RESULTS AND DISCUSSION

In this chapter, NiMo metal supported on different ZSM-5 was investigated to estimate the activity of the catalyst including conversion and yield of jet fuel using PFAD as feedstock. In addition, the effect of hydrotreated parameters including reaction temperature, reaction time were also studied to obtain optimal condition for high yield of jet fuel. Nevertheless, characterization of ZSM-5 supports were discussed in this chapter. In order to determine the characteristics of zeolite support, ZSM-5 were analyzed by the X-ray diffraction (XRD) for determine the characteristic of support and type of crystal form, the scanning electron microscopy (SEM) and Transmission Electron Microscope (TEM) to study the morphology, nitrogen adsorption-desorption isotherm to study the textural and ammonia temperature program desorption for study the acidity of ZSM-5. Generally, many researchers studied hierarchical ZSM-5 synthesis by using TEOS as a Si source, aluminium nitrate as a Al source, TPABr as an organic template cation and amphiphilic organosilane as a mesoporous directing agent [13, 28, 42]. Their raw materials are efficient precursor to obtain high crystalline ZSM-5 but it has a drawback in economic due to high raw material cost. Sodium silicate is one of silica forms which can produce by using cheap raw materials like rice husk ash (RHA). RHA is a waste product from rice industry. Hence, Sodium silicate was used to replace TEOS as a Si source in the synthesis and using ODAC to adjust the morphology of zeolite. Synthesized ZSM-5 using sodium silicate with ODAC was successfully in the research. Led to synthesize ZSM-5 from sodium silicate which was leached form RHA.

#### 5.1. Characterization of ZSM-5 supports

Figure 6. showed the XRD pattern of ZSM-5 samples that were used a different silica sources, TEOS, sodium silicate and rice husk ash. All samples showed the XRD pattern indicated that ZSM-5 phase existed and corresponding to the MFI structure. The patterns showed the characteristic diffraction peaks at  $2\text{-theta} = 7.89^\circ$ ,

8.73°, 23.04°, 23.86° and 24.26° Figure 6 a. shows only ZSM-5 phase. But, Figure 6 b. and Figure 6 c. which added ODAC as a mesoporous directing agent showed less intensity because the formation of mesoporous structure. This result was similar with Xu et al. and Lei et al. It suggested that amorphous aluminosilicate walls were not completely converted into MFI structure. According to this wall, there were more spaces for large molecule to access in active site of the catalyst [43-45]. From the Figure 6 b and c, it showed only main peak of silica quartz at 26.6° of 2-Theta. This quartz presented only in ZSM-5 sample which added ODAC as a mesoporous directing agent. It should be due to a metastable phase in zeolite. During the crystallization process of ZSM-5, the metastable phase could develop to quartz, which was the most stable phase of silica [46, 47]. It should notice that there are no quartz in ZTco sample (Figure 6 d.) which synthesized using TEOS as Si source and added ODAC. The effect of Si source between TEOS and sodium silicate was ascribed to the nucleation and crystal growth of ZSM-5 which were more quickly when using monomeric silica source, such as fumed silica, colloidal silica and TEOS, than using condensed Si source, such as sodium metasilicate. Therefore, using TEOS as a Si source had a good effect to synthesized ZSM-5 [48]. Metastable phase in zeolite could be also saw when using rice husk ash (RHA) as a silica source in Figure 6 e. In this sample, cristobalite and SSZ-13 were found in XRD pattern. Cristobalite is the Si phase that present in the RHA before and Cristobalite phase will disappear while ZSM-5 phase will form during hydrothermal process. It was interesting that SSZ-13 was found in this sample. SSZ-13 was the chabazite (CHA) zeolite of aluminosilicate with 8-membered ring openings connected with large cavities. CHA zeolite was interesting used in methanol to olefin reaction due to the advantage of lower deactivation rate and lower temperature reaction than SAPO-34. The differences of SSZ-13 and SAPO-34 were that the SSZ-13 is an aluminosilicate which has Al as the heteroatom but SAPO-34 is silicoaluminophosphates which has Si as a heteroatom [49-51]. From Wu studied, he found that ZSM-5 phase presented as a competing phase in SSZ-13(TPOAC, 0.08) sample [51].

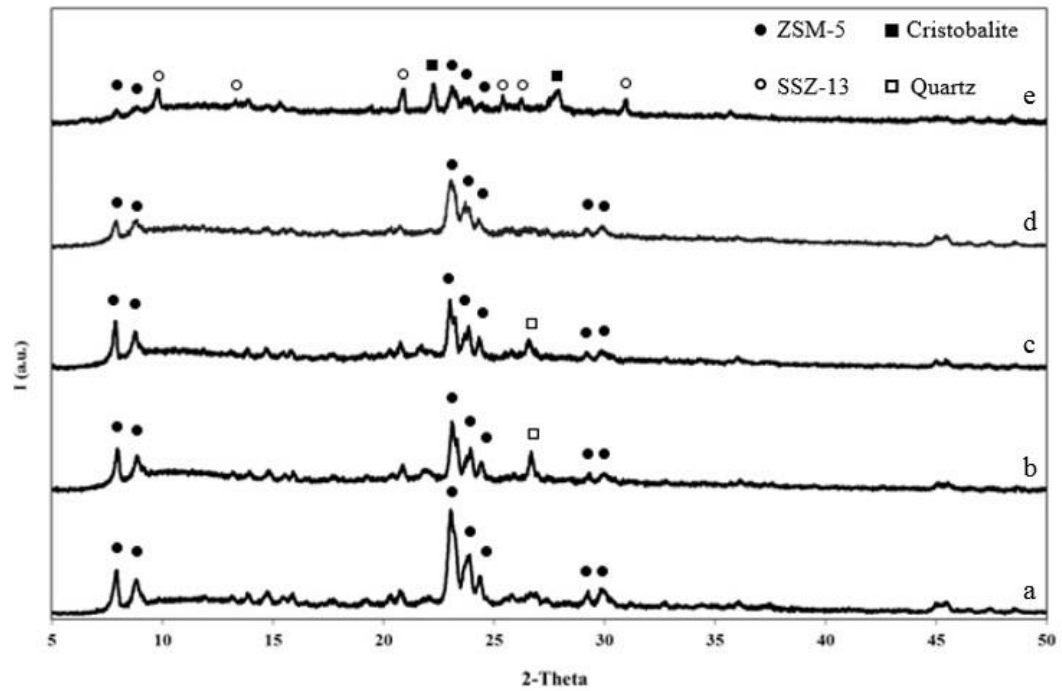


Figure 6. XRD pattern of ZSM-5 synthesized by using (a) Sodium silicate (ZNwo), (b) Sodium silicate and add ODAC with Si sources (ZNco), (c) Sodium silicate and add ODAC after add Si source (ZNpost), (d) TEOS and add ODAC with Si sources (ZTco). And (e) rice husk ash and add ODAC with Si sources (ZRco).



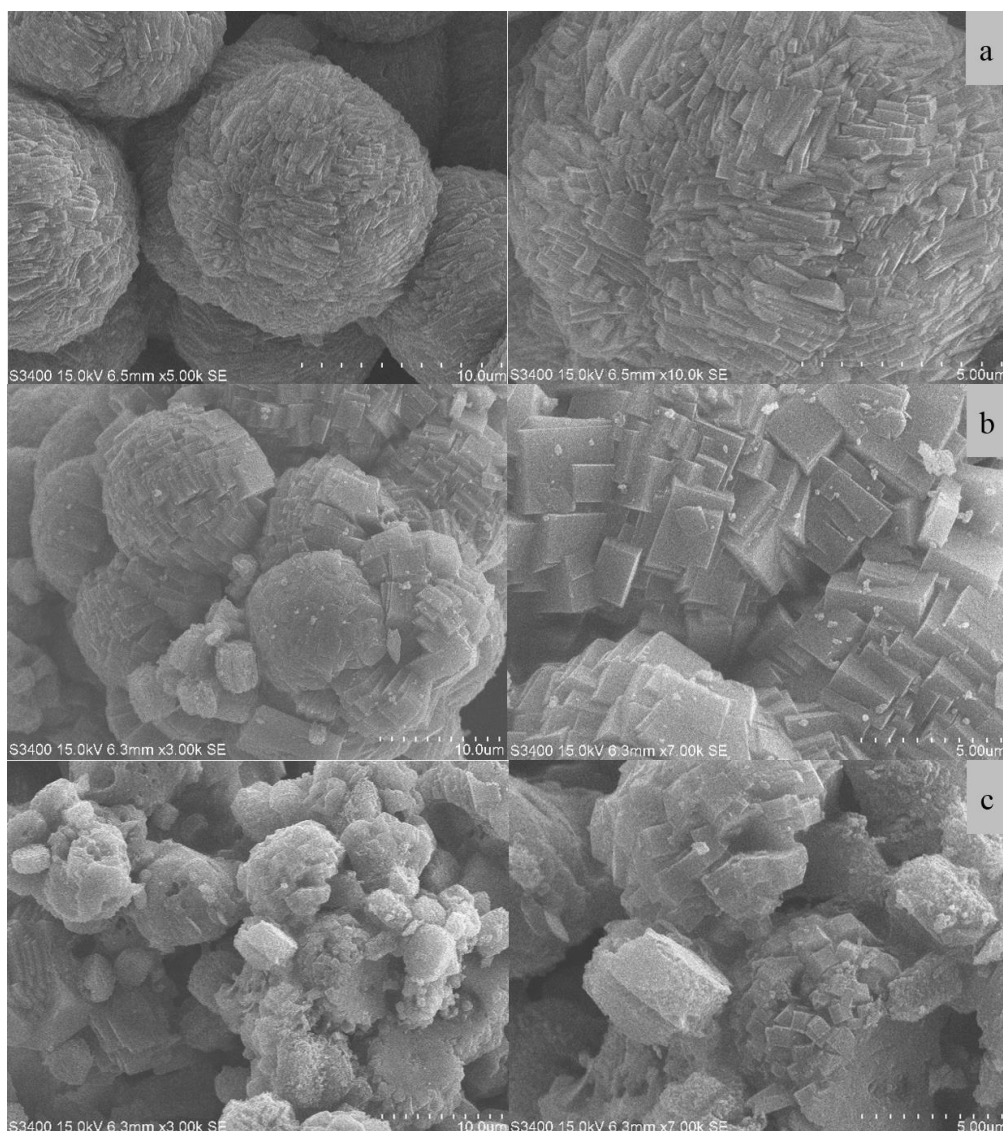


Figure 7. SEM images for the major morphology of ZSM-5 using (a) Sodium silicate (ZNwo), (b) Sodium silicate and add ODAC with Si sources (ZNco), (c) Sodium silicate and add ODAC after add Si source (ZNpost)

The SEM photographs of ZSM-5 supports were shown in Figure 7. The ZSM-5 products were mainly cubical structure agglomerated to form spheroidal crystal. Moreover, ZSM-5 without mesoporous directing agent had cubical structure agglomerated to form sphere with very uniform shape and not show flake crystal or other amorphous crystalline impurities. The ZSM-5 modified with mesoporous directing agent showed the same appearance with some solid fragments. This characteristic was similar to Chareonpanich et al, Armaroli et al., Shirazi et al., and Shetti et al. All images indicated that there are intergrowth, aggregation and

amorphous substance impurity [23, 42, 52, 53]. SEM image of ZSM-5 with addition of ODAC after added Sodium silicate showed in Figure 7 c. suggested that the coarse agglomerated ZSM-5 crystals were appeared. Based on SEM images observation, addition of ODAC after added Sodium silicate led to get the ZSM-5 with more amorphous and coarser ZSM-5 crystal.

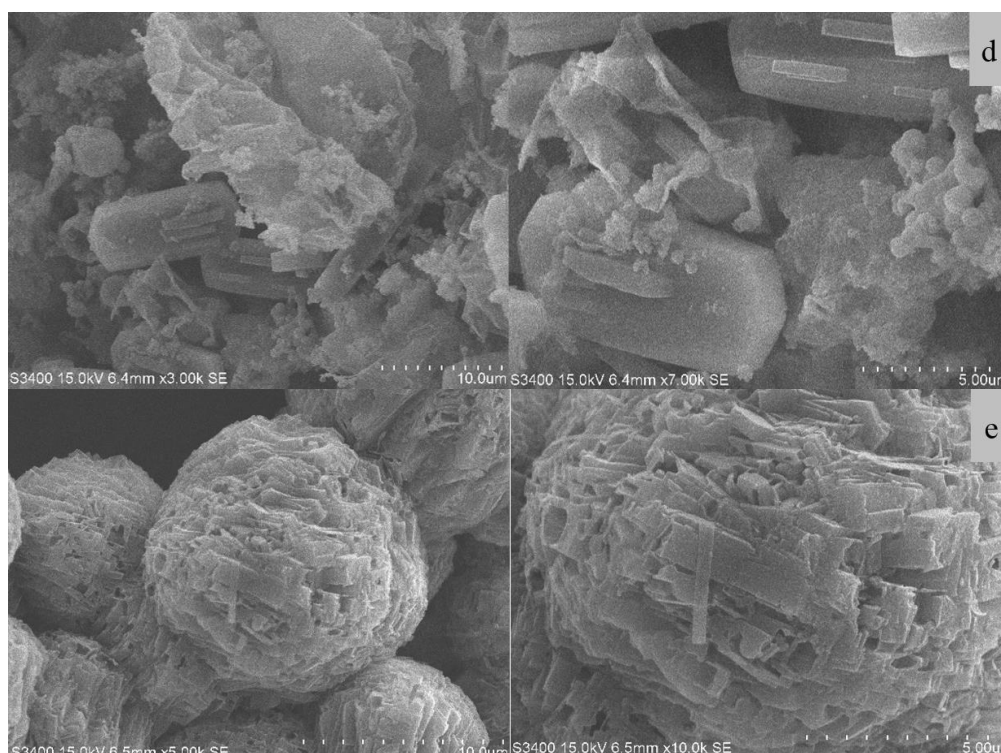


Figure 8. SEM images of ZSM-5 synthesized from TEOS and add ODAC with Si sources (ZTco). And (e) rice husk ash and add ODAC with Si sources (ZRco)

The SEM photographs of the zeolite products of different Si sources using TEOS and RHA were showed in Figure 8 d. and e. ZSM-5 sample using TEOS as Si source showed slight difference of crystal shape. On the other hand, this sample showed the typical MFI hexagonal morphology of ZSM-5 crystal with the partially amorphous structure because addition of mesoporous directing agent. From SEM image of ZSM-5 using RHA as Si source revealed that the morphologies of the solid seem to be very spongy and agglomerated but the particles were sphere without impurity fragments.

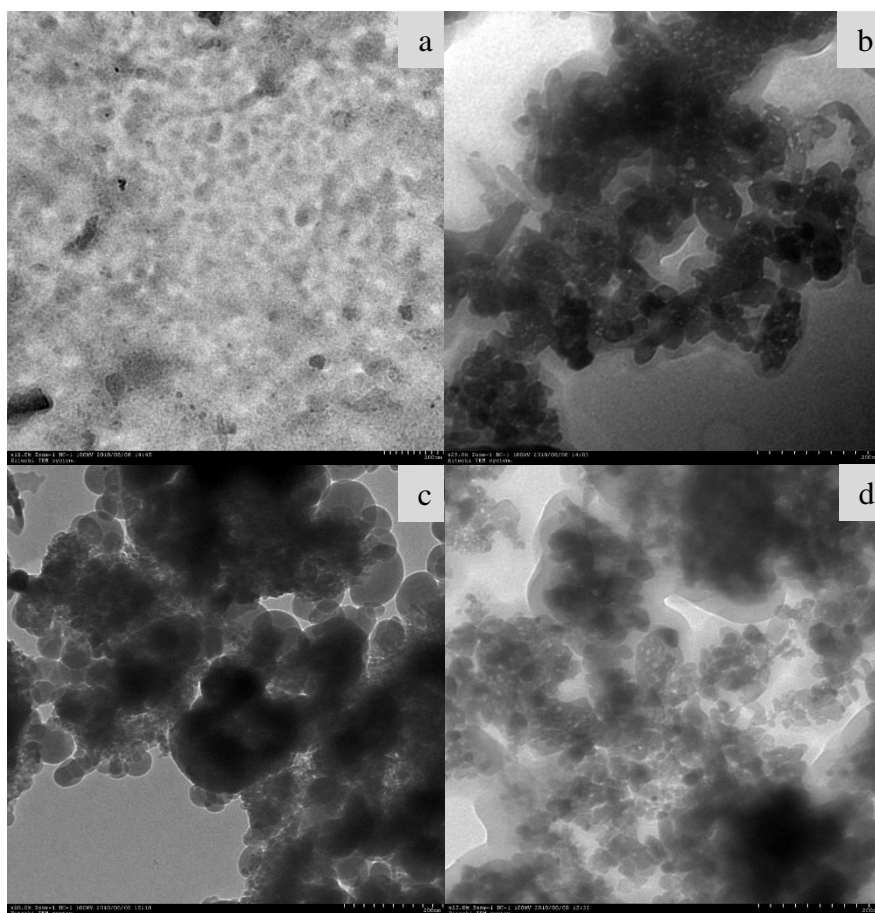


Figure 9. TEM images of catalysts at 200 nm. (a) ZNwo, (b) NiMo/ZNwo, (c) NiMo/ZNco and (d) NiMo/ZNpost

The TEM images of catalysts at 200 nm were showed in Figure 9. In Figure 9 a., ZNwo without metal loading was clearly no dark spot which represent the metal deposit on the support. Moreover, the modified ZSM-5 with mesoporous directing agent in Figure 9 c and d. presented the agglomerate ZSM-5 particle by small ZSM-5 unit. Figure 9 b, c, and d. present NiMo loading on ZSM-5 support. The impregnated catalysts indicated that Ni particles were located on the external surface. However, in the modified ZSM-5 supports (Figure 9. C and d.) Ni particle were obviously within the secondary porosity of agglomerated ZSM-5 which had better dispersion of Ni metal. The size of round dark spot of Ni metal is in the 10 – 50 nm. On the other hands, The Mo species almost located inside the pore system of ZSM-5. Mo metal was small particle and highly dispersed on the supports [40, 45, 54].



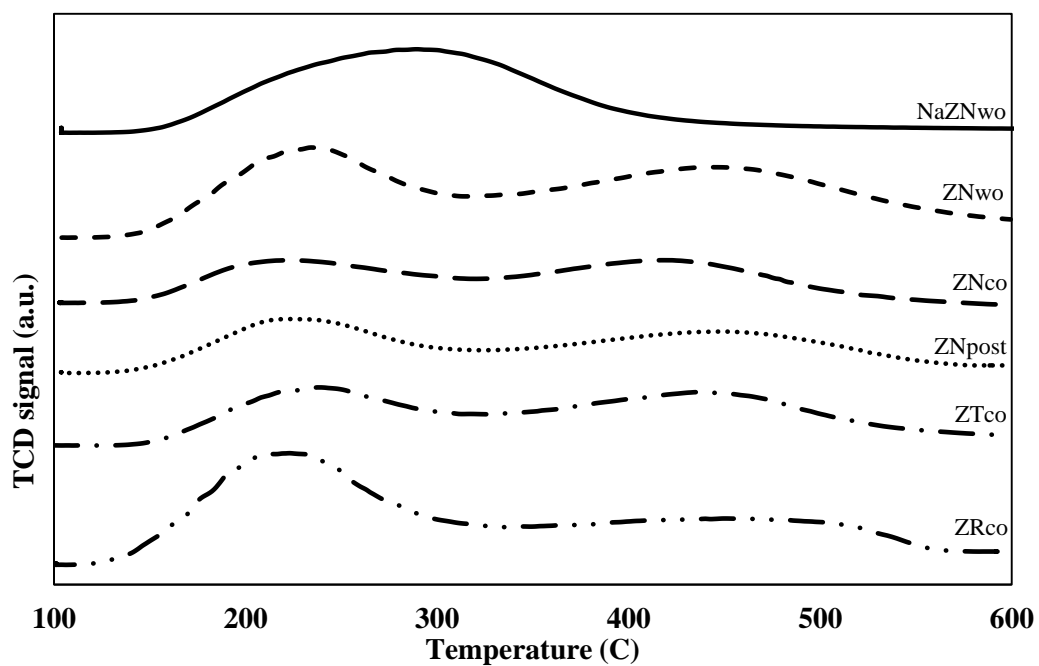


Figure 10. NH<sub>3</sub>-TPD profiles of NaZNwo, ZNwo, ZNco, ZNpost ZTco, and ZRco.

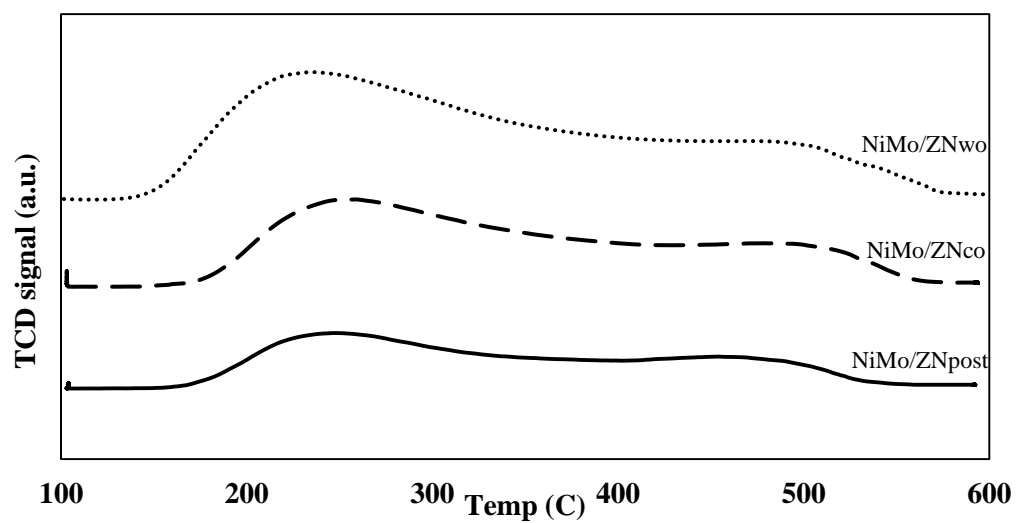


Figure 11. NH<sub>3</sub>-TPD profiles of NiMo/ZNwo, NiMo/ZNco and NiMo/ZNpost

Table 3. Acidity of ZSM-5 supports determined by temperature programmed desorption of ammonia

Acid site					
Catalyst	T < 300°C		T > 300°C		Total acid site mmol NH <sub>3</sub> /g
	mmol NH <sub>3</sub> /g	T (°C)	mmol NH <sub>3</sub> /g	T (°C)	
NaZNwo	1.102	289.9	-	-	1.102
ZNwo	0.505	233.9	0.795	445.5	1.300
ZNco	0.400	224.6	0.511	439.5	0.911
ZNpost	0.403	223.3	0.535	450.2	0.938
ZTco	0.490	239.1	0.527	447.6	1.017
ZRco	0.598	225.4	0.535	460.3	1.133
NiMo/ZNwo	0.752	220.9	0.289	469.7	1.041
NiMo/ZNco	0.481	234.2	0.291	464.5	0.772
NiMo/ZNpost	0.400	222.6	0.292	475.1	0.692

Figure 10., Figure 11. and table 3. showed acidic properties of ZSM-5 supports. The amount and strength of the acid sites on various ZSM-5 supports were investigated using the temperature programmed desorption of ammonia. Figure 10. demonstrated NH<sub>3</sub>-TPD peak profile of ZSM-5 supports. The peaks profile revealed two main NH<sub>3</sub> desorption peaks. The first peak appeared at lower 300°C region corresponding to weak acid site. The second peak appeared at higher 300°C region corresponding to strong acid site, respectively. The weak acid sites were accounted for the acidic structure of Si-OH-Si group, in another case, the strong acid sites were claimed to the acidic structure of Si-OH-Al group. To compared the acidity distribution of supports. Fityk program was used to deconvolute the two peaks to calculate the ammonia amount of weak and strong acid by using Gaussian function as shown in Table 3. The NaZSM-5 presented the highest amount of total acidic sites. And this amount started to decrease when impregnated metal on the support. In consequence, the incorporation of Ni and Mo affected both the amount acid site and maximum temperature of NH<sub>3</sub>-TPD. The results revealed the impregnation with Ni and Mo decreased both the amount of strong acid sites and desorption temperature shifted to lower region. Moreover, the increasing of weak acid sites were attributed to the formation of new weak acid sites by NiMo species. However, the addition of ODAC as a microporous directing agent can cover the acid sites and make the desorption peak shifted to lower temperature [55]. The other reason for the reduction of acid sited on the modified ZSM-5 support using mesoporous directing agent was that the acid sites located on external surface of mesoporous structure had lower acid strength than acid sites on microporous structure. These result suggested that the reduction of total acid sites of modified ZSM-5 could ascribed to the loss of acid framework and formation of mesoporous structure [56].

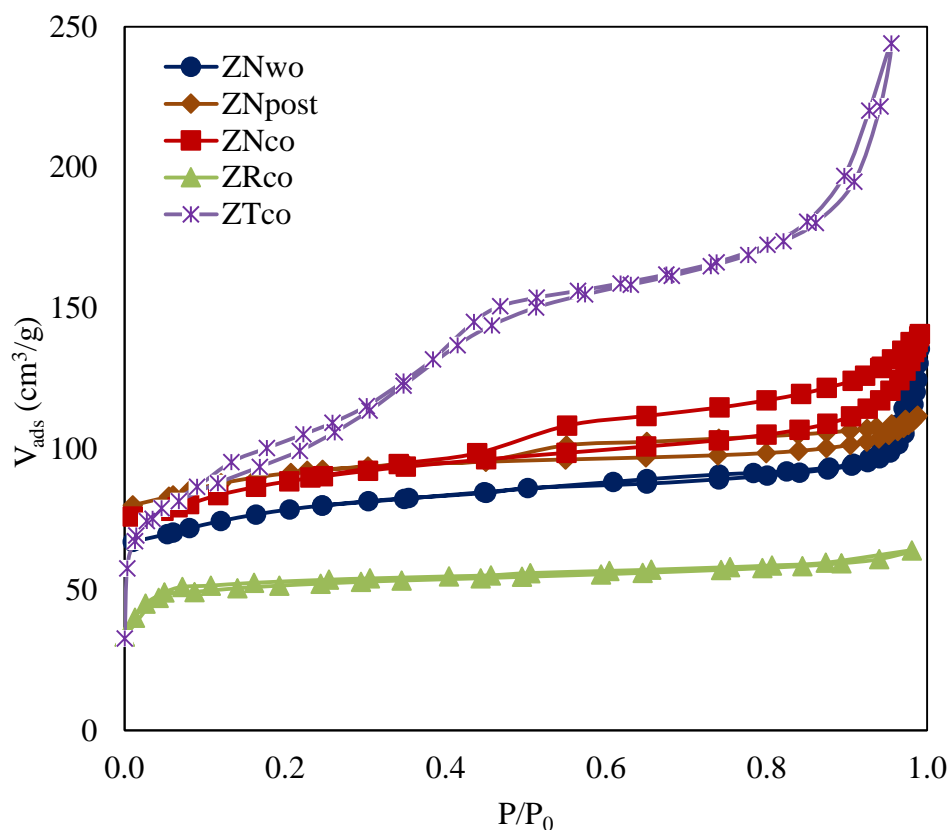


Figure 12. Nitrogen adsorption – desorption isotherm of ZSM-5 supports with different Si source and modified with ODAC as a mesoporous directing agent

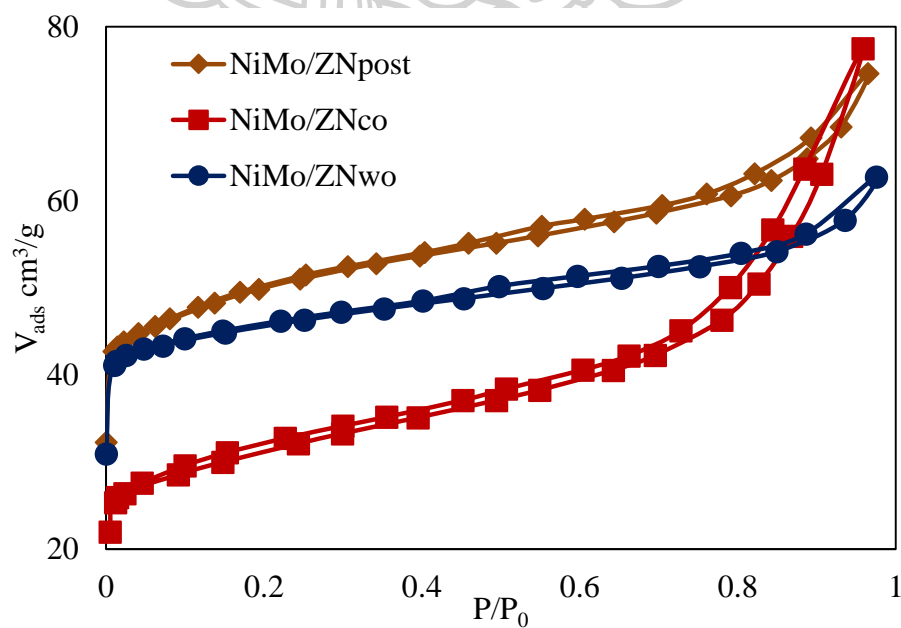


Figure 13. Nitrogen adsorption – desorption isotherm of NiMo impregnated on ZSM-5 and modified ZSM-5 with ODAC

Table 4. Textural properties of the samples

Sample	$S^a_{\text{BET}}$ ( $\text{m}^2/\text{g}$ )	$V^b_{\text{total}}$ ( $\text{cm}^3/\text{g}$ )	$V^c_{\text{micro}}$ ( $\text{cm}^3/\text{g}$ )	$V^d_{\text{meso}}$ ( $\text{cm}^3/\text{g}$ )	$D^e$ (nm)
ZNwo	248	0.162	0.137	0.025	3
ZNpost	284	0.224	0.179	0.045	3.7
ZNco	281	0.204	0.160	0.044	3.6
ZRco	140	0.11	0.084	0.026	3.3
ZTco	345	0.49	0.189	0.301	4.4
NiMo/ZNwo	125	0.109	0.075	0.034	
NiMo/ZNpost	118	0.127	0.076	0.051	
NiMo/ZNco	128	0.120	0.034	0.086	

<sup>a</sup> Specific BET surface area obtained from nitrogen adsorption isotherm.

<sup>b</sup> Total pore volumes obtained at  $P/P_0 = 0.95$ .

<sup>c</sup> Measured by MP plot method.

<sup>d</sup>  $V_{\text{meso}} = V_{\text{total}} - V_{\text{micro}}$

<sup>e</sup> Average pore diameters obtain form BET method

The nitrogen adsorption-desorption isotherm for all samples showed in Figure 12., Figure 13. and Table 4. BET results indicated that ZSM-5 synthesized with sodium silicate as Si source showed combination of Type I and type IV adsorption-desorption isotherm as showed in Figure 12. Moreover, the adsorption-desorption at low relative pressure appeared to be nearly horizontal typical for nitrogen adsorbed inside micropore and there was significant hysteresis loop at relative pressure higher than  $P/P_0 = 0.4$ , denoting the presence of mesoporous structure in the ZSM-5. The numerical data of ZSM-5 presented in Table 4. The specific BET surface area of supports is approximately 250 to 290  $\text{m}^2/\text{g}$  and average pore diameters were around 3 nm. Thus, to synthesize ZSM-5 using sodium silicate as Si source yielded ZSM-5 with mesoporous structure. The presence of a mixture of ZSM-5 crystal and amorphous structure on ZSM-5 synthesized with TEOS as Si source led to have nonuniform pore structure. The shape of the isotherm of ZTco showed that there were three steps of adsorption with hysteresis loop. This was suggested that there was mesoporous in the support with many pore type structures to adsorb nitrogen in three steps. This ZTco also had the highest specific BET surface area and volume of mesoporous as showed in Table 4. ZSM-5 synthesized with RHA as Si source had the lowest specific BET surface area and the nitrogen adsorption-desorption isotherm revealed that there was mostly microporous structure.

The specific surface area obtained by BET analysis and total pore volume especially the volume of mesopore of ZSM-5 modified with ODAC as a mesoporous directing agent slightly increased. The characterization of addition Ni and Mo into ZSM-5 support analyzed by nitrogen adsorption-desorption were showed in Figure 13. The impregnated of NiMo led to specific BET surface area and total pore volume were significant decreased through partially filled up with metal particle. The blocking pore of metal lead to the major reduction volume of micropore as showed in Table 4.

## 5.2. Hydroprocessing of PFAD

The studies of reaction activity and yield were operated on hydroprocessing of PFAD over NiMo catalyst using different ZSM-5 as a support. First of all, Effect of pressure was studied due to finding the optimal operating pressure. The effect of pressure was studied at 10, 40 and 60 bar. Conversion of hydroprocessing increases to approximately 70% when increased pressure to 40 and 60 bar. However, yield of diesel was constant at every value of pressure. But yield of jet fuel and gasoline increased to the maximum at 40 bar and then constant although pressure was increased to 60 bar. According to the result, it was reasonable to choose the operating pressure at 40 bar for all experiments to obtain the suitable catalyst activity and yield. The effect of operating pressure on conversion and yield was shown in Figure 11.

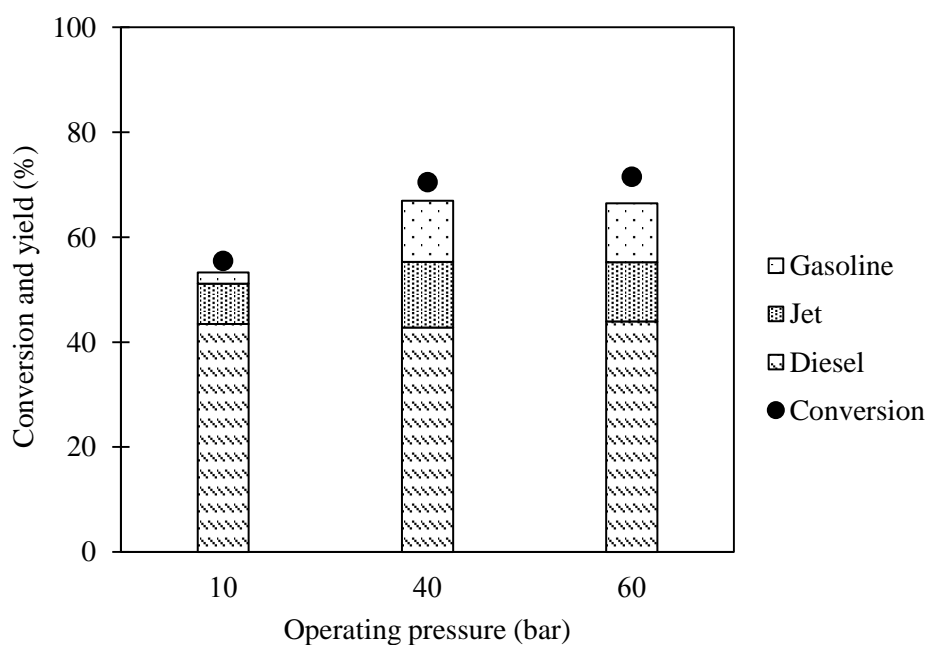


Figure 14. The effect of operating pressure on conversion and yield of NiMo/ZNco at operating temperature = 360°C and reaction time = 1 h

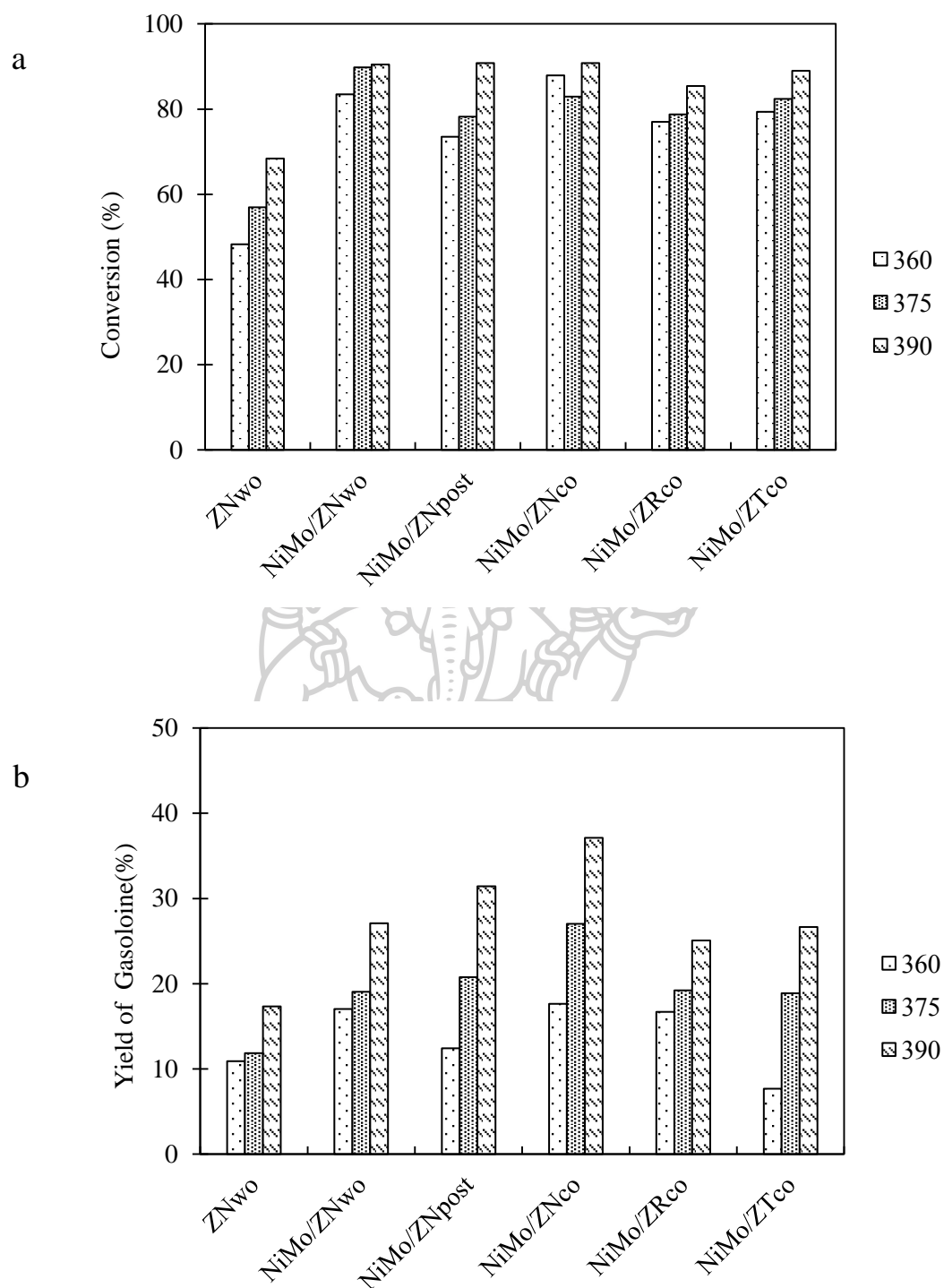


Figure 15. The effect of operating temperature on conversion (a) and yield of gasoline (b) of all catalysts (operating pressure = 40 bar and reaction time = 2 h)



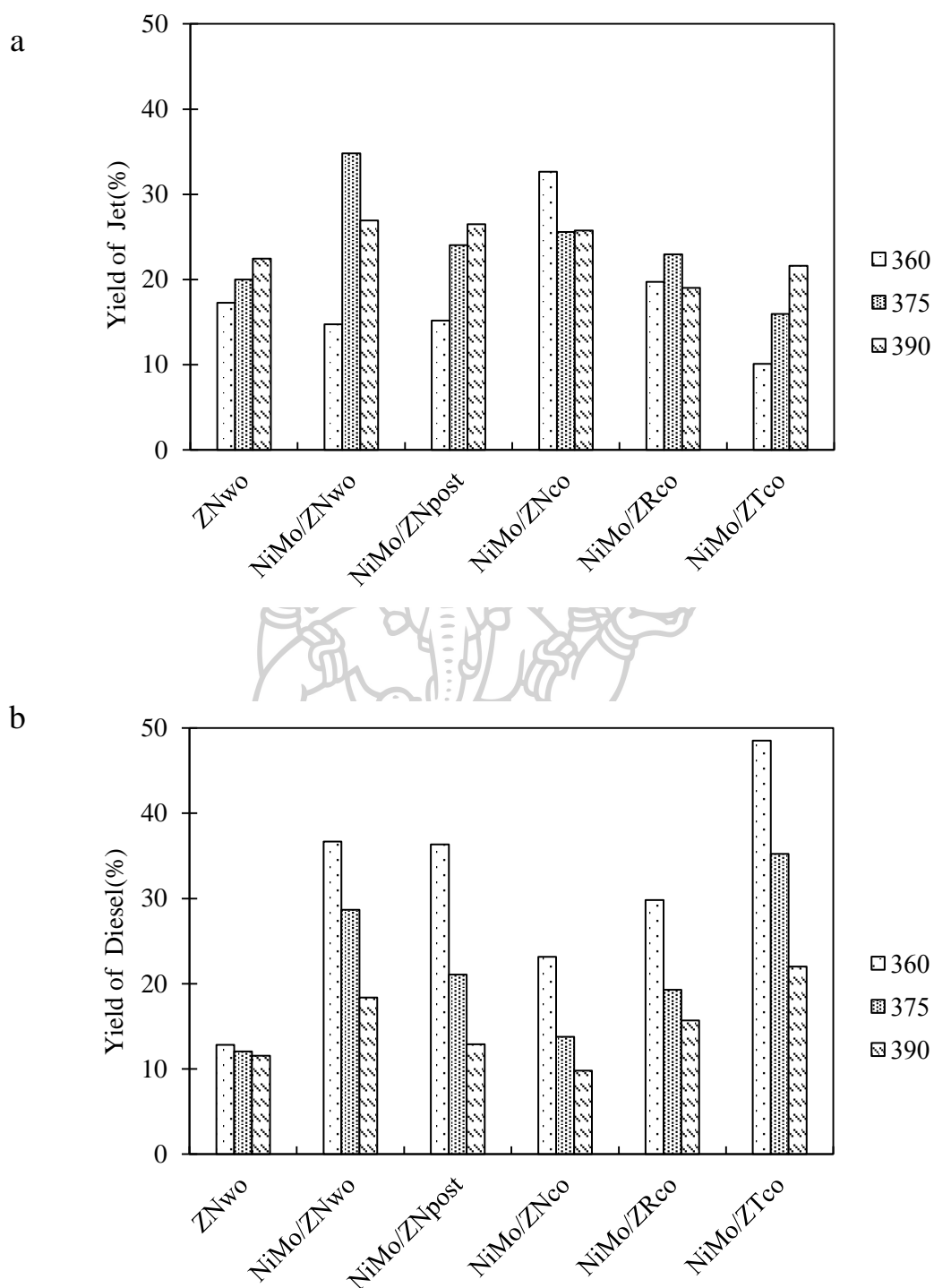


Figure 16. The effect of operating temperature on yield of jet fuel (a) and yield of diesel (b) of all catalysts (operating pressure = 40 bar and reaction time = 2 h)

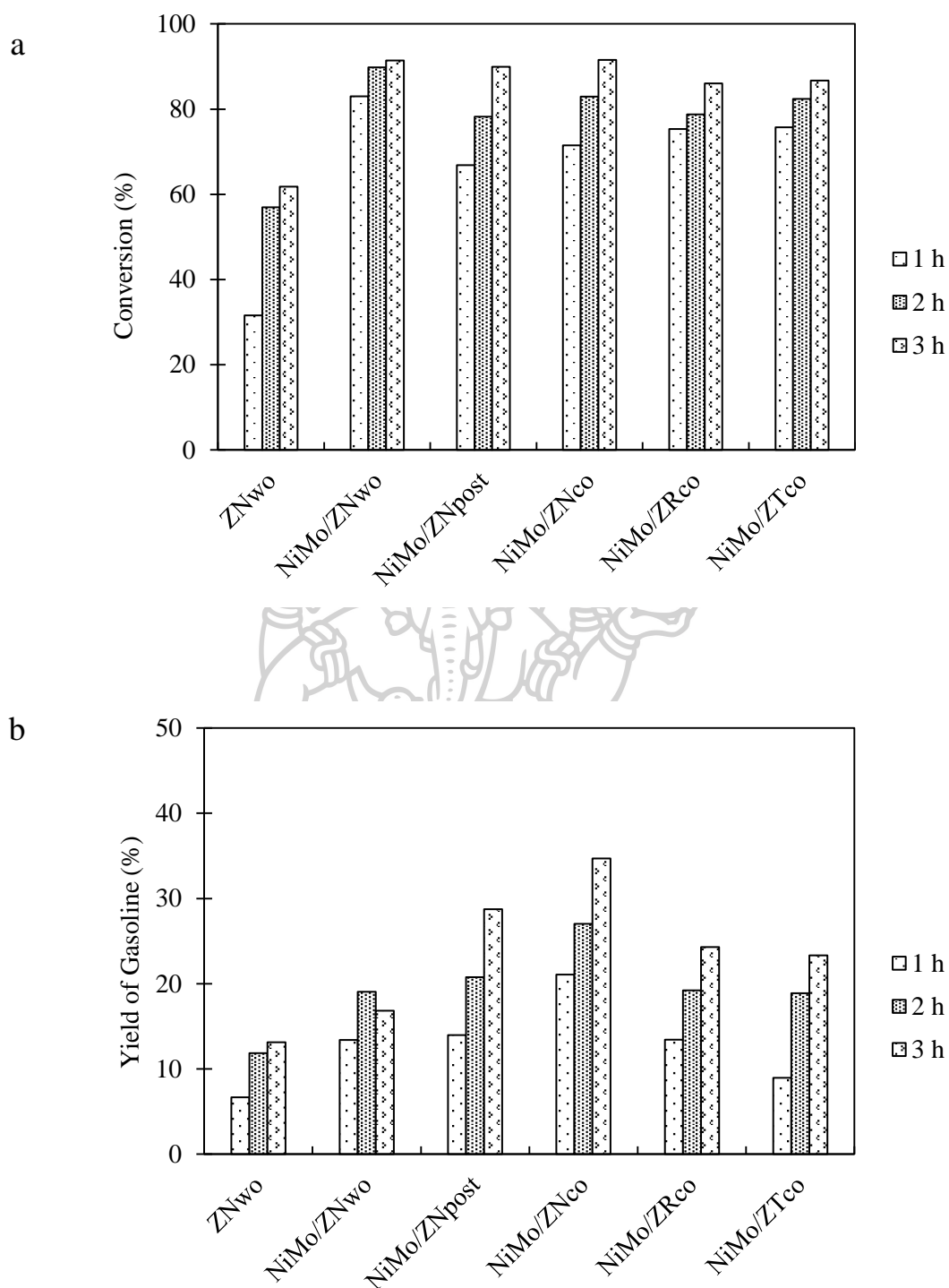


Figure 17. The effect of reaction time on conversion (a) and yield of gasoline (b) of all catalysts (operating pressure = 40 bar and operating temperature = 375°C)

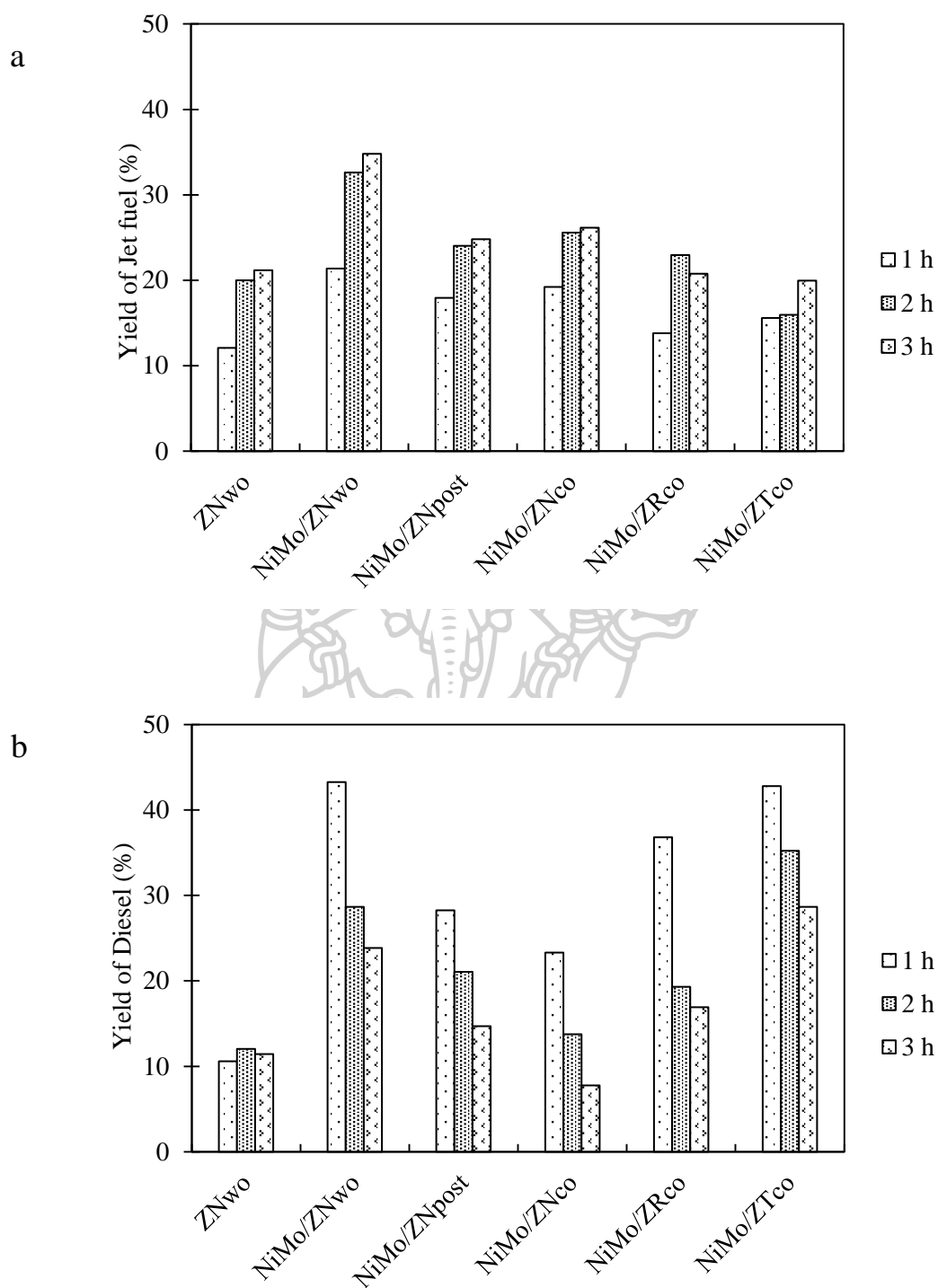


Figure 18. The effect of reaction time on yield of jet fuel (a) and diesel fuel (b) of all catalysts (operating pressure = 40 bar and operating temperature = 375°C)

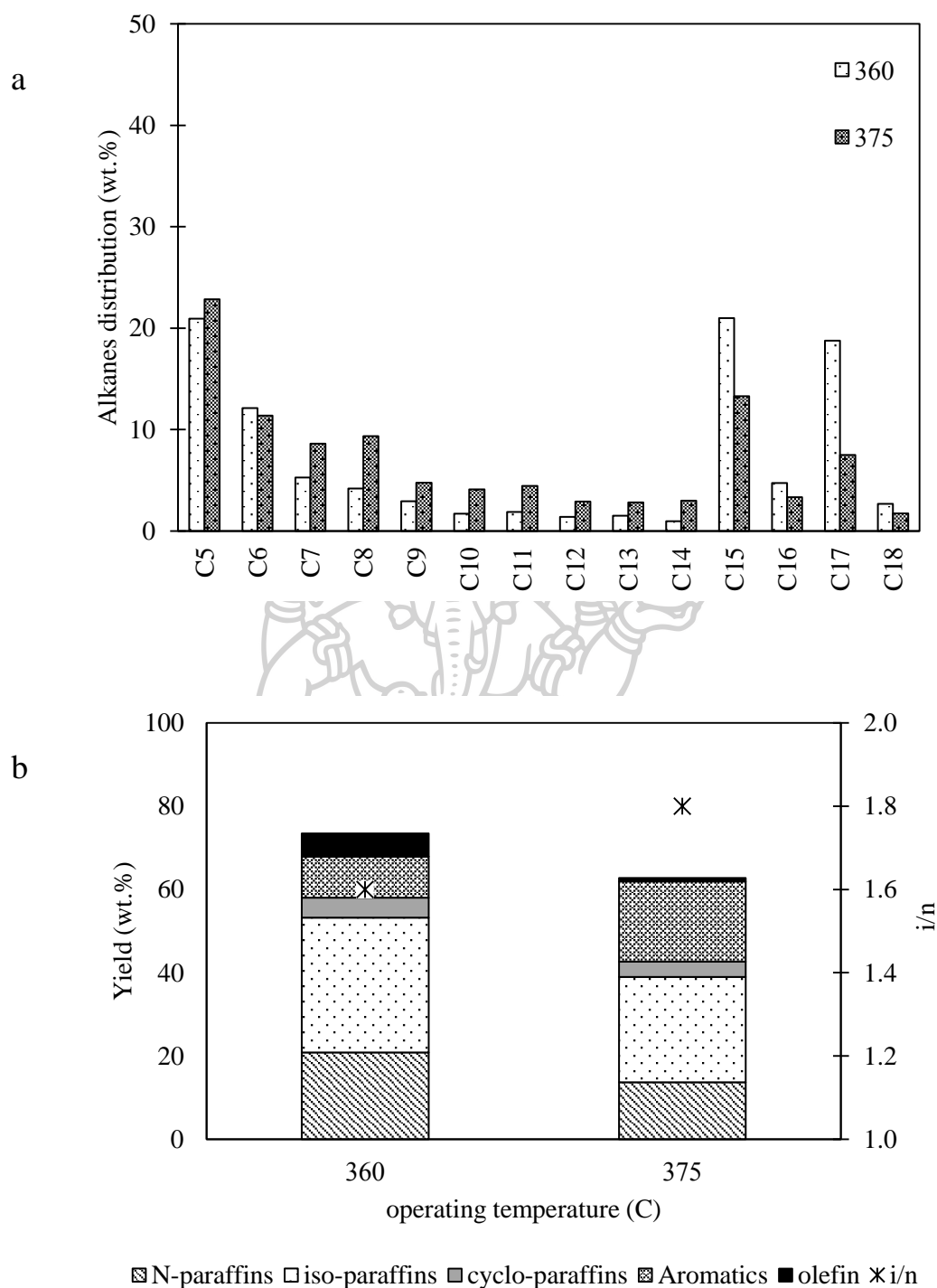


Figure 19. The effect of operating temperature on n-alkanes distribution (a), and hydrocarbon composition using NiMo/ZNco at operating temperature = 360°C and 375°C (b) (operating pressure = 40 bar and reaction time = 2 h)

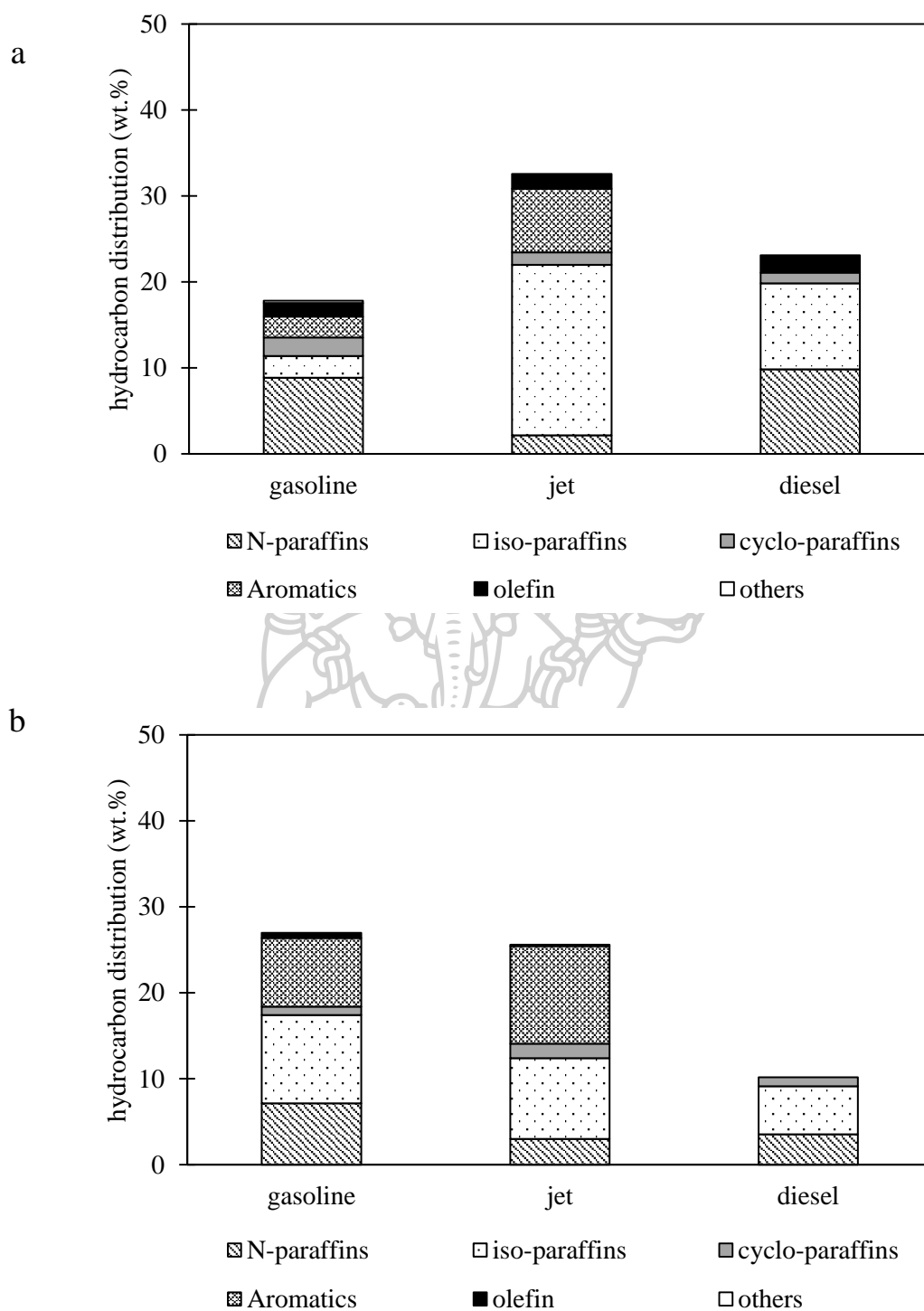


Figure 20. The effect of operating temperature on hydrocarbon distributions in gasoline, jet and diesel range using NiMo/ZNco at operating temperature = 360°C (a) and at operating temperature = 375°C (b) (operating pressure = 40 bar and reaction time = 2 h)

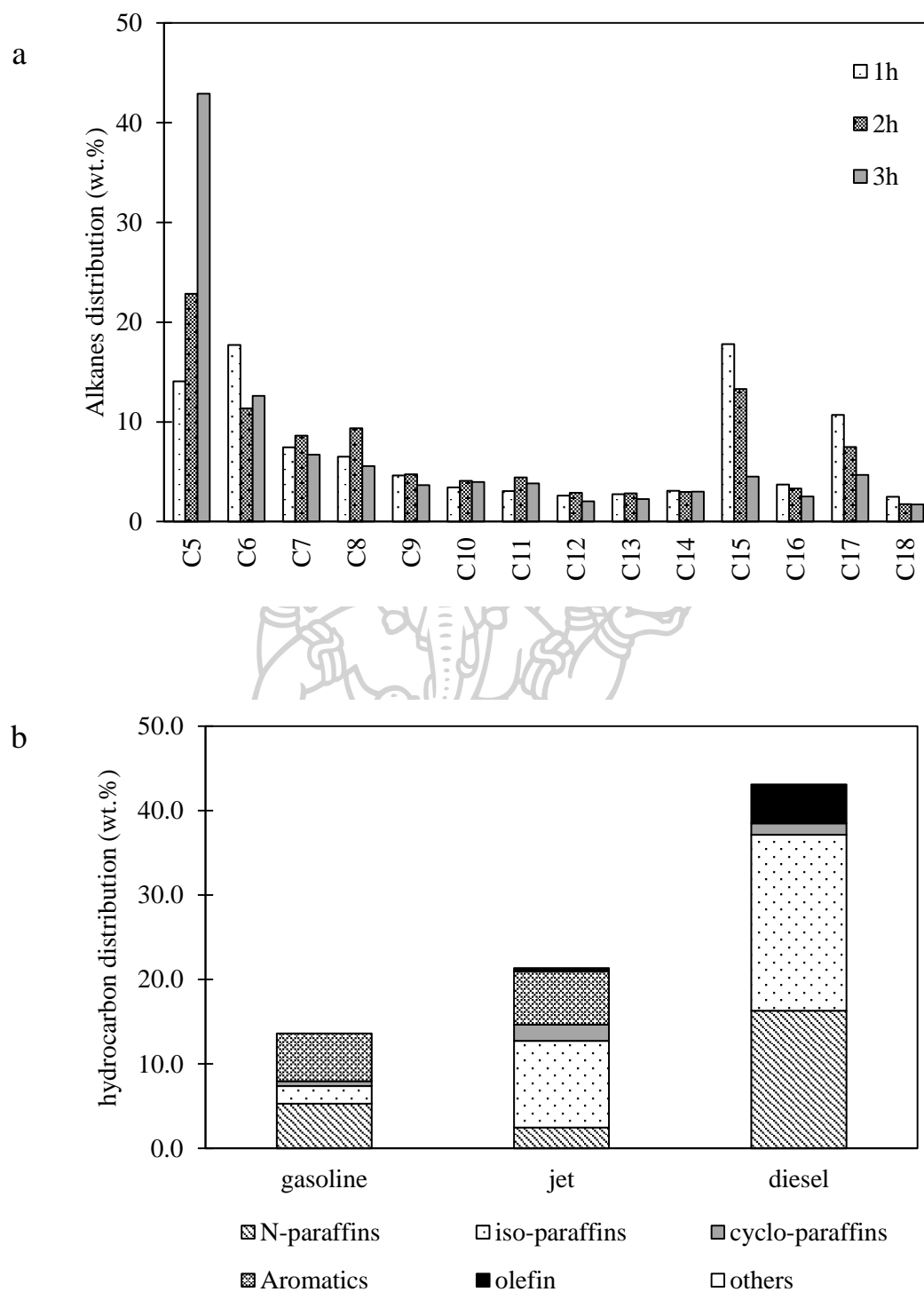


Figure 21. The effect of operating time on n-alkanes distribution (a), and hydrocarbon distributions in gasoline, jet and diesel range at reaction time = 1 h (b) using NiMo/ZNwo (operating pressure = 40 bar and operating temperature = 375°C )

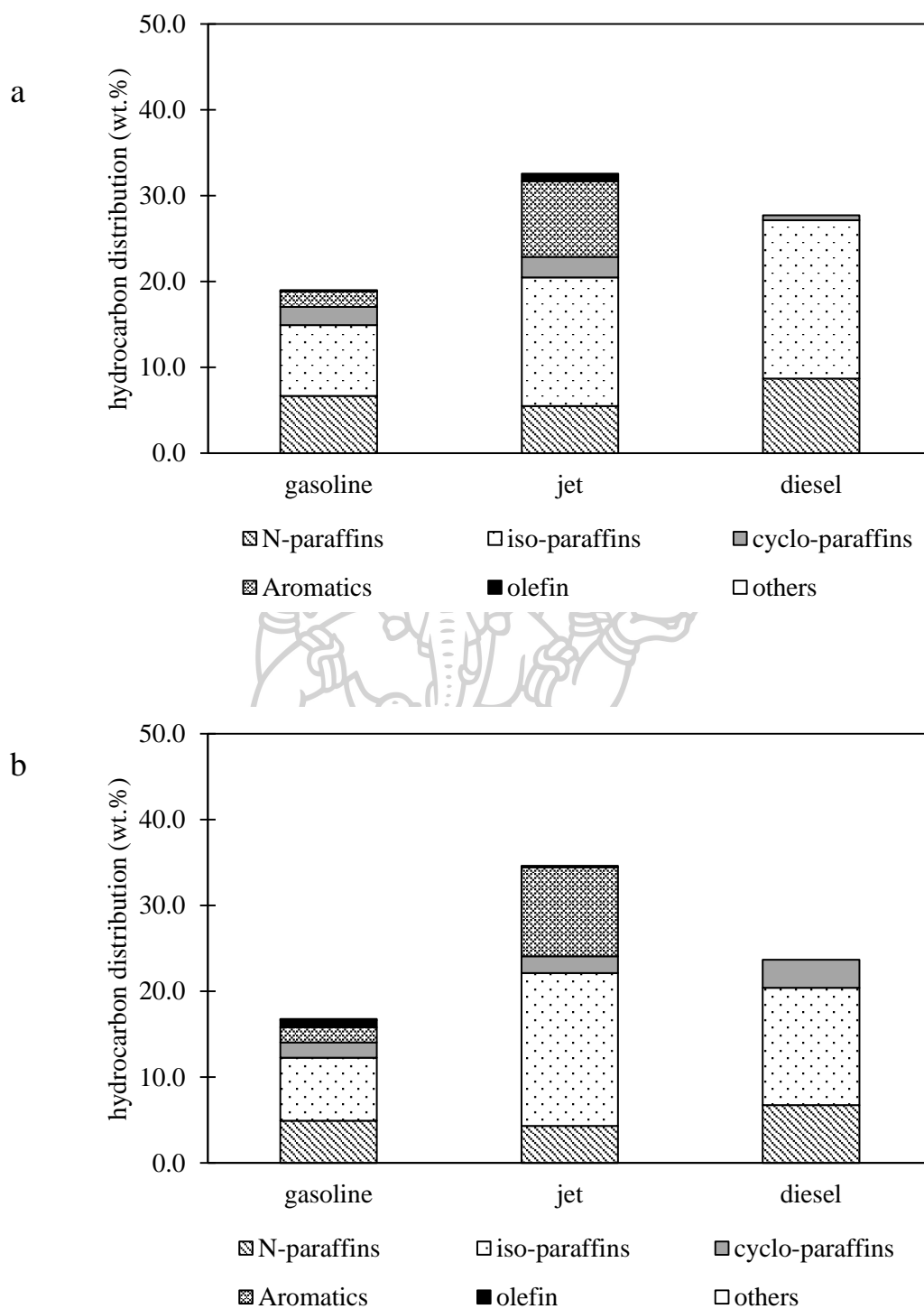


Figure 22. The hydrocarbon distributions in gasoline, jet and diesel range at reaction time = 2 h (a), and 3 h (b) using NiMo/ZNwo (operating pressure = 40 bar and operating temperature = 375°C )

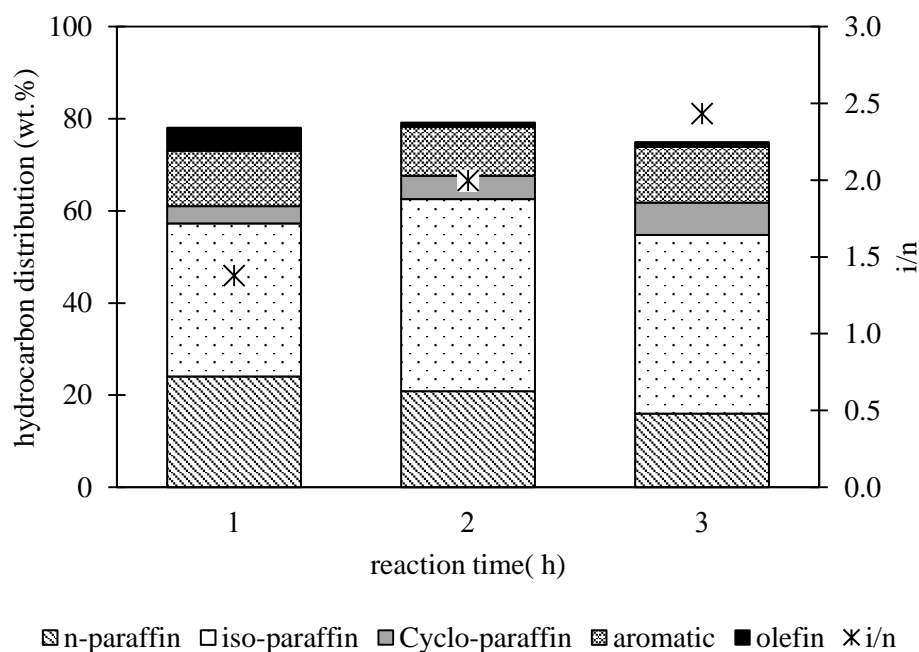


Figure 23. The effect of reaction time on hydrocarbon composition using NiMo/ZNwo (operating pressure = 40 bar and operating temperature = 375°C)

### 5.2.1. Effect of operating temperature and reaction time.

The effect of operation temperature was one of the most outstanding effect on conversion and product yield. The conversion of palm fatty acid distillate referred to the hydroprocessing activity and productiveness. The effect of reaction temperature was studying at 360°C, 375°C and 390°C. Figure 15. (a) and (b) showed the effect of reaction temperature on conversion (a) and yield of gasoline (b) of all catalysts. The conversion increased with an increasing reaction temperature. The increasing temperature was not only affected to the hydroprocessing activity but also the yield of gasoline. At higher reaction temperature, the yield of gasoline increased due to hydrocracking activity which is favored with temperature. The conversion and yield of gasoline were higher up to approximately 90% and 37% when temperature increased to 390°C. But yield of diesel as demonstrated in Figure 16. (b). was decreased rapidly when reaction temperature reached to 390°C. The reason for explanation of reduction of long chain molecule in the diesel range could be that the long chain cracked to the lighter molecule due to cracking reaction. However the yield



of jet fuel seem to be constant when increase reaction temperature as showed in Figure 16. (a). which affected from cracking reaction. Some middle distillate in jet fuel range were cracked into lighter molecule meanwhile some heavy molecule including PFAD were cracked to middle distillate and light hydrocarbon range. Moreover, the yield of jet fuel is highest at 34.81% when using NiMo/ZNwo. On the other hand, NiMo supported on modified ZSM-5 exhibited the highest yield of gasoline fuel in 2-3 h. of reaction time these result demonstrated that the interconnected pores of modified supports with mesoporous directing agent promoted light hydrocarbon formation by secondary cracking reaction. After cracking reaction, hydrocarbon products were in the gasoline and jet fuel range. The result of yield of jet fuel in Figure 16. (a). showed that percent yield of jet fuel of NiMo supported on ZNco could reached to 32% at 360°C in lower reaction temperature than conventional ZSM-5 which had highest yield of jet at 375°C [57].

#### 5.2.2. Characterization of liquid product.

Considering in n-alkane distribution, at 360°C and 2 hours of reaction temperature using NiMo/ZNco as a catalyst, the main components of n-alkanes were pentane, pentadecane and heptadecane. From the Figure 21. (a)., at the beginning, the most abundant hydrocarbon were C15 and C17 which indicated that decarboxylation and decarbonylation were the dominant pathway. When increasing reaction temperature, heavier molecule will further cracking to lighter hydrocarbon. The result revealed that at highest temperature, pentane was the most dominant molecule due to cracking reaction. [55, 58, 59].

The analysis results of biofuel from GC-MS were shown in Figure 19. (b)., using NiMo/ZNco as a catalyst, at 360°C and 375°C respectively. At 360°C, the dominate hydrocarbon compositions as showed in Figure 19 (b). were iso-paraffins, n-paraffins and aromatics. From the distinct aromatization activity, yield of aromatic increased from 9.8 to 19.3% when increased reaction temperature from 360 to 375°C. Hence, isomerization and aromatization were favor with temperature. However, the mechanism of isomerization started with the formation of carbenium ions in the acid sites. The role of NiMo in the ZSM-5 support, n-olefins could formed through the hydrogenation of n-paraffins on the metal sites. Then, the addition of proton to n-

olefin resulting to form the normal carbenium ion. Therefore, at the acid site, the normal carbenium ion would isomerize to a branched carbenium ion followed by the elimination of proton of branch carbenium to get an iso-olefin. Eventually, the iso-olefin is hydrogenated again to obtain an iso-paraffin on the metal sites. Accordingly, NiMo play a role as a function of hydrogenation or dehydrogenation and acid site play a role as a function of isomerization. It was obviously that carbenium ion could be formed on the acid sites therefore amount of acid sites and acidic strength played important role to the isomerization, aromatization and cracking reaction [60]. The high reaction temperature and long reaction time favored isomerization, aromatization and cracking reaction, resulting in the increasing of isomerized, aromatized and lighter carbon products. These were because high temperature and long reaction time could activated acid function of catalysts to the high activity of isomerization, aromatization and cracking. The reason of high aromatic activity could explain from the activity of NiMo which can encourage the formation of gas product and combination with the formation of light hydrocarbon which led to offer materials for aromatization. Moreover, Mo species might enhance the transfer of electron between Ni and Mo by allowed partial electrons to Ni species. This were resulting to increase the carbenium ions and reaction activity. The addition mesoporous directing agent in NiMo supported on ZNco showed higher mesoporous volume which improved the reaction accessibility by allowing the bulky molecule can access to the active center of the catalyst. This benefits might confirmed by the yield of aromatic hydrocarbon of NiMo/ZNco was higher than NiMo/ZNwo [56]. As seen in Figure 20., especially in operating temperature at 360°C, highest yield of jet fuel which consist of a lot amount of iso-paraffin and aromatic. The advantage of consist of appropriate iso-paraffin and aromatic in biofuel was that the biofuel can act as drop-in with existing fuel specifications without blending. Some results of hydrocarbon distribution of biofuel using NiMo/ZNwo as a catalyst were showed in Figure 21 - 23.

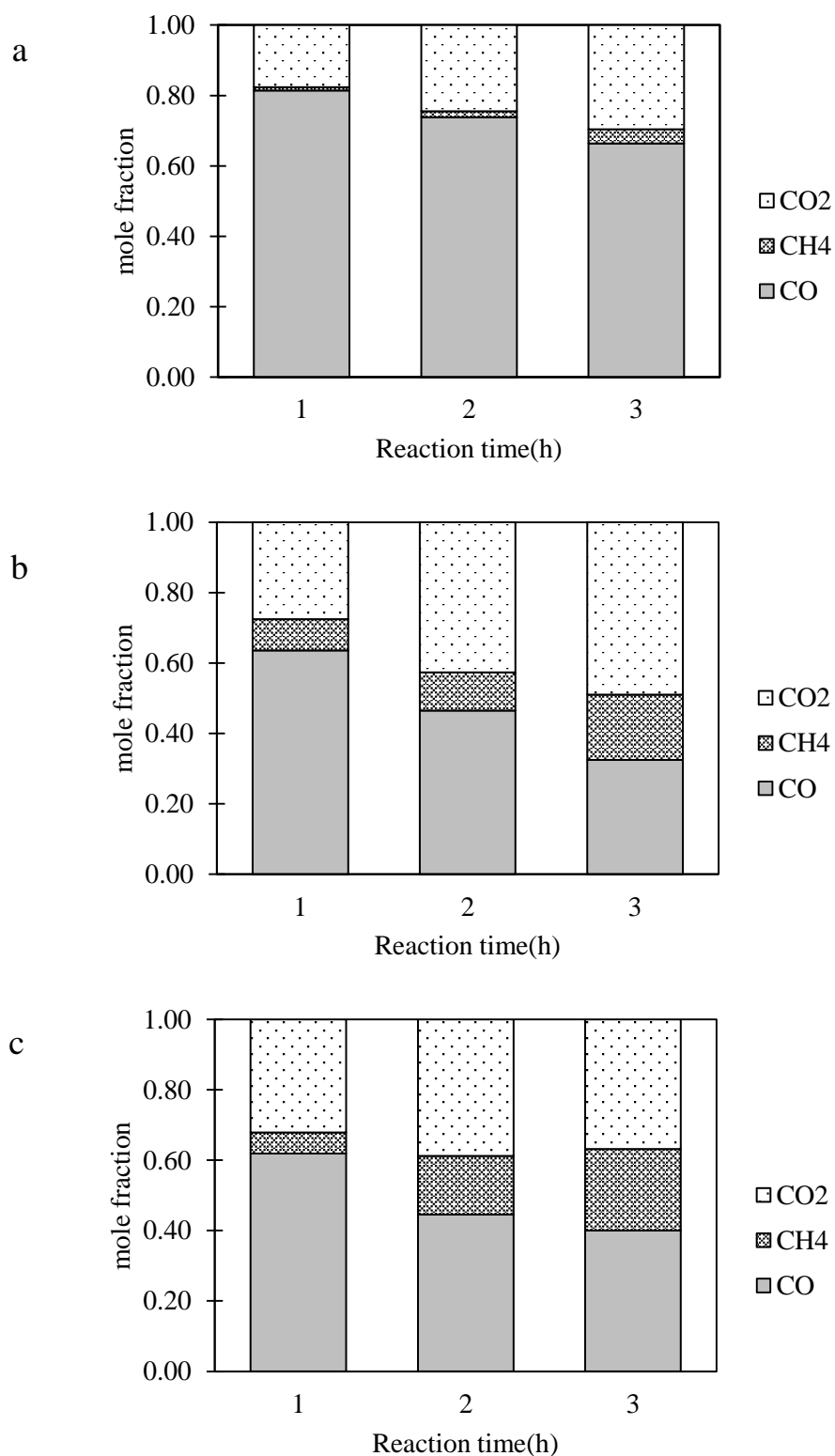


Figure 24. Mole fraction of gaseous products using NiMo/ZNwo at operating temperature = 360°C (a), 375°C (b), and 390°C (c) (operating pressure = 40 bar)

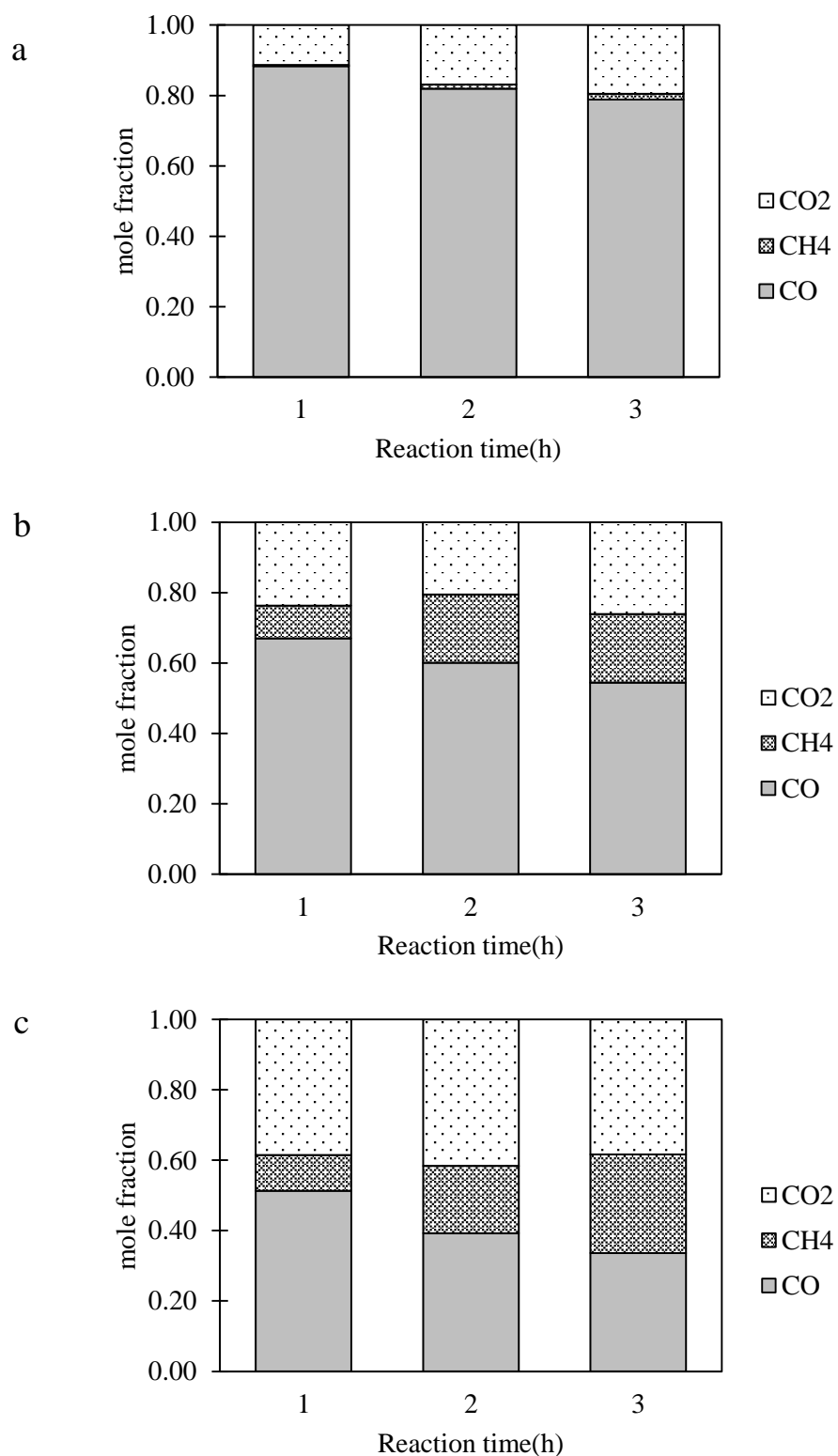


Figure 25. Mole fraction of gaseous products using NiMo/ZnCo at operating temperature = 360°C (a), 375°C (b), and 390°C (c) (operating pressure = 40 bar)

### 5.2.3 Characterization of gas product.

All gaseous product of hydroprocessing was similar to Kiatkittipong et.al and Veriansyah et al. From the results of gaseous product analysis, the dominant large amount of CO indicated that decarbonylation was dominant pathway when the hydroprocessing reaction was taken place at lower operating temperature and shorter reaction time. But, CO mole fraction decreased while CH<sub>4</sub> and CO<sub>2</sub> increased with operation temperature and reaction time. The amount of CO<sub>2</sub> increased due to the limitation of H<sub>2</sub> consumption while H<sub>2</sub> was consumed in the reaction, the limitation of H<sub>2</sub> as feed caused the hydroprocessing reaction pathway [10, 59]. A small amount of ethane and trace amount of propane were also observed in long reaction time and high operating temperature. The formation of CH<sub>4</sub> implied that the catalyst could able to crack feed into a smaller hydrocarbon. The CH<sub>4</sub> mole fraction increased with reaction time and operating temperature. CH<sub>4</sub> might was produced from the cleavage of C – C bond of short chain hydrocarbon [61]. From gas results as showed in Figure 24. and Figure 25., these result showed that, the formation rate of CH<sub>4</sub> was lower than CO and CO<sub>2</sub>. This was suggesting that the catalyst had more DCO and DCO<sub>2</sub> activity. Nevertheless, the methanation and water gas shift reaction by the present of CO, CO<sub>2</sub> and H<sub>2</sub> in the reaction system were accountable for the formation of CH<sub>4</sub>. Because of the present of methanation reaction in the system, the ratio of CO/CO<sub>2</sub> unable to represent the activity of DCO and DCO<sub>2</sub> [14, 41].

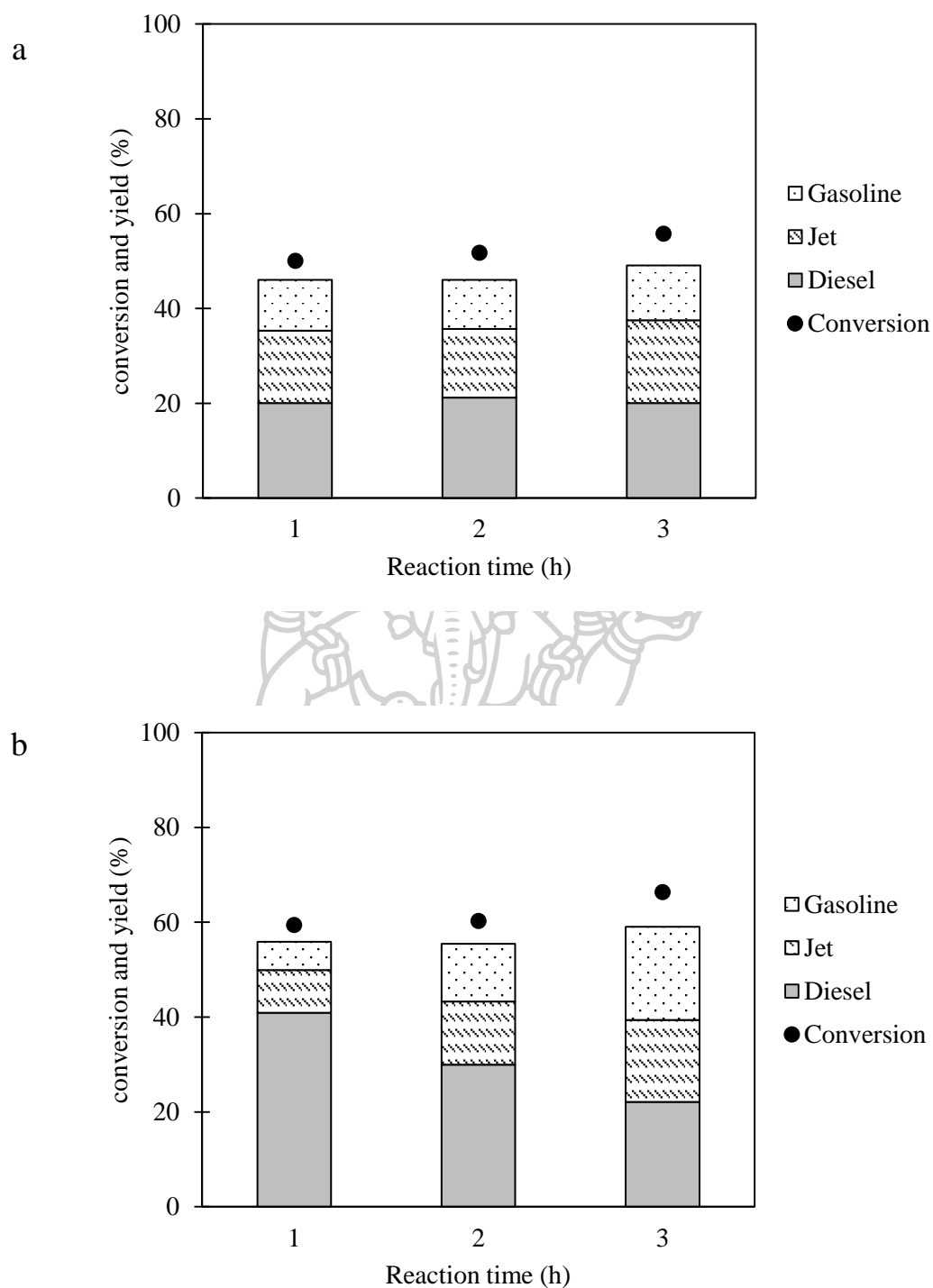


Figure 26. The effect of reaction time on conversion, yield of gasoline, jet and diesel when using *Pongamia Pinnata* oil as feedstock and using NiMo/ZNwo (a) and NiMo/ZNco (b) (operating pressure = 40 bar and operating temperature = 360°C)

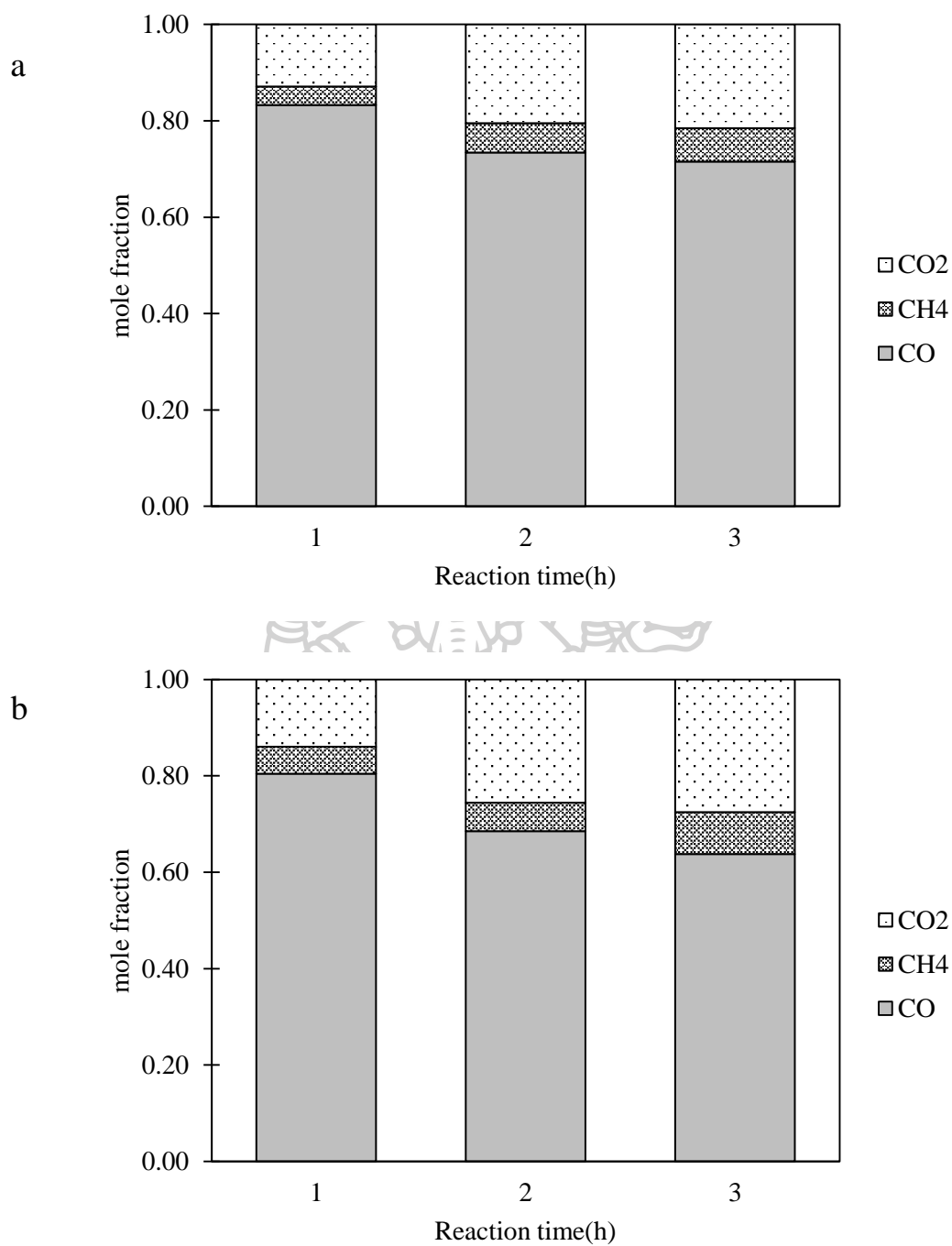


Figure 27. The effect of reaction time on gaseous products when using *Pongamia Pinnata* oil as feedstock and using NiMo/ZNwo (a) and NiMo/ZNco (b) (operating pressure = 40 bar and operating temperature = 360°C)

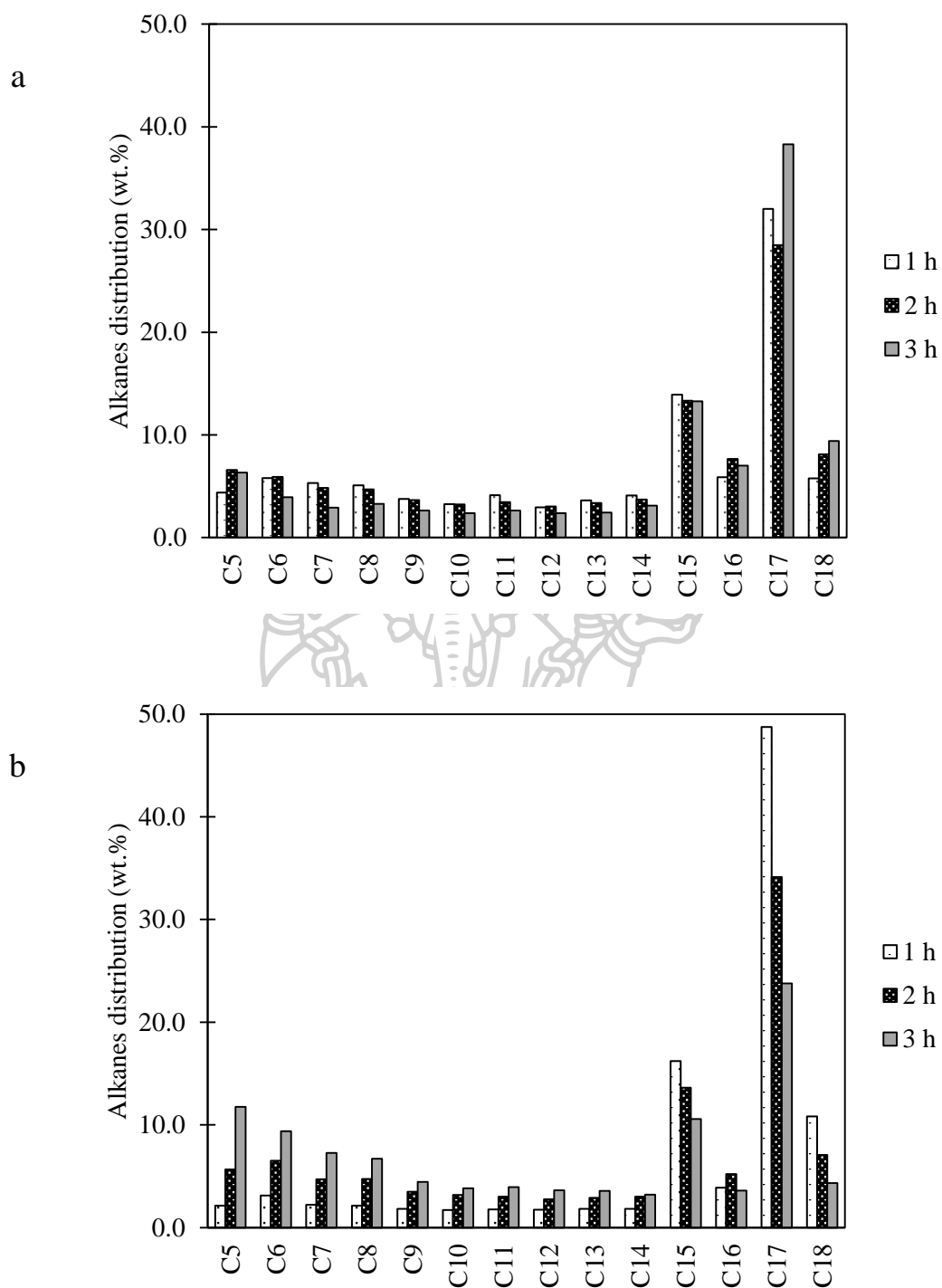


Figure 28. The effect of reaction time on n-alkanes distribution when using *Pongamia Pinnata* oil as feedstock and using NiMo/ZNwo (a) and NiMo/ZNco (b) (operating pressure = 40 bar and operating temperature = 360°C)



#### 5.2.4. Effect of feedstock structure; Comparison between free fatty acid and triglyceride molecule.

This study aimed to compare the structure of feedstock molecule which affected to the activity of ZSM-5. The two abundant fatty acids in PFAD were palmitic acid (C16:0) and oleic acid (C18:1) as showed in table 1. A triglyceride was an ester which has glycerol as a backbone and consisted of three fatty acid chains. A glycerol had hydroxyl (-OH) group and a fatty acid has carboxyl (COOH) group as showed in Figure 29.

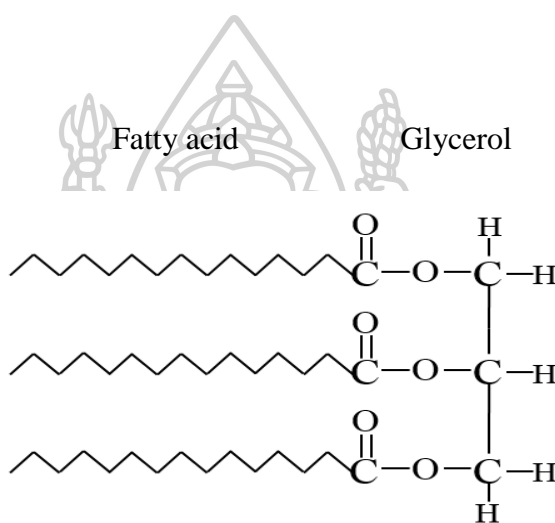


Figure 29. structure of triglyceride.

From the data above, it was obviously that triglyceride is bigger molecule than fatty acid. The main disadvantage of ZSM-5 was the diffusion limitation of their microporous structure. To study the effect of feedstock structure, *Pongamia Pinnata* oil were used in this reaction. Fatty acid distribution of *Pongamia Pinnata* oil were showed in table 5.

The catalytic performances for hydroprocessing reaction of *Pongamia Pinnata* oil were shown in Figure 26 – 28. NiMo/ZNco showed higher activity for conversion of *Pongamia Pinnata* oil than NiMo/ZNwo. 66.33% conversion was achieved at 360°C of operating temperatue, 3 h of reaction time and using NiMo/ZNco as a catalyst. The obtain result indicated that the activity of modified ZSM-5 with ODAC as a mesoporous directing agent is higher compare to ZSM-5 without modified.

Moreover, NiMo/ZNco exhibited the yield of jet and gasoline increase, while the diesel decrease. These results proved that ZNco promoted cracking reaction. The difference in catalytic performance was attributed to the present of more mesopore. The NiMo/ZNco showed higher mesoporous volume which enhance the reaction accessibility by allowing the bulky molecule can access to the active site of the catalyst. Depending on feedstock structure, in case of use PFAD as feedstock which the molecule was smaller than triglyceride. The activity of hydroprocessing using PFAD as feedstock in all catalysts seemed not much different. But when using *Pongamia Pinnata* oil as feedstock, very bulky molecule, this was crucial to perform the reaction with suitable catalyst. As can be seen, NiMo/ZNco exhibited the extremely enhanced active site accessibility due to the modification of ZSM-5 by adding the mesoporous directing agent.

Table 5. Fatty acid distribution of *Pongamia Pinnata* oil

Fatty acid	wt.%
C 16:0 (Palmitic acid)	15.09
C 18:0 (Stearic acid)	4.66
C 18:1 ( <i>n</i> -9 cis, Oleic acid)	54.41
C 18:2 ( <i>n</i> -6 cis, Linoleic acid)	13.45
C 18:3 ( <i>n</i> -3, Linolenic acid)	0.205
C 20:0 (Arachidic acid)	1.05
C 20:1 ( <i>n</i> -9, Eicosenoic acid)	1.46
C 22:0 (Behenic acid)	8.27

### 5.2.5. The thermogravimetric analysis of the used catalysts.

The used NiMo/ZNwo and NiMo/ZNco catalysts were analyzed by the TGA. The mass loss of used catalysts at different temperature and derivative thermogravimetric analysis were investigated.

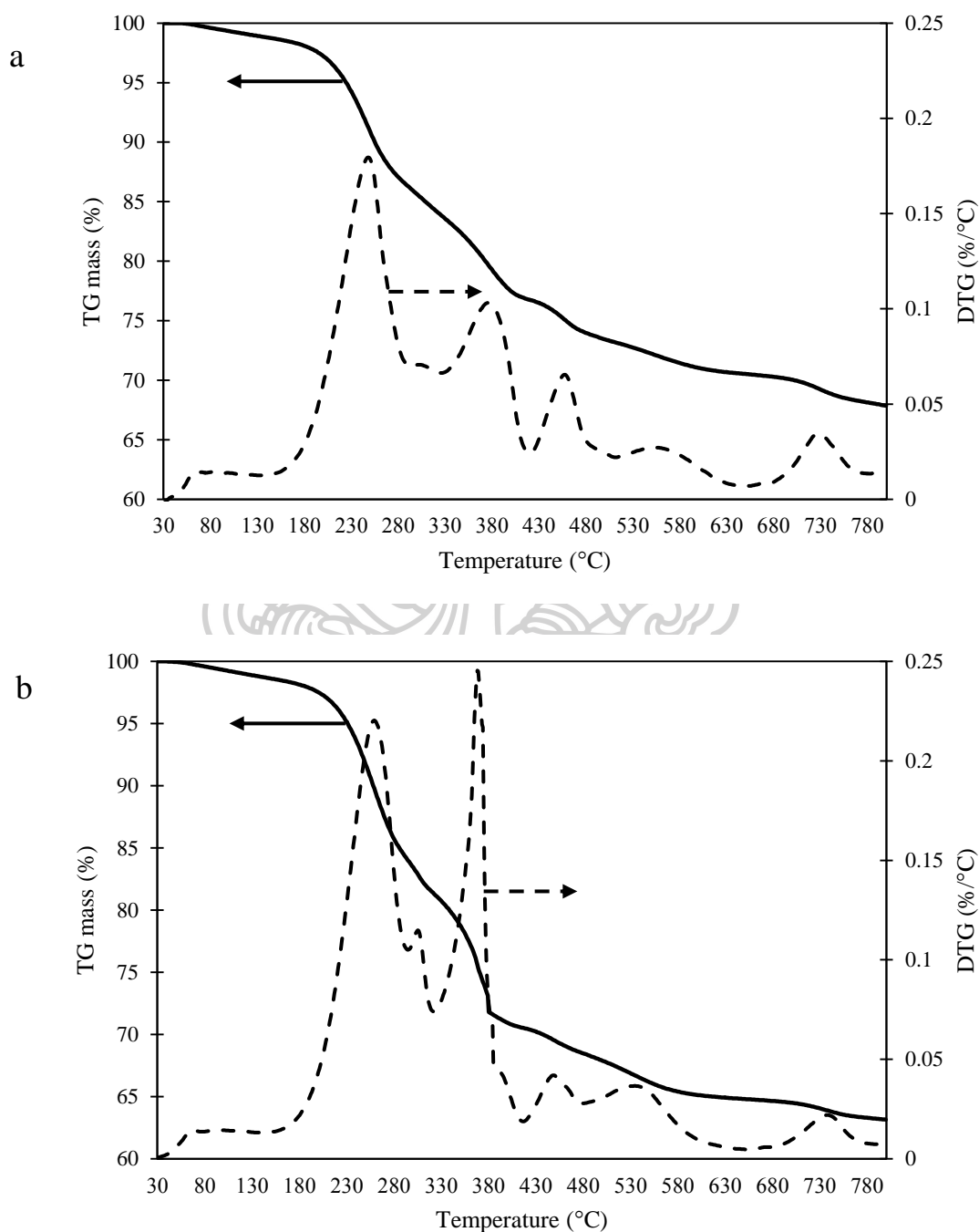


Figure 30. TG-DTA profiles of used NiMo/ZNwo (a) and used NiMo/ZNco (b).

Figure 30. showed TG-DTG profiles of used NiMo/ZNwo (a) and used NiMo/ZNco (b). It was obviously that the mass of used NiMo/ZNwo and used NiMo/ZNco catalysts decreased around 33% and 38% respectively after tested in hydroprocessing reaction at 40 bar of operating pressure, 375°C of operating temperature and 2 h of reaction time. The carbon content of the deactivated mesoporous-modified ZSM-5 is higher than without modified ZSM-5 because the improved accessibility of the catalyst [62]. The degradation of organic compounds of ZSM-5 produced a carbonaceous residue which still remain in the pore and surface of ZSM-5. The used NiMo/ZNwo and used NiMo/ZNco showed weight loss between 30 and 800°C. The removal of coke including carbonaceous residues and hydrogen were considered using DTG curve. The mass loss at 30 - 180°C represented the water content and physical adsorbents. The main mass lost was in 200 - 400°C region which indicated that the degradation of hydrocarbon compounds. The mass lost in 400 - 600°C region inferred to the soft coke. From the literature, hard coke of zeolite almost appeared at 600°C. The peak around 700°C was corresponding to the graphitization [63-66]. The mass loss of NiMo/ZNwo and NiMo/ZNco at above 400°C were around 10% but the main loss in 200 - 400°C were slightly different. It is interesting that Javiad and co-worker have studied the effect of conversion of each reactant on BTX reaction and found the relationship between the formation coke and BTX [67]. The BTX would be form inside the pore and could further convert into larger aromatic molecule which could deposit in the pore or the surface resulting to easily convert into coke. The higher of the mass loss of NiMo/ZNco than NiMo/ZNwo in the 200 - 400°C region could relate to the amount of aromatic content of these two catalyst at Figure 19. and Figure 23. The yield of aromatic which consisted of mainly BTX components of NiMo/ZNco was two times higher than NiMo/ZNwo at 40 bar of operating pressure, 375°C of operating temperature and 2 h reaction time [66, 67].

## CHAPTER 6

### CONCLUSIONS AND RECOMMENDATIONS

#### 6.1 . Conclusion

##### 6.1.1. Hydroprocessing of PFAD

In this study, hydroprocessing in a single-step process of palm fatty acid distillate (PFAD) is investigated. Catalysts employed in this study includes 5wt% Ni and 18wt% Mo supported on ZSM-5 (ZNwo), modified ZSM-5 with mesoporous-directing agent (ZNco and ZNpost), ZSM-5 using rice husk ash as a silica source (ZRco) and ZSM-5 from TEOS as a silica source (ZTco). The obtain product consist of liquid and gas phase. For all catalyst, the most abundant n-paraffins were n-pentadecane (n-C<sub>15</sub>) and n-heptadecane (n-C<sub>17</sub>), which one carbon atom shorter than the total carbon atom of corresponding palm fatty acid distillate such as palmitic acid and oleic acid. This result suggested that decarbonylation and decarboxylation are more dominant pathway than hydrodeoxygenation pathway which its alkane product containing the same carbon atom of feedstock. The dominant hydrocarbon compositions detected by GC-MS were iso-paraffins, n-paraffins and aromatics. The addition mesoporous directing agent in NiMo supported on ZNco showed higher mesoporous volume which improved the reaction accessibility by allowing the bulky molecule can access to the active center of the catalyst. This benefits might confirmed by the yield of aromatic hydrocarbon of NiMo/ZNco was higher than NiMo/ZNwo.

#### 6.2. Recommendations

In this study, the conversion is not completed hence some oxygenate and heavy molecule might effect to the properties of liquid product. For future work, analysis of the effect of oxygenate and heavy molecule should be considered.

The synthesized ZSM-5 by using RHA showed CHA phase which is competitive phase wjth ZSM-5. For future work, the effect of suitable synthesis temperature and time is necessary to find out.

## REFERENCES



- [1] A. Anger and J. Köhler, "Including aviation emissions in the EU ETS: Much ado about nothing? A review," *Transport Policy*, vol. 17, no. 1, pp. 38-46, 2010.
- [2] O. Dessens, M. O. Köhler, H. L. Rogers, R. L. Jones, and J. A. Pyle, "Aviation and climate change," *Transport Policy*, vol. 34, pp. 14-20, 2014.
- [3] J. Hileman and R. Stratton, "Alternative jet fuel feasibility," *Transport Policy*, vol. 34, pp. 52-62, 2014.
- [4] E. Dahlquist, *Biomass as energy source: resources, systems and applications*. CRC Press, 2013.
- [5] J. I. Hileman et al., "Near-term feasibility of alternative jet fuels," RAND Corporation and Massachusetts Institute of Technology: Santa Monica, CA, USA, 2009.
- [6] T. Choudhary and C. Phillips, "Renewable fuels via catalytic hydrodeoxygenation," *Applied Catalysis A: General*, vol. 397, no. 1, pp. 1-12, 2011.
- [7] M. Mohammad, T. K. Hari, Z. Yaakob, Y. C. Sharma, and K. Sopian, "Overview on the production of paraffin based-biofuels via catalytic hydrodeoxygenation," *Renewable and Sustainable Energy Reviews*, vol. 22, pp. 121-132, 2013.
- [8] S. Baroutian, M. K. Aroua, A. A. A. Raman, A. Shafie, R. A. Ismail, and H. Hamdan, "Blended aviation biofuel from esterified *Jatropha curcas* and waste vegetable oils," *Journal of the Taiwan Institute of Chemical Engineers*, vol. 44, no. 6, pp. 911-916, 2013.
- [9] E. Santillan-Jimenez and M. Crocker, "Catalytic deoxygenation of fatty acids and their derivatives to hydrocarbon fuels via decarboxylation/decarbonylation," *Journal of Chemical Technology and Biotechnology*, vol. 87, no. 8, pp. 1041-1050, 2012.
- [10] W. Kiatkittipong, S. Phimsen, K. Kiatkittipong, S. Wongsakulphasatch, N. Laosiripojana, and S. Assabumrungrat, "Diesel-like hydrocarbon production

- from hydroprocessing of relevant refining palm oil," Fuel processing technology, vol. 116, pp. 16-26, 2013.
- [11] J. Mikulec, J. Cvengroš, E. Joríková, M. Banič, and A. Kleinová, "Second generation diesel fuel from renewable sources," Journal of Cleaner Production, vol. 18, no. 9, pp. 917-926, 2010.
- [12] M. J. McCall, J. A. Kocal, A. Bhattacharyya, T. N. Kalnes, and T. A. Brandvold, "Production of aviation fuel from renewable feedstocks," ed: Google Patents, 2011.
- [13] D. Verma, R. Kumar, B. S. Rana, and A. K. Sinha, "Aviation fuel production from lipids by a single-step route using hierarchical mesoporous zeolites," Energy & Environmental Science, vol. 4, no. 5, pp. 1667-1671, 2011.
- [14] S. Phimsen et al., "Oil extracted from spent coffee grounds for bio-hydrotreated diesel production," Energy Conversion and Management, vol. 126, no. Supplement C, pp. 1028-1036, 2016/10/15/ 2016.
- [15] S. Phimsen et al., "Nickel sulfide, nickel phosphide and nickel carbide catalysts for bio-hydrotreated fuel production," Energy Conversion and Management, vol. 151, no. Supplement C, pp. 324-333, 2017/11/01/ 2017.
- [16] N. Corp. (10/11). Palm fatty acid distillate (PFAD) – a residue from palm oil refining process. Available: <https://www.neste.com/en/corporate-info/sustainability/sustainable-supply-chain/pfad-residue-palm-oil-refining-process-0>
- [17] T. S. T. K.Y. Cheah, and P.M. Koh. (2010, 10 ). Palm fatty acid distillate biodiesel: Next-generation palm biodiesel. Available: <https://www.aocs.org/stay-informed/read-inform/featured-articles/palm-fatty-acid-distillate-biodiesel-next-generation-palm-biodiesel-may-2010>
- [18] R. J. Argauer and G. R. Landolt, "Crystalline zeolite ZSM-5 and method of preparing the same," ed: Google Patents, 1972.
- [19] S. M. Auerbach, K. A. Carrado, and P. K. Dutta, Handbook of zeolite science and technology. CRC press, 2003.



- [20] J. Perez-Ramirez, C. H. Christensen, K. Egeblad, C. H. Christensen, and J. C. Groen, "Hierarchical zeolites: enhanced utilisation of microporous crystals in catalysis by advances in materials design," *Chemical Society Reviews*, 10.1039/B809030K vol. 37, no. 11, pp. 2530-2542, 2008.
- [21] C. S. Cundy and P. A. Cox, "The hydrothermal synthesis of zeolites: history and development from the earliest days to the present time," *Chemical Reviews*, vol. 103, no. 3, pp. 663-702, 2003.
- [22] K. Na, M. Choi, and R. Ryoo, "Recent advances in the synthesis of hierarchically nanoporous zeolites," *Microporous and Mesoporous Materials*, vol. 166, pp. 3-19, 2013.
- [23] T. Armaroli et al., "Effects of crystal size and Si/Al ratio on the surface properties of H-ZSM-5 zeolites," *Applied Catalysis A: General*, vol. 306, pp. 78-84, 2006.
- [24] D. Serrano, J. Aguado, J. Escola, and J. Rodríguez, "Influence of nanocrystalline HZSM-5 external surface on the catalytic cracking of polyolefins," *Journal of analytical and applied pyrolysis*, vol. 74, no. 1, pp. 353-360, 2005.
- [25] D. P. Serrano, J. Aguado, J. M. Escola, J. M. Rodríguez, and Á. Peral, "Hierarchical zeolites with enhanced textural and catalytic properties synthesized from organofunctionalized seeds," *Chemistry of materials*, vol. 18, no. 10, pp. 2462-2464, 2006.
- [26] L. Frunz, R. Prins, and G. D. Pirngruber, "ZSM-5 precursors assembled to a mesoporous structure and its subsequent transformation into a zeolitic phase— from low to high catalytic activity," *Microporous and mesoporous materials*, vol. 88, no. 1, pp. 152-162, 2006.
- [27] K. Suzuki, Y. Aoyagi, N. Katada, M. Choi, R. Ryoo, and M. Niwa, "Acidity and catalytic activity of mesoporous ZSM-5 in comparison with zeolite ZSM-5, Al-MCM-41 and silica–alumina," *Catalysis Today*, vol. 132, no. 1, pp. 38-45, 2008.

- [28] M. Choi, H. S. Cho, R. Srivastava, C. Venkatesan, D.-H. Choi, and R. Ryoo, "Amphiphilic organosilane-directed synthesis of crystalline zeolite with tunable mesoporosity," *Nature materials*, vol. 5, no. 9, pp. 718-723, 2006.
- [29] W. K. Craig and D. W. Soveran, "Production of hydrocarbons with a relatively high cetane rating," ed: Google Patents, 1991.
- [30] J. Monnier, G. Tourigny, D. W. Soveran, A. Wong, E. N. Hogan, and M. Stumborg, "Conversion of biomass feedstock to diesel fuel additive," ed: Google Patents, 1998.
- [31] M. Stumborg, A. Wong, and E. Hogan, "Hydroprocessed vegetable oils for diesel fuel improvement," *Bioresource Technology*, vol. 56, no. 1, pp. 13-18, 1996.
- [32] J. Satyarthi, T. Chiranjeevi, D. Gokak, and P. Viswanathan, "An overview of catalytic conversion of vegetable oils/fats into middle distillates," *Catalysis Science & Technology*, vol. 3, no. 1, pp. 70-80, 2013.
- [33] J. Myllyoja, P. Aalto, and E. Harlin, "Process for the manufacture of diesel range hydrocarbons," ed: Google Patents, 2012.
- [34] J. A. Petri and T. L. Marker, "Production of diesel fuel from biorenewable feedstocks," ed: Google Patents, 2009.
- [35] G. W. Huber, P. O'Connor, and A. Corma, "Processing biomass in conventional oil refineries: Production of high quality diesel by hydrotreating vegetable oils in heavy vacuum oil mixtures," *Applied Catalysis A: General*, vol. 329, pp. 120-129, 2007.
- [36] G. Liu, B. Yan, and G. Chen, "Technical review on jet fuel production," *Renewable and Sustainable Energy Reviews*, vol. 25, pp. 59-70, 2013.
- [37] A. Llamas, A.-M. Al-Lal, M. Hernandez, M. Lapuerta, and L. Canoira, "Biokerosene from babassu and camelina oils: Production and properties of their blends with fossil kerosene," *Energy & fuels*, vol. 26, no. 9, pp. 5968-5976, 2012.

- [38] E. Nygren, K. Aleklett, and M. Höök, "Aviation fuel and future oil production scenarios," *Energy Policy*, vol. 37, no. 10, pp. 4003-4010, 2009.
- [39] J. P. Brady, T. N. Kalnes, and T. L. Marker, "Production of transportation fuel from renewable feedstocks," ed: Google Patents, 2012.
- [40] H. Chen, Q. Wang, X. Zhang, and L. Wang, "Hydroconversion of jatropha oil to alternative fuel over hierarchical ZSM-5," *Industrial & Engineering Chemistry Research*, vol. 53, no. 51, pp. 19916-19924, 2014.
- [41] S. Gong, A. Shinozaki, and E. W. Qian, "Role of support in hydrotreatment of jatropha oil over sulfided NiMo catalysts," *Industrial & Engineering Chemistry Research*, vol. 51, no. 43, pp. 13953-13960, 2012.
- [42] V. N. Shetti, J. Kim, R. Srivastava, M. Choi, and R. Ryoo, "Assessment of the mesopore wall catalytic activities of MFI zeolite with mesoporous/microporous hierarchical structures," *Journal of Catalysis*, vol. 254, no. 2, pp. 296-303, 2008.
- [43] Q. Lei, T. Zhao, F. Li, L. Zhang, and Y. Wang, "Catalytic cracking of large molecules over hierarchical zeolites," *Chemical communications*, no. 16, pp. 1769-1771, 2006.
- [44] L. Xu et al., "Synthesis, characterization of hierarchical ZSM-5 zeolite catalyst and its catalytic performance for phenol tert-butylation reaction," *Catalysis Communications*, vol. 9, no. 6, pp. 1272-1276, 2008.
- [45] J. Botas, D. Serrano, A. García, and R. Ramos, "Catalytic conversion of rapeseed oil for the production of raw chemicals, fuels and carbon nanotubes over Ni-modified nanocrystalline and hierarchical ZSM-5," *Applied Catalysis B: Environmental*, vol. 145, pp. 205-215, 2014.
- [46] M. Conte et al., "Enhanced selectivity to propene in the methanol to hydrocarbons reaction by use of ZSM-5/11 intergrowth zeolite," *Microporous and Mesoporous Materials*, vol. 164, pp. 207-213, 2012.
- [47] B. Wang, H. Wang, G. Liu, X. Li, and J. Wu, "Conversion of dimethyl ether to toluene under an O<sub>2</sub> stream over W/HZSM-5 catalysts," *Catalysis Science & Technology*, vol. 5, no. 3, pp. 1813-1820, 2015.

- [48] R. M. Mohamed, H. M. Aly, M. F. El-Shahat, and I. A. Ibrahim, "Effect of the silica sources on the crystallinity of nanosized ZSM-5 zeolite," *Microporous and mesoporous materials*, vol. 79, no. 1, pp. 7-12, 2005.
- [49] T. Fjermestad, S. Svelle, and O. Swang, "Mechanistic Comparison of the Dealumination in SSZ-13 and the Desilication in SAPO-34," *The Journal of Physical Chemistry C*, vol. 117, no. 26, pp. 13442-13451, 2013.
- [50] B. Liu et al., "Synthesis of low-silica CHA zeolite chabazite in fluoride media without organic structural directing agents and zeolites," *Microporous and Mesoporous Materials*, vol. 196, pp. 270-276, 2014.
- [51] L. Wu, "Mesoporous CHA and MFI zeolite catalysts for methanol conversion reactions," Doctoral degree, Department of Chemical Engineering and Chemistry, Technische Universiteit Eindhoven, Eindhoven : Technische Universiteit Eindhoven, 2014, 2014.
- [52] M. Chareonpanich, T. Namto, P. Kongkachuichay, and J. Limtrakul, "Synthesis of ZSM-5 zeolite from lignite fly ash and rice husk ash," *Fuel processing technology*, vol. 85, no. 15, pp. 1623-1634, 2004.
- [53] L. Shirazi, E. Jamshidi, and M. Ghasemi, "The effect of Si/Al ratio of ZSM-5 zeolite on its morphology, acidity and crystal size," *Crystal Research and Technology*, vol. 43, no. 12, pp. 1300-1306, 2008.
- [54] J. Botas, D. Serrano, A. García, J. De Vicente, and R. Ramos, "Catalytic conversion of rapeseed oil into raw chemicals and fuels over Ni-and Mo-modified nanocrystalline ZSM-5 zeolite," *Catalysis today*, vol. 195, no. 1, pp. 59-70, 2012.
- [55] S. Liu, Q. Zhu, Q. Guan, L. He, and W. Li, "Bio-aviation fuel production from hydroprocessing castor oil promoted by the nickel-based bifunctional catalysts," *Bioresource technology*, vol. 183, pp. 93-100, 2015.
- [56] X. Yang, J. Liu, K. Fan, and L. Rong, "Hydrocracking of Jatropha Oil over non-sulfided PTA-NiMo/ZSM-5 Catalyst," *Scientific Reports*, vol. 7, p. 41654, 2017.

- [57] P. Kham-or, P. Suwannasom, and C. Ruangviriyachai, "Effect of agglomerated NiMo HZSM-5 catalyst for the hydrocracking reaction of *Jatropha curcas* oil," *Energy Sources, Part A: Recovery, Utilization, and Environmental Effects*, vol. 38, no. 24, pp. 3694-3701, 2016.
- [58] S. K. Kim, J. Y. Han, H.-s. Lee, T. Yum, Y. Kim, and J. Kim, "Production of renewable diesel via catalytic deoxygenation of natural triglycerides: comprehensive understanding of reaction intermediates and hydrocarbons," *Applied Energy*, vol. 116, pp. 199-205, 2014.
- [59] B. Veriansyah et al., "Production of renewable diesel by hydroprocessing of soybean oil: effect of catalysts," *Fuel*, vol. 94, pp. 578-585, 2012.
- [60] Y. Liu, R. Sotelo-Boyás, K. Murata, T. Minowa, and K. Sakanishi, "Hydrotreatment of Vegetable Oils to Produce Bio-Hydrogenated Diesel and Liquefied Petroleum Gas Fuel over Catalysts Containing Sulfided Ni–Mo and Solid Acids," *Energy & Fuels*, vol. 25, no. 10, pp. 4675-4685, 2011/10/20 2011.
- [61] X. Zhao, L. Wei, J. Julson, Q. Qiao, A. Dubey, and G. Anderson, "Catalytic cracking of non-edible sunflower oil over ZSM-5 for hydrocarbon bio-jet fuel," *New biotechnology*, vol. 32, no. 2, pp. 300-312, 2015.
- [62] F. Schmidt et al., "Coke location in microporous and hierarchical ZSM-5 and the impact on the MTH reaction," *Journal of Catalysis*, vol. 307, pp. 238-245, 2013/11/01/ 2013.
- [63] S. B. Abusriwil, O. A. Sharif, and A. M. Dabah, "Hydrocracking of Heavy Gas Oil Fraction Over NiMo/H-ZSM5 and Ni/Mordinite Catalysts."
- [64] M. Ali, M. Siddiqui, and S. Zaidi, "Thermal analysis of crude oils and comparison with SIMDIST and TBP distillation data," *Journal of thermal analysis and calorimetry*, vol. 51, no. 1, pp. 307-319, 1998.
- [65] Z. Zhang, Q. Wang, H. Chen, and X. Zhang, "Hydroconversion of Waste Cooking Oil into Bio-Jet Fuel over a Hierarchical NiMo/USY@ Al-SBA-15 Zeolite," *Chemical Engineering & Technology*, vol. 41, no. 3, pp. 590-597, 2018.

- [66] H. Zhang, S. Shao, R. Xiao, D. Shen, and J. Zeng, "Characterization of coke deposition in the catalytic fast pyrolysis of biomass derivatives," *Energy & Fuels*, vol. 28, no. 1, pp. 52-57, 2013.
- [67] R. Javaid, K. Urata, S. Furukawa, and T. Komatsu, "Factors affecting coke formation on H-ZSM-5 in naphtha cracking," *Applied Catalysis A: General*, vol. 491, pp. 100-105, 2015.





**INDEX**

## Appendix A

### A.1. Calculation H<sub>2</sub> to feed ratio

Table 6. Fatty acid distribution of palm fatty acid distilled (PFAD).

Fatty acid	Formular	Molecular weight (g/mole)	Wt% Normalization	Mass fraction
Palmitic	C <sub>16</sub> H <sub>32</sub> O <sub>2</sub>	256.42	57.8	0.58
Oleic	C <sub>18</sub> H <sub>34</sub> O <sub>2</sub>	282.46	42.2	0.42

Molecular weight of PFAD =  $(0.58 \times 256.42) + (0.42 \times 282.46) = 267.36 \text{ g/mole}_{\text{PFAD}}$

In each batch experiment, the volume of feedstock was fix at 2 ml.

The density of PFAD at 30°C is 0.9 g/cm<sup>3</sup>.

The weight of feedstock =  $0.9 \times 2 = 1.8 \text{ ml}$ .

Mole of PFAD in feedstock =  $1.8 \div 267.36 = 0.00673 \text{ mole}$

The space volume in reactor is 25 cm<sup>3</sup>.

The mole of hydrogen in reaction was calculated, as follow:

$$PV = nRT$$

$$n = \frac{PV}{RT}$$

For example, the initial pressure of hydrogen is 40 bar and room temperature is 303 K, the calculation of mole of initial hydrogen:

$$n = \frac{40 \text{ bar} \times (25 \times 10^{-6} \text{ m}^3)}{\left(8.314 \times 10^{-5} \frac{\text{m}^3 \text{bar}}{\text{mole K}}\right) \times 303 \text{ K}} = 0.0397 \text{ mole}$$

The calculation of H<sub>2</sub> to feed ratio:



$$\text{H}_2:\text{feed ratio} = \frac{0.0397}{0.00673} = 5.899 \left( \frac{\text{mole}}{\text{mole}} \right)$$

### A.2. Calculation of metal loading for catalyst preparation

For example, preparation of 5%Ni and 18%Mo supported on ZSM-5 was calculated as follow:

Basis: 2 g. of ZSM-5 support

$\text{Ni}(\text{NO}_3)_2 \cdot 6\text{H}_2\text{O}$  was used as Ni precursor.

$$\begin{aligned} &= (2 \text{ g. ZSM-5}) \times \left( \frac{5 \text{ g. Ni}}{77 \text{ g. ZSM-5}} \right) \times \left( \frac{1 \text{ mol Ni}}{58.6932 \text{ g. Ni}} \right) \times \left( \frac{1 \text{ mol Ni}(\text{NO}_3)_2 \cdot 6\text{H}_2\text{O}}{1 \text{ mol Ni}} \right) \\ &\times \left( \frac{290.81 \text{ g. Ni}(\text{NO}_3)_2 \cdot 6\text{H}_2\text{O}}{1 \text{ mol Ni}(\text{NO}_3)_2 \cdot 6\text{H}_2\text{O}} \right) \times \left( \frac{1}{0.97} \right) \\ &= 0.663 \text{ g. Ni}(\text{NO}_3)_2 \cdot 6\text{H}_2\text{O} \end{aligned}$$

$(\text{NH}_4)\text{Mo}_7\text{O}_{24} \cdot 4\text{H}_2\text{O}$  was used as Mo precursor.

$$\begin{aligned} &= (2 \text{ g. ZSM-5}) \times \left( \frac{18 \text{ g. Mo}}{77 \text{ g. ZSM-5}} \right) \times \left( \frac{1 \text{ mol Mo}}{95.96 \text{ g. Mo}} \right) \times \left( \frac{1 \text{ mol}(\text{NH}_4)\text{Mo}_7\text{O}_{24} \cdot 4\text{H}_2\text{O}}{7 \text{ mol MO}} \right) \\ &\times \left( \frac{1235.86 \text{ g.}(\text{NH}_4)\text{Mo}_7\text{O}_{24} \cdot 4\text{H}_2\text{O}}{1 \text{ mol}(\text{NH}_4)\text{Mo}_7\text{O}_{24} \cdot 4\text{H}_2\text{O}} \right) \times \left( \frac{1}{0.82} \right) \\ &= 1.048 \text{ g.}(\text{NH}_4)\text{Mo}_7\text{O}_{24} \cdot 4\text{H}_2\text{O} \end{aligned}$$

Preparaion of of 5%Ni and 18%Mo used 0.663 g.  $\text{Ni}(\text{NO}_3)_2 \cdot 6\text{H}_2\text{O}$  and 1.048 g.  $(\text{NH}_4)\text{Mo}_7\text{O}_{24} \cdot 4\text{H}_2\text{O}$  supported on 2 g. ZSM-5.

A.3. The calculation of the composition solution used to synthesize ZSM-5 from rice husk ash as a Si precursor.

1. The calculation of the Si precursor from rice husk ash used to synthesize ZSM-5 zeolite.

The preparation a sodium silicate solution from rice husk ash at molar ratio of Si to Al equal to 20. The data of the composition of silica and alumina in rice husk ash and molecule mass of silica and alumina showed as follows:

The composition of silica in rice husk ash = 99.0 wt%

The composition of alumina in rice husk ash = 0.060 wt%

The composition of alumina in sodium aluminate solution = 53 wt%

Molecular mass of silica = 60.09

Molecular mass of alumina = 101.96

The molar ratio of Si to Al (Si/Al) = 20

Amount of rice husk ash = X

Weight  $\text{Al}_2\text{O}_3$  in sodium aluminate is g/mole =  $\frac{0.35}{101.96} \times 0.53 \times X = 1.8193 \times 10^{-3}$  gmole

Weight  $\text{SiO}_2$  in rice husk ash =  $(X) \times 0.99 = 0.99(X)$  g

$$= \frac{0.99 \times (X)}{60.09}$$

= 0.01648 (X) gmole

Weight  $\text{Al}_2\text{O}_3$  in rice husk ash =  $(X) \times 0.0006 = 0.0006(X)$  g

$$= \frac{0.0006 \times (X)}{101.96}$$

=  $9.8078 \times 10^{-6}$  (X) gmole

From Si/Al ratio = 20 or  $\text{SiO}_2/\text{Al}_2\text{O}_3$  ratio = 40

$$20 = \frac{0.01648 \times (X)}{1.8193 \times 10^{-3} + 9.8078 \times 10^{-6} (X)}$$

$$X = 4.49 \text{ g.}$$

Therefore weight of rice husk ash used to synthesize was 4.49 g. And sodium silicate solution contains  $\text{SiO}_2$  27 wt % .

$$\text{Weight of silicate in rice husk ash} = 4.49 \times 0.99 = 4.486 \text{ g}$$

Weight of sodium hydroxide in sodium silicate solution was 10% and 99% purity.

$$= \frac{4.486 \times 0.1}{0.27 \times 0.99} = 1.678 \text{ g}$$

And amount of  $\text{H}_2\text{O}$  was 63%

$$= 0.63 \times \frac{4.486}{0.27} = 10.47 \text{ g or } 10.47 \text{ ml}$$

Therefore, the solution of sodium silicate by using rice husk ash contained 4.486 g of rich husk ash in solid, 1.678 g. of NaOH and adjusts the volume by 10.47 ml of distilled water.

2. The calculation of the Al precursor used to synthesize ZSM-5 zeolite.

From calculation above; weight of rice husk ash used to synthesize was 4.49 g.

$$\text{Weight } \text{SiO}_2 \text{ in rice husk ash} = 4.49 \times 0.01648 = 0.074 \text{ gmol}$$

$$\text{Si/Al ratio} = 20 \text{ or } \text{SiO}_2/\text{Al}_2\text{O}_3 \text{ ratio} = 40$$

The volume of sodium aluminate is equal to =Y ml

$$\text{Weight } \text{Al}_2\text{O}_3 \text{ in rice husk ash} = 4.49 \times 0.0006 = 2.694 \times 10^{-3} \text{ g.}$$

$$= \frac{2.694 \times 10^{-3}}{101.96}$$

$$= 2.642 \times 10^{-5} \text{ gmole}$$

$$\text{Weight of } \text{Al}_2\text{O}_3 \text{ in sodium aluminate solution} = 0.53Y \text{ g}$$

$$= \frac{0.53Y}{101.96} = 5.1981 \times 10^{-3} Y \text{ gmol}$$

To obtain  $\text{SiO}_2/\text{Al}_2\text{O}_3$  ratio equal to 40

$$\frac{\text{SiO}_2}{\text{Al}_2\text{O}_3} = 40 = \frac{0.074}{2.642 \times 10^{-3} + 5.1981 \times 10^{-3}Y}$$

$$Y = 0.35 \text{ g.}$$

Therefore, to synthesize ZSM-5 with Si/Al ratio was 20, 0.35 g. of aluminate was added to the synthesized solution.

3. The calculation an amount of tetrapropylammonium bromide (TPABr) template used to synthesize ZSM-5 zeolite.

$$\text{Si/Al ratio} = 20 \text{ or SiO}_2/\text{Al}_2\text{O}_3 \text{ ratio} = 40$$

$$\text{The tetrapropylammonium bromide to alumina ratio (TPABr/Al}_2\text{O}_3) = 0.5$$

$$\text{The amount mole of tetrapropylammonium bromide (gmole)} = Z$$

From calculation above;

$$\text{Weight of Al}_2\text{O}_3 \text{ in rice husk ash} = 4.404 \times 10^{-5} \text{ gmole}$$

$$\text{Weight of Al}_2\text{O}_3 \text{ in sodium aluminate solution} = 1.8193 \times 10^{-3} \text{ gmole}$$

$$\frac{\text{TPABr}}{\text{Al}_2\text{O}_3} = 0.5 = \frac{Z}{(1.8193 \times 10^{-3}) + (4.404 \times 10^{-5})}$$

$$Z = 9.3167 \times 10^{-4} \text{ gmole}$$

Molecular mass of TPABr is 266.27 g/gmole and 98% purity.

$$(9.3167 \times 10^{-4}) \times \left(\frac{266.27 \text{ g}}{1 \text{ gmole}}\right) \times \frac{1}{0.98} = 0.2531 \text{ g.}$$

Therefore, to synthesize ZSM-5, the amount of tetrapropylammonium bromide template was 0.2531 g.

#### A.4. The calculation of selectivity and yield of liquid hydrocarbon and conversion of PFAD

The calculations of product yield classified to gasoline, jet and diesel were based on area of GC without using external or internal standards. The peak area normalization method based on peak area fraction was used to quantify results. For analysis the performance of the catalyst, the conversion of PFAD, gasoline, jet and diesel selectivity were determined by using following equations:

$$\text{conversion(\%)} = \frac{\text{Feed}_{\text{TG}} - \text{Product}_{\text{TG}}}{\text{Feed}_{\text{TG}}} \times 100$$

The conversion was defined as the mole of triglycerides (TG) as feedstock converted to hydrocarbons.

Where  $\text{Feed}_{\text{C18+}}$  is area fraction of the TG as a feed. And,  $\text{Product}_{\text{TG}}$  is area fraction of the TG in product having fraction of hydrocarbon more than C18.

The selectivity of gasoline, jet and diesel was also defined based on peak area fraction as follows.

$$\text{Gasoline selectivity} = \left( \frac{\text{Product}_{\text{C5-C8}}}{\text{Product}_{\text{C5-C8}} + \text{Product}_{\text{C9-C14}} + \text{Product}_{\text{C15-C18}}} \right)$$

$$\text{Jet selectivity} = \left( \frac{\text{Product}_{\text{C9-C14}}}{\text{Product}_{\text{C5-C8}} + \text{Product}_{\text{C9-C14}} + \text{Product}_{\text{C15-C18}}} \right)$$

$$\text{Diesel selectivity} = \left( \frac{\text{Product}_{\text{C15-C18}}}{\text{Product}_{\text{C5-C8}} + \text{Product}_{\text{C9-C14}} + \text{Product}_{\text{C15-C18}}} \right)$$

Where  $\text{Product}_{\text{C5 - C8}}$  is an area fraction of the product in the range of hydrocarbon C5 – C8,  $\text{Product}_{\text{C9 - C14}}$  is an area fraction of the product in the range of hydrocarbon C9 – C14, and  $\text{Product}_{\text{C15 - C18}}$  is an area fraction of the product in the range of hydrocarbon C15 – C18.

Liquid and gas fraction can be calculated by following equations:

$$\text{Liquid fraction of product} = \frac{\text{weight of liquid product}}{\text{weight of feed}}$$

$$\text{Gas fraction of product} = 1 - \frac{\text{weight of liquid product}}{\text{weight of feed}}$$

Gasoline, jet, and diesel yield can be calculated by following equations:

Gasoline yield = Gasoline selectivity  $\times$  conversion  $\times$  Liquid fraction of product

Jet yield = Jet selectivity  $\times$  conversion  $\times$  Liquid fraction of product

Diesel yield = Diesel selectivity  $\times$  conversion  $\times$  Liquid fraction of product-

Yield of liquid fuel = Gasoline yield + Jet yield + Diesel yield

Table 7. The chemical composition of rice husk ash (RHA)

Chemical compositions in Silica source	Rice husk ash (wt.%)
SiO <sub>2</sub>	99.0
Al <sub>2</sub> O <sub>3</sub>	0.060
K <sub>2</sub> O	0.062
CaO	0.062

## A.4. The SEM-EDX images of catalysts

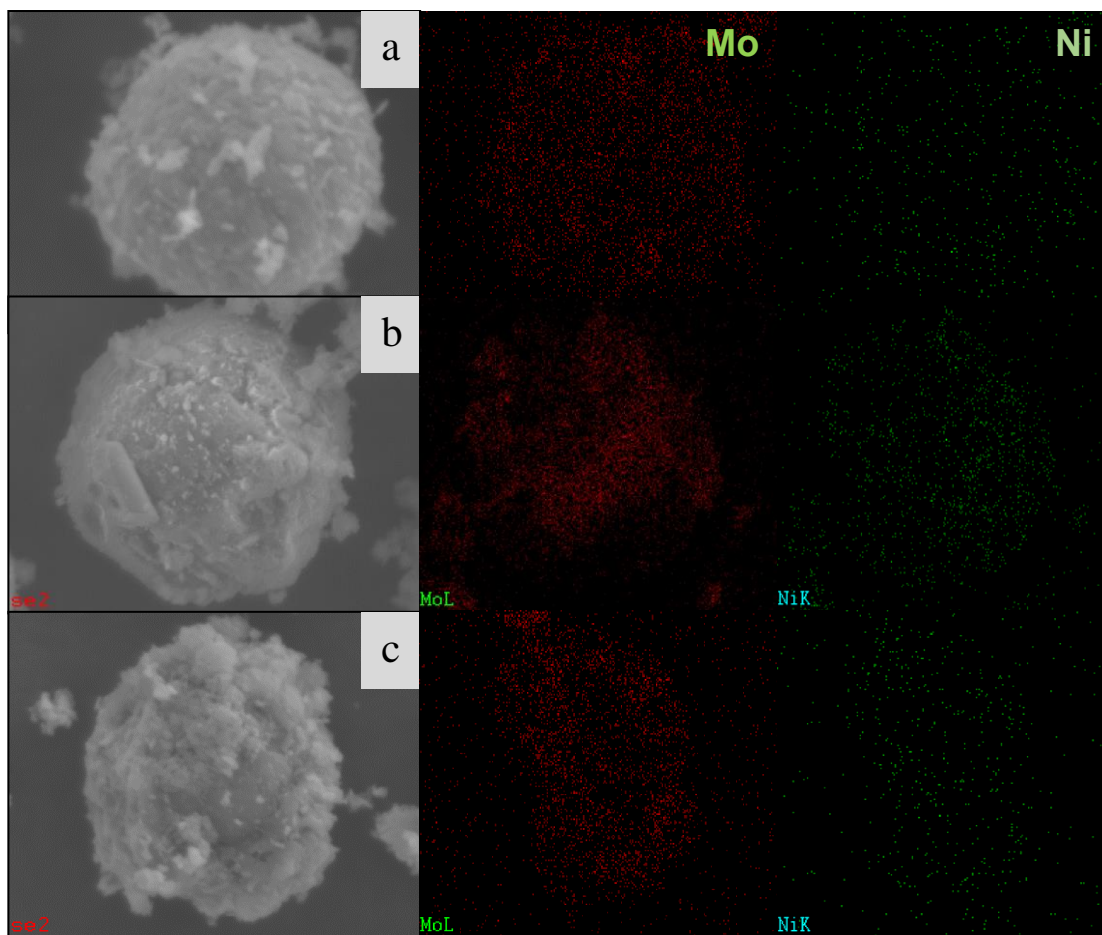


Figure 31 SEM-EDX images of NiMo/ZNwo (a), NiMo/ZNco (b), and NiMo/ZNpost (c).

**VITA**

**NAME** Boontarika Akassupha

**DATE OF BIRTH** 24 April 1991

**PLACE OF BIRTH** Lopburi

**INSTITUTIONS  
ATTENDED** Silpakorn University

**HOME ADDRESS** 35/1 Moo 8, Patal sub district, Mueng district, Lopburi,  
Thailand 15000

